Universidade de Aveiro Departamento de Biologia
Ano 2019

Carla Patrícia da Silva Leite

Toxic impacts of titanium dioxide nanoparticles in *Mytilus galloprovincialis* exposed to warming conditions

Impactos tóxicos de nanopartículas de dióxido de titânio em *Mytilus galloprovincialis* expostos ao aquecimento global

DECLARAÇÃO

Declaro que este relatório é integralmente da minha autoria, estando devidamente referenciadas as fontes e obras consultadas, bem como identificadas de modo claro as citações dessas obras. Não contém, por isso, qualquer tipo de plágio quer de textos publicados, qualquer que seja o meio dessa publicação, incluindo meios eletrónicos, quer de trabalhos académicos.

Universidade de Aveiro Departamento de Biologia
Ano 2019

Carla Patrícia da Silva Leite

Toxic impacts of titanium dioxide nanoparticles in *Mytilus galloprovincialis* exposed to warming conditions

Impactos tóxicos de nanopartículas de dioxido de titânio em *Mytilus galloprovincialis* expostos ao aquecimento global

Dissertação apresentada à Universidade de Aveiro para cumprimento dos requisitos necessários à obtenção do grau de Mestre em Toxicologia e Ecotoxicologia, realizada sob a orientação científica da Doutora Rosa de Fátima Lopes de Freitas, investigadora auxiliar do Departamento de Biologia da Universidade de Aveiro e da professora Doutora Maria Eduarda da Cunha Pereira, professora associada do Departamento de Química da Universidade de Aveiro

o júri

Presidente

Doutora Isabel Maria Cunha Antunes Lopes
Investigadora principal do centro de estudos do ambiente e do mar (CESAM) da Universidade de Aveiro

Doutora Montserrat Solé
Investigadora principal do Instituto de Ciências Marinhas do Conselho Superior de Investigações Científicas (ICM-CSIC) em Barcelona, Espanha.

Doutora Rosa de Fátima Lopes de Freitas
Investigadora pós-doutorada e professora auxiliar do Departamento de Biologia e Centro de Estudos do Ambiente e do Mar (CESAM) da Universidade de Aveiro

agradecimentos

Às minhas orientadoras, Doutora Rosa Freitas e professora Doutora Maria Eduarda Pereira, pelo apoio prestado para a realização deste trabalho, por toda a disponibilidade e paciência e pela oportunidade de trabalhar com as suas excelentes equipas de investigação. À Doutora Rosa Freitas pela oportunidade de aprender novos métodos noutro País.

Ao Rui Monteiro por toda a ajuda no planeamento e execução do ensaio experimental e pelos esclarecimentos das minhas várias dúvidas em relação à parte química. À Francesca pela ajuda prestada na realização dos parâmetros bioquímicos e juntamente com os seus pais pela ajuda e disponibilidade da sua casa quando estive em Nápoles. Aos restantes colegas do laboratório da Biologia e da Química pelo apoio, ajuda e motivação prestada. Ao professor Gianluca Polese e à Tania pelo ensinamento e por toda a ajuda em Nápoles.

Ao Marcelo pela motivação, paciência, companhia, carinho e apoio. Aos restantes amigos de Ciências do Mar, Leninha, João, Alexandre e Miguel que sempre estiveram presentes quando precisei. À Cláudia pelos momentos de descontração que me fizeram desanuviar.

À minha mãe pelo esforço durante todos estes anos para que eu conseguisse continuar a estudar e ter um futuro melhor, pelo seu apoio incondicional quando mais precisei e pela sua compreensão quando não estava muito bem disposta.

palavras-chave

Mexilhões; rutílio; anatase; alterações climáticas; parâmetros bioquímicos; histopatologia.

resumo

As nanopartículas de dióxido de titânio (NPs de TiO_2) têm sido amplamente utilizadas em várias aplicações industriais e produtos de consumo. Devido à sua grande produção e uso, acabam por entrar nos ambientes aquáticos. Uma vez no ambiente aquático, as NPs de TiO_2 podem interagir com os organismos e induzir efeitos tóxicos. Além da contaminação, os organismos também estão expostos a alterações climáticas, responsáveis por um aumento gradual da temperatura nos oceanos, que pode causar danos fisiológicos e bioquímicos nos organismos aquáticos e maior sensibilidade a poluentes. Além disso, já foi reportado que o aquecimento pode alterar as propriedades e a toxicidade dos poluentes. Como as formas mais comuns das NPs de TiO_2 são o rutílio e a anatase, o presente estudo avaliou os efeitos destas duas formas em *Mytilus galloprovincialis* à temperatura controlo e os efeitos das NPs de rutílio sob condições de aquecimento global. Para isto, os mexilhões foram distribuídos em duas salas climáticas para manter os organismos em duas temperaturas diferentes: 18 ± 1 e 22 ± 1 °C. As concentrações testadas de NPs de rutílio e anatase a 18 °C e de rutílio a 22 ºC foram 0 µg/L; 5 µg/L; 50 µg /L; e 100 µg/L. A exposição durou 28 dias e no final foram avaliadas as concentrações de Ti no tecido dos mexilhões, as alterações histopatológicas e os efeitos bioquímicos. Os resultados histopatológicos demonstraram que ambas as formas de TiO_2 induziram alterações nas brânquias e nas glândulas digestivas ao longo do aumento das concentrações de exposição, independentemente da temperatura. Os parâmetros bioquímicos mostraram que os mexilhões expostos a NPs de rutílio na temperatura controle mantiveram a capacidade metabólica (avaliada pela atividade da cadeia de transporte de eletrões, ETS), enquanto o metabolismo dos mexilhões expostos a NPs de rutílio a 22 °C aumentou quando expostos a 5 e 50 µg/L de Ti e os mexilhões expostos a NPs de anatase também aumentaram a capacidade metabólica. Os mexilhões expostos a NPs de rutílio à temperatura controlo aumentaram as defesas desintoxicantes que, devido às baixas concentrações testadas, foram suficientes para evitar danos celulares. Por outro lado, os mexilhões expostos a NPs de anatase sofreram danos celulares, apesar do aumento das defesas antioxidantes, o que pode estar relacionado com a maior atividade da cadeia de transporte de eletrões. Além disso, os mexilhões expostos a NPs de rutílio sob temperaturas mais elevadas ativaram as defesas antioxidantes, porém ainda ocorreram danos celulares nessas condições. No geral, este estudo mostrou que as NPs de rutílio e anatase são tóxicas para *M. galloprovincialis*, com maior stress oxidativo exercido pela anatase e que o aumento da temperatura pode aumentar significativamente a sensibilidade de bivalves para as NPs de rutílio, demonstrando impactos tóxicos mais elevados em mexilhões expostos a NPs de rutílio sob condições de aquecimentom global.

keywords

Mussels; rutile; anatase; climate changes; biochemical parameters; histopathology.

abstract

Titanium dioxide nanoparticles (TiO_2 NPs) have been widely used in various industrial applications and consumer products. Due to their large production and use, they will eventually enter into aquatic environment. Once in the aquatic environment TiO_2 NPs may interact with the organisms and induce toxic effects. Beside contamination, organisms are also exposed to climate change, responsible for a gradual increase in the ocean temperature, which can cause physiological and biochemical impairments in aquatic organisms as well as increased the sensibility of organisms to pollutants. Furthermore, it is already reported that warming may change the properties and toxicity of pollutants. Since the most common forms of TiO_2 NPs are rutile and anatase, the present study evaluated the effects of these two forms in *Mytilus galloprovincialis* at control temperature and the effects of rutile NPs under warming conditions. For this, mussels were distributed into two climatic rooms to maintain organisms at two different temperatures: 18±1 and 22±1 °C. The tested concentrations of rutile and anatase NPs at 18 °C and of rutile ate 22 °C were 0 µg/L; 5 µg/L; 50 µg/L; and 100 µg/L. The experimental exposure lasted 28 days and at the end Ti concentrations, histopathological alterations and biochemical effects were evaluated. Histopathological results demonstrated that both forms of TiO_2 induced alterations on gills and digestive glands along the increasing exposure concentrations regardless the temperature. Biochemical markers showed that mussels exposed to rutile NPs at control temperature maintained their metabolic capacity (assessed by the activity of the electron transport system, ETS), while the metabolism of mussels exposed rutile NPs under higher temperature increased at 5 and 50 µg/L of Ti and in mussels exposed to anatase NPs the metabolic capacity was increased. Mussels exposed to rutile NPs at control temperature increased their detoxificant defenses which, due to the low tested concentrations, were sufficient to avoid cellular damage. On the other hand, mussels exposed to anatase NPs suffered cellular damages despite the increased in antioxidant defenses which may be related to higher activity of the electron transport system. Also, mussels exposed rutile NPs under higher temperature activated the antioxidant defenses, however still cellular damage occurred under these conditions. Overall, this study showed that rutile and anatase NPs were toxic to *M. galloprovincialis*, with higher oxidative stress exerted by anatase form and that temperature rise may significantly increase the sensitivity of bivalves towards rutile NPs, revealing higher toxic impacts in mussels exposed to rutile NPs under warming conditions.

Contents

List of figures

List of tables

Chapter 1

Introduction

1. INTRODUCTION

1.1. Marine coastal systems: major stressors

Marine coastal systems are among the most productive ecosystems in the world (Dayton *et al*., 2005). These dynamic areas are usually defined as the interface between land and sea and for this reason are subjected to natural and anthropogenic changes (FAO, 1998). Coastal systems such as estuaries and lagoons are water bodies that connect terrestrial, freshwater and marine systems (Dame, 2008) and because of that they are expected to be the ultimate sink for contaminants (Islam and Tanaka, 2004; Dauvin and Ruellet, 2009). In fact, coastal systems have been exposed to a variety of contaminants including "classical" (like metals and organic) (Huang *et al*., 2014; Artifon *et al*., 2019; Gao *et al*., 2019) and emerging contaminants (ECs) such as rare-earth elements (REEs) (Elderfield *et al*., 1990; Casse *et al*., 2019), nanoparticles (NPs) (Baalousha *et al*., 2011; Gondikas *et al*., 2014) or pharmaceuticals (Desbiolles *et al*., 2018; Fernández-Rubio *et al*., 2019). Besides contamination, marine coastal systems are increasingly subject to climate change related factors, including warming and acidification (Angel, 1991; Murawski, 1993; Caldeira and Wickett, 2003; Orr *et al*., 2005).

1.1.1. Emerging contaminants

In the last few decades, population growth and the expansion of the chemical, agrochemical, cosmetic and pharmaceutical industries led to the synthesis and increased manufacture and usage of innumerous compounds known as emerging contaminants (ECs) (Starling *et al*., 2019). These substances are not commonly monitored in the environment because they have only recently being considered potentially toxic (Rodriguez-Narvaez *et al*., 2017; Martín-Pozo *et al*., 2019). Emerging contaminants are a heterogeneous group of compounds that includes REEs, pharmaceuticals, personal care products, flame retardants and endocrine disrupting chemicals (Martín-Pozo *et al*., 2019).

Among anthropogenic ECs are also manufactured NPs that include carbonaceous nanomaterials, metal oxides, semiconductor materials (quantum dots (QDs)), zero-valent metals (iron (Fe), silver (Ag), and gold (Au)) and nanopolymers (Fadeel and Garcia-Bennett, 2010; Măruţescu *et al*., 2019). Nanoparticles can be in an unbound state, as an aggregate (hard bonds between particles) or as an agglomerate (weak bonds between particles) (Jiang

et al., 2009; Maskos and Stauber, 2016) and at least one dimension must have 1–100 nm to be considered as NPs (Hood, 2004; The European Commission, 2011; ISO, 2015). Nanoparticles exhibit different properties than their bulk counterparts as they have a very large surface area-to-volume ratio (D'Agata *et al*., 2014; Măruţescu *et al*., 2019) allowing the production of new technologies with novel or improved specificities and applications (Măruţescu *et al*., 2019). These particles can be produced by chemical (''bottom-up methods''), physical (''top-down methods'') and biological (green methods) synthesis (Yazdi *et al*., 2016) and in various shapes such as rod (Mnasri *et al*., 2016), cube (Zhou *et al*., 2019), sphere (Zhang and Zheng, 2019) and nanoplate (Im *et al*., 2019). It is difficult to characterize NPs due to their tendency to aggregate or agglomerate when there is a change in surrounding environment and also due to their small size which is usually below the wavelength limit of direct optical detection via light microscopy (Maskos and Stauber, 2016). Nanoparticles have received considerable attention in physics, chemistry, biology, and technology because their use is more efficiency compared to bulk particles due to their unique characteristics (mechanical, physical, catalytic, optical, and electrical conductivity) and their small dimensions (Hosseinzadeh *et al*., 2016; Măruţescu *et al*., 2019). For these reasons their applications in various industries have rapidly expanded (Banerjee *et al*., 2017; Cai *et al*., 2017; Dey *et al*., 2017; Gao *et al*., 2017; Priyadarshini and Pradhan, 2017; Liu, 2006).

The increasing production of several NPs caused its increase in the environment and, therefore, doubts concerning nanoparticle effects on the environment and human health has rised (Zanjani *et al*., 2018), although these materials can be used in biological applications, such as water treatment (Coppola *et al*., 2019; Masunga *et al*., 2019) in order to improve aquatic environment health (Zanjani *et al*., 2018). However, several studies have shown that NPs induced adverse effects to marine and freshwater organisms. Gambardella *et al*. (2015) shown that silica NPs (SiO_2) induced anomalies in sea urchin offspring and neurotoxicity in sea urchin (*Paracentrotus lividus*). Ale *et al*. (2019) demonstrated that Ag NPs cause cellular damage and Ag accumulation in the mussel *Mytilus galloprovincialis*. Also, Barreto *et al*. (2019) shown that the fish species *Sparus aurata* had decreased their swimming performance and increased oxidative damage in gills and liver when exposed to Au NPs. According to De Marchi *et al*. (2018; 2019 a,b) carbon nanotubes induce oxidative damage and neurotoxicity

in clams (*Ruditapes philippinarum)* and polychaetes (*Nereis diversicolor, Diopatra neapolitana*).

Titanium dioxide nanoparticles as emerging contaminants

Titanium dioxide (TiO_2) displays properties including a bright white color, ability to block UV light, long-term stability, antimicrobial activity, hydrophilicity as well as a relatively low cost (Hoffmann *et al*., 1995; Su *et al*., 2006; Wang *et al*., 2009; Cho *et al*., 2013). TiO_2 NPs are metal oxide nanoparticles which have been extensively used in various industrial applications and consumer products including personal care products as sunscreen, creams and toothpastes (Wahie *et al*., 2007; Johnson *et al*., 2011; Lu *et al*., 2015; de la Calle *et al*., 2017; Sureda *et al*., 2018), as pigment in paints, plastics, and paper (Winkler, 2003; Kaegi *et al*., 2008; Amorim *et al*., 2018); as well as in food storage acting as an antibacterial agent (Cui *et al*., 2016; Zhu *et al*., 2018). For this reason it is estimated that the worldwide TiO_2 NPs will reach 2.5 million tons by 2025 (Mezni *et al*., 2018).

There are mainly three crystalline forms of TiO_2, namely anatase (tetragonal), rutile (tetragonal), and brookite (orthorhombic) (Fig. 1) (Cho *et al*., 2013; Iswarya, 2018). Among these, rutile and anatase are the most common forms of TiO_2 due to their properties such as high photocatalysis, refractive index and transparency to visible light and high UV absorption (Braydich-Stolle *et al*., 2009; Iswarya, 2018). Brookite has been rarely used and studied so far, due to its scarcity in the environment (Allen *et al*., 2010) and difficulties in preparing significant amounts of good quality material (Gong and Selloni, 2007). Both rutile and anatase are widely employed in consumer products like toothpaste, sunscreens, food, paints, plastics, paper, and biomedical devices (Wang *et al*., 2007; Yang *et al*., 2009; Middlemas *et al*., 2013; de la Calle *et al*., 2017; Barbosa *et al*., 2018; Leong and Oh, 2018; Dorier *et al*., 2019). Furthermore, they are also used in environmental oriented applications including water treatment (Yuzer *et al*., 2016; Abdel-Maksoud *et al*., 2018), air purification (Paz, 2010) and soil remediation (Yang and Xing, 2009). Rutile is commonly used in optical elements, since it has one of the highest refractive indices at visible wavelengths of any known crystal and also exhibits a particularly large birefringence and high dispersion (Iswarya *et al*., 2016, 2018). It is also used as a dielectric material in ceramics (Amtout and Leonelli, 1995; Wang *et al*., 2019). Anatase is applied as a catalytic support for the production of nanotubes and nanoribbons (Mogilevsky *et al*., 2008) and used in

photovoltaics (Grätzel, 2001). Due to their worldwide production and usage, both forms of TiO_2 NPs are released in enormous quantities in urban and industrial sewage and, consequently, reach aquatic environments (Colvin, 2003; Lecoanet and Wiesner, 2004; Guzman *et al*., 2006; Nowack and Bucheli, 2007; Gottschalk and Nowack, 2011; Nowack *et al*., 2012).

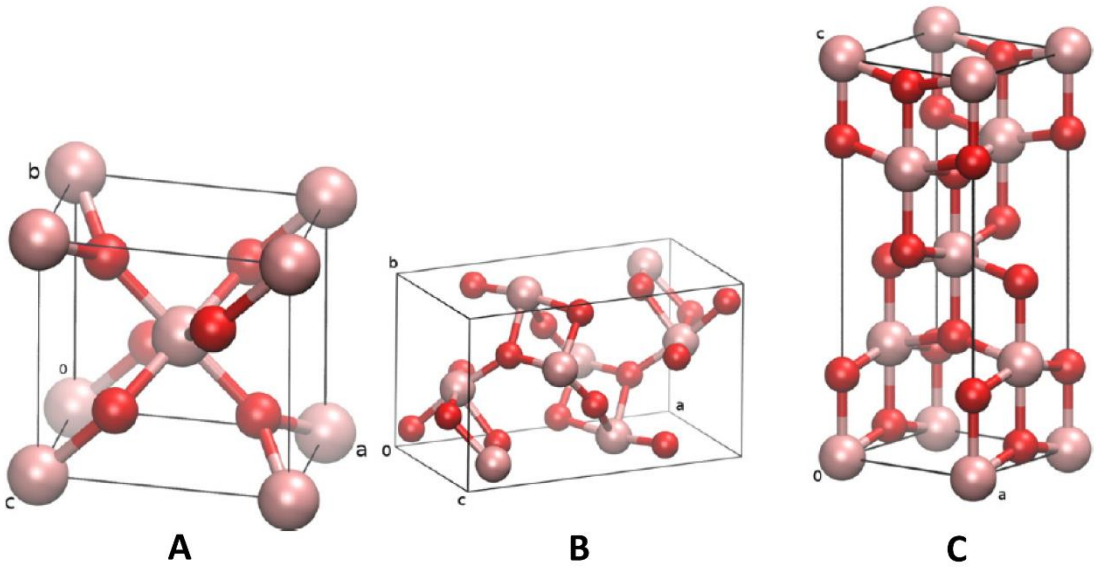

Fig. 1 Crystal structures of TiO_2. A: rutile; B: brookite; and C: anatase (Moellmann et al., 2012).

Dissolved Ti is usually present at very low concentrations in marine systems with concentrations ranging between 0.01 and 5.5 µg/L (Yan *et al*., 1991; Yokoi *et al*., 1991; Skrabal, 2006). With the increased use of TiO_2 NPs and low capacity of wastewater treatment plants (WWTPs) to eliminate these NPs (Shi *et al*., 2016), Ti concentration has been increasing in aquatic systems (Batley *et al*., 2013; Gondikas *et al*., 2014). TiO_2 NPs are found in domestic sewage, wastewater, industrial effluents and surface runoff from the paints on building facades (Kaegi *et al*., 2008; Kiser *et al*., 2009; Brar *et al*., 2010; Weir *et al*., 2012). Kiser *et al*. (2009) demonstrated that raw sewage contains 100–3000 µg/L of Ti and after the removal at WWTPs the resulting effluent contains only 5 – 15 µg/L of Ti. Shi *et al*. (2016) detected concentrations ranging between 52 and 86 µg/L of Ti in the Xiaohe River (China). Also, Gondikas *et al*. (2014) quantified TiO_2 at the Old Danube Recreational Lake (Vienna) with concentrations between 1.7 – 27.1 µg/L of Ti.

Once in the aquatic environment TiO_2 NPs may interact with the organisms and induce toxic effects (Iswarya *et al*., 2019). Previous studies demonstrated that these NPs caused severe toxicity towards aquatic organisms. Monteiro *et al*. (2019 a,b) demonstrated that the estuarine mussel *M. galloprovincialis* is affected by TiO_2, with alterations of organism's metabolic capacity, oxidative damage and defense mechanisms. Barmo *et al*. (2013) showed that TiO_2 NPs affected mussels immune system and digestive gland function. Other studies showed the impacts of different forms of TiO_2 NPs. Braydich-Stolle *et al*. (2009) observed that rutile NPs were capable of initiating apoptosis, while anatase NPs triggered cell necrosis in mouse keratinocytes. Also, Iswarya *et al*. (2015) demonstrated that rutile and anatase NPs caused damage in different parts of the green algae *Chlorella sp*. with rutile NPs causing damages in chloroplast and internal organelles and anatase NPs originating nucleus and cell membrane damages. Nevertheless, information on the impacts of these two forms of TiO_2 NPs on aquatic species, and especially marine and estuarine organisms, is still limited. Therefore, it is of upmost relevance to understand the impacts of rutile and anatase NPs on aquatic environments, namely on their inhabiting organisms.

1.1.2. Impact of climate changes: warming

Since the beginning of the industrial revolution, atmospheric concentration of carbon dioxide (CO_2) has been increasing, reaching for the first time levels above 400 ppm (IPCC, 2014). This increased of atmospheric CO_2 is related with the cumulative emissions of anthropogenic greenhouse gases that besides CO_2, release methane (CH_4) and nitrous oxide (N_2O) (IPCC, 2014). Furthermore, unless CO_2 emissions are reduced as a result of policy actions, it is expected that CO_2 in the atmosphere may reach up to ~1000 ppm until the end of the century (Pörtner *et al*., 2014). The oceans act as CO_2 sinks because nearly 30% of the atmospheric CO_2 is absorbed by the oceans. The continuous CO_2 uptake by the oceans result in seawater chemistry alterations, including the predicted decrease of seawater pH up to 0.42 units by the year of 2100 (IPCC, 2014). However, besides changes in seawater properties, the increase of CO_2 in combination with other "greenhouse" gases has triggered a continuous rise in mean ocean temperature (nowadays increased by 0.76 °C from pre-industrial levels), with predictions indicating that temperature may rise up to 4 °C in the sea surface by the end of the century (Collins *et al*., 2013; IPCC, 2014). Additionally, models studying global

climate patterns have predicted that the frequency and extent of extreme weather events, including drought periods, will increase at a global scale (Pörtner *et al*., 2014).

The increase in temperature that exceeds the organism's thermal tolerance range may cause deleterious effects in the organisms (IPCC, 2007; Hofmann and Todgham, 2010). Recent studies already demonstrated that seawater warming is expected to induce major shifts in species spatial distribution and abundance (Clarke, 2003; Hoffmann *et al*., 2003; Harley *et al*., 2006). Organisms exposed to warming conditions showed also physiological perturbations, such as growth and reproductive patterns (Pörtner *et al*., 2007; Pörtner and Knust, 2007; Santos *et al*., 2011; Boukadida *et al*., 2016), as well as biochemical alterations (Verlecar *et al*., 2007; Freitas *et al*., 2017; Nardi *et al*., 2017; Velez *et al*., 2017; Andrade *et al*., 2019). Warming is known to induce the production of reactive oxygen species (ROS) in cells and activate the mechanisms of defense, such as superoxide dismutase (SOD), catalase (CAT), glutathione peroxidase (GPx), glutathione reductase (GRed) and glutathione S-transferases (GSTs) (Verlecar *et al*., 2007). Warming may influence the respiratory and aerobic capacity as well as metabolic rate of aquatic organisms (Pörtner *et al*., 2005; Jansen *et al*., 2009; Pörtner, 2010; Velez *et al*., 2017). Besides the direct effects of temperature rise in aquatic organisms, increased temperature may also change organism's responses when exposed to pollutants, through alterations in biochemical and physiological processes as well as pollutants bioavailability and toxicity (Banni *et al*., 2014; Izagirre *et al*., 2014; Manciocco *et al*., 2014; Nardi *et al*., 2017; Coppola *et al*., 2018). It is known that warming may increase the sensibility of organisms to pollutants, for example Coppola *et al*. (2017; 2018) shown that *M. galloprovincialis* increased the sensitive to mercury (Hg) and arsenic (As) respectively, when exposed to increased temperature. Sokolova (2004) demonstrated that warming increased the sensitivity of *Crassostrea virginica* to cadmium. Also, it was already reported that warming influences the accumulation of the pollutants, for example Mubiana and Blust (2007) showed a higher accumulation of cadmium and lead in *M. edulis* under warming conditions, and Coppola *et al*. (2018) demonstrated that *M. galloprovincialis* increased the accumulation of As when exposed to increased temperature.

1.2. *Mytilus galloprovincialis* as bioindicator species

A biological indicator is an organism (or a community of organisms) which represents the impact of environmental pollutants on a habitat, community or ecosystem

(Markert *et al*., 2003). Bioindicators must show wide geographical distribution, display a sessile lifestyle or a restricted territory, be easily collected and be well understood in biochemical, physiological and biological terms (Lower and Kendall, 1990). Mussels are globally used as bioindicators of pollution in coastal environments, since the monitoring programme known as 'mussel watch' (Kimbrough *et al*., 2008). In fact, mussels have wide distribution, dominate coastal and estuarine communities, accumulate and respond to many pollutants, do not show a prolonged handling stress, and many aspects of their biology and responses to intrinsic and extrinsic factors are well understood (Livingstone *et al*., 1989).

M. galloprovincialis (Lamark, 1819) (Fig. 2), also known as Mediterranean mussel, is widely distributed from warm temperate to subpolar areas (Grant and Cherry, 1985), being present in intertidal zones to 40 m deep attached to rocks and piers, within sheltered harbours, estuaries and on rocky shores (FAO, 2019). This species is native to the Mediterranean coasts but has colonised several regions around the globe, such as South Africa, Hong Kong, Japan, Korea, Australia, Hawaii, Mexico, California, Washington and the west coast of Canada, and it is establishing as an invasive species (Branch and Steffani, 2004). This species plays a significant ecologic and economic role in marine ecosystems, being commonly used as bioindicator (Wang *et al*., 1996; Viarengo *et al*., 2007; Banni *et al*., 2014). A variety of studies in laboratory conditions worked with this species exposed to a combination of pollutants and higher temperature, such as studies conducted by Coppola *et al*. (2018), Andrade *et al*. (2019), Banni *et al*. (2014) and Freitas *et al*. (2019). This species is also used in biomonitoring programs to evaluate the distributions and biological effects of pollutants (Catsiki and Florou, 2006; Benali *et al*., 2017; Azizi *et al*., 2018).

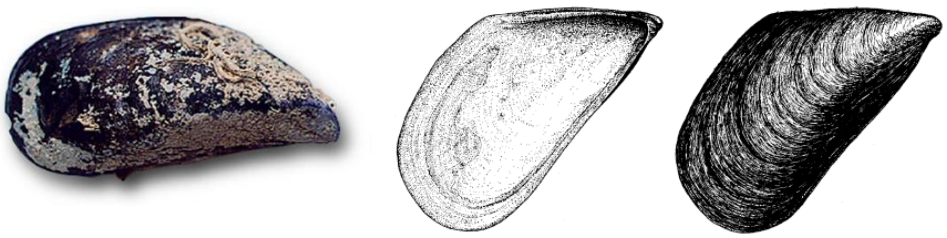

Fig. 2 Mytilus galloprovincialis (FAO, 2019).

1.3. Objectives

Several studies already revealed the impacts of TiO_2 NPs in *M. galloprovincialis* (Canesi *et al*., 2010; Canesi *et al*., 2012; Ciacci *et al*., 2012; Barmo *et al*., 2013; D'Agata *et al*., 2014; Mezni *et al*., 2018), but to my knowledge no information is available on the toxic effects of rutile and anatase forms on this mussel species. Furthermore, in most of the aquatic environments, especially coastal systems, both pollution and climate change related factors act in combination, and so it is important to understand how temperature may change the effects induced by TiO_2 NPs as well as the sensitivity of *M. galloprovincialis* to this pollutant. Therefore, the present study evaluated: i) the impacts induced by different concentrations of rutile and anatase NPs in *M. galloprovincialis*, by measuring histopathological and metabolic alterations as well as oxidative and neurotoxic status; ii) the impacts of different concentrations of rutile NPs induced in *M. galloprovincialis*, under actual and predicted warming conditions, to understand the effects of predicted temperature rise on the toxicity of rutile and sensitivity of mussels to this NP.

Chapter 2

Materials and Methods

2. MATERIALS AND METHODS

2.1. Rutile and Anatase characterization

In the present study two TiO_2 NPs of different morphology were tested: the rutile form acquired from Alfa Aesar, and the anatase form, acquired from Merck. The structural and microstructural characterization were performed by X-ray diffraction (XRD), and scanning electron microscopy (SEM) techniques, respectively (Table 2). The textural properties of the samples were achived by -196 °C N_2 adsorption-desorption isotherms. XRD data were collected with a Phillips X'Pert MPD diffractometer using Cu-Kα radiation. SEM images were acquired on a SEM-FEG Hitachi S4100 microscope operated at 15 kV. Nitrogen adsorption-desorption isotherms were recorded at -196 °C using a Gemini V 2.00 instrument model 2380. The samples were dehydrated overnight at 120 °C to an ultimate pressure of 1024 mbar and then cooled to room temperature prior to adsorption.

For particles characterization in the exposure medium, water samples (5 mL each) were collected from each aquarium immediately after medium contamination. The measurements of the particles was made by Dynamic Light Scattering (DLS) analysis.

2.2. Sampling area

M. galloprovincialis specimens were collected in September 2018 during low tide in the Ria de Aveiro (Fig. 3). Ria de Aveiro is a coastal lagoon located on the northwest coast of Portugal, with 10 km wide and 45 km long (Dias *et al*., 1999; Dias *et al*., 2000) and it is constituted by four main channels: S. Jacinto , Mira, Espinheiro and Ílhavo (Dias *et al*., 1999; Lopes *et al*., 2013). The average depth is about 1 m, except in navigation channels (15 m depth) (Dias *et al*., 1999; Lopes *et al*., 2013). This lagoon is separated from the Atlantic ocean through an artificial channel, and supplied with freshwater by Antua and Vouga rivers (Dias *et al*., 1999; Dias *et al*., 2000). Ria de Aveiro is considered one of the most important coastal system of Portugal, presenting several biotopes with biological importance, such as salt marshes (Sousa *et al*., 2017). Regarding the benthic community, the most abundant taxa found in Ria de Aveiro are annelids followed by bivalves (Quintino *et al*., 2012).

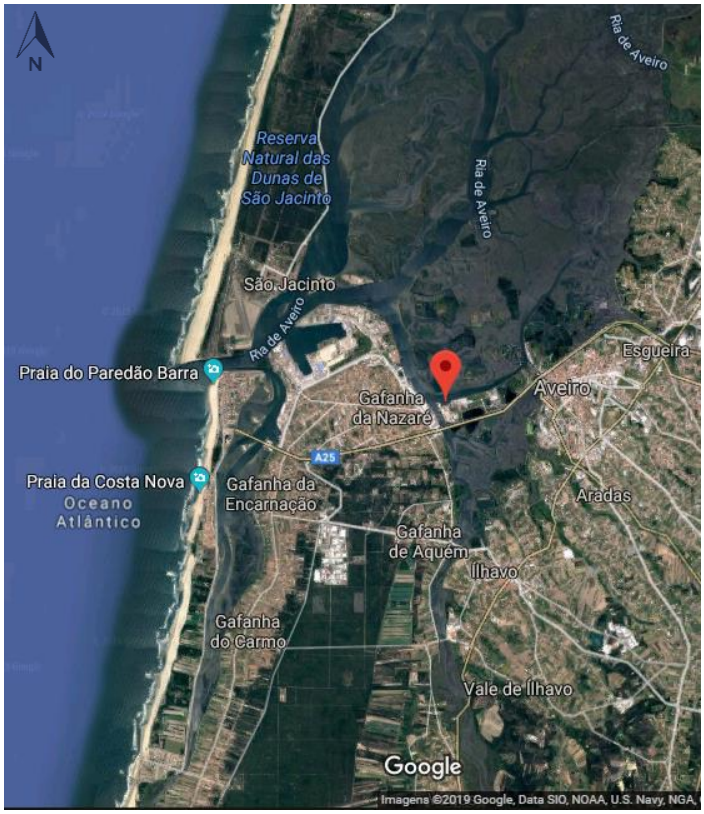

Fig. 3 Sampling area (Google Maps, 2019).

2.3. Experimental conditions

After sampling, mussels were transported to the laboratory, where they were maintained for two weeks in different aquaria for depuration and acclimation to laboratory conditions. During this period organisms were maintained in synthetic seawater (salinity 30 ± 1, temperature 18.0 ± 1.0 °C; pH 8.0 ± 0.1), prepared with reverse osmosis water with commercial salt (Tropic Marin® SEA SALT). Seawater was renewed every day for the first three days and every three days until the end of this period and mussels were fed with Algamac protein plus (150,000 cells/animal) three times per week.

During the experimental exposure (twenty-eight days), mussels were distributed into two climatic rooms to maintain organisms at two different temperatures: 18±1 (control) and 22±1 °C (control + 4 °C, resembling predicted warming conditions). Within each temperature mussels were divided into different aquaria, with the following gradient of rutile and anatase NPs concentration at 18 °C: CTL (control) 0 µg/L; C1) 5 µg/L; C2) 50 µg/L; and C3) 100 µg/L and the same gradient for rutile NPs at 22 °C. Per condition three replicates (3 aquaria of 3 L) were used with five mussels per aquaria. Fig. 4 demonstrates the experimental setup performed in this study.

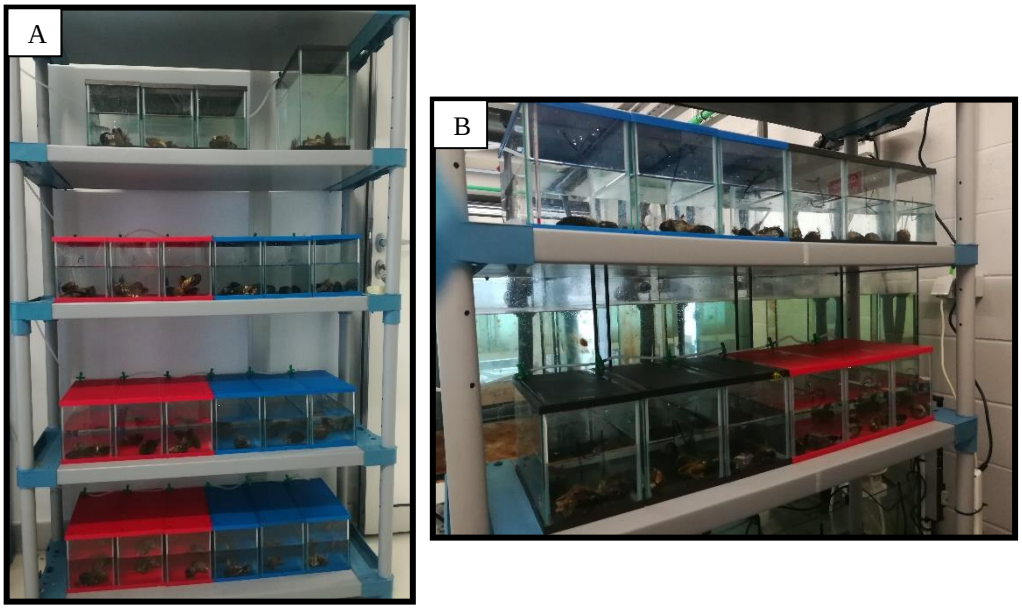

Fig. 4 Experimental setup of this study. A: Control room 18±1 °C; B: Warming room 22±1 °C.

The tested Ti concentrations were selected according to the values reported in previous works for pristine and contaminated aquatic systems (Kennedy *et al*., 1974; Yan *et al*., 1991; Yokoi *et al*., 1991; Skrabal, 2006; Kiser *et al*., 2009; Menard *et al*., 2011; Gondikas *et al*., 2014; Shi *et al*., 2016). For the exposure assay, TiO_2 NPs in a powder form were dispersed in ultrapure water using a bath sonicator to obtain stock solution of 60 and 600 mg/L of Ti. From these dispersions, appropriate contamination ones were prepared so that the intended contaminated levels in aquaria were achieved.

The control temperature (18 °C) was selected considering the average temperature measured at the bivalves sampling site. Salinity and pH conditions were the same as those used during acclimation and containers were continuously aerated, with a 12 light: 12 dark

photoperiod. Temperature (18±1 or 22±1 °C), pH (8.0± 0.1) and salinity (30 ± 1) were daily checked and adjusted if necessary. Mortality was also daily checked. During the entire experimental period organisms were fed with Algamac protein plus (150,000 cells/animal) three times a week. Seawater was renewed once a week after which Ti concentration was re-established. Immediately after the rutile and anatase NPs spiking into the water, samples of water were collected from each aquarium for further quantification and characterization of Ti, aiming to compare real and nominal concentration.

At the end of the exposure period, with the exception of one mussel per aquarium (three per condition) used for histopathological analyses, the remaining organisms were frozen with liquid nitrogen and stored at -80 °C. Three frozen mussels per aquarium (nine per condition) were homogenized with a mortar and a pestle under liquid nitrogen (Fig. 5). Each homogenized organism was divided into 0.5 g fresh weight (FW) aliquots for biomarkers analyses and the remaining tissue was used for Ti quantification.

Fig. 5 Homogenization of mussel's frozen tissue with liquid nitrogen.

2.4. Titanium quantification in water and mussel's samples

For the determination of Ti concentration in water, the samples were stirred and then sonicated for 10 min to ensure proper dispersion of the potentially present TiO_2 NPs. For the digestion 10 mL of reagent mixture (4 mL of sample, 0.5 mL HNO_3, 0.1 mL HF and 5.4 mL of H_2O) were added to Teflon vessels (Fig. 6A). Samples were digested in a CEM MARS 5 (Fig. 6B) by increasing temperature to 180 °C in 10 min, which was then maintained for 10 min. After cooling down, the resultant 10 mL of digest was promptly analyzed by inductively coupled plasma optical emission spectrometry (ICP-OES) (Fig. 7A). Quality control was

kept by blank analysis (0.5 mL HNO_3, 0.1 mL HF and 9.4 mL of H_2O), which was below quantification limit (2 µg/L).

For the determination of Ti in *M. galloprovincialis* soft tissues, freeze-dried samples of mussel's (0.2 g) were homogenized and weighted into a Teflon vessel (Fig. 6A) to which 1 mL HNO_3 65% (v/v), 1 mL HF (40%) and 2 mL H_2O_2 (30%) were added. Samples were digested in a CEM MARS 5 (Fig. 6B) using the same procedure as described for water samples. After cooling, samples were transferred into 25 mL polyethylene vessels, the remaining volume made up with ultrapure water and analyzed by ICP-OES (Fig. 7A). The quality control was assured by running procedural blanks (reaction vessels with only reagent mixture), certified reference material BCR-060 (Aquatic Plant, Lagarosiphon major) and duplicates. Blanks were always below the quantification limits for Ti (2 µg/L and 0.25 mg/kg). The coefficient of variation of samples duplicates varied from 1 to 22% and mean percentage of recovery in BCR-60 was 79 ± 2 %.

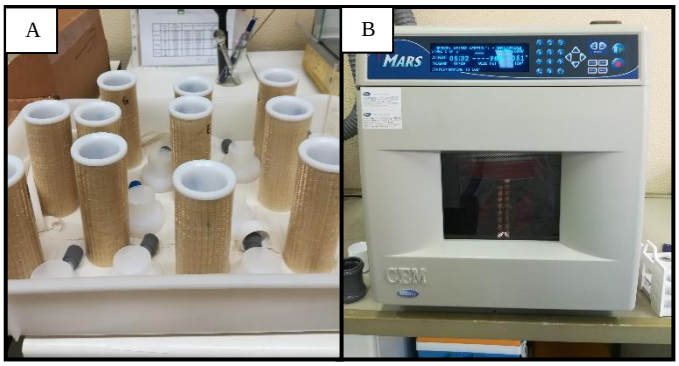

Fig. 6 A: Teflon vessels; B: CEM MARS 5 microwave.

2.4.1. Inductively coupled plasma optical emission spectrometry

Total Ti concentrations in water samples and *M. galloprovincialis* soft tissues were determined by ICP-OES (*Jobin Yvon Activa M.*) (Fig. 7A), after microwave-assisted acid digestion. In this equipment the samples are normally analyzed in liquid form. The liquid sample is aspirated into the nebulizer chamber, where the liquid is converted into an aerosol. Then the aerosol is transported to the plasma where it is vaporized, desolvated and atomized, as well as excited and/or ionized by the plasma. The excited atoms and ions when return of an electron from a higher (excited) state of energy to a state of fundamental energy emit their characteristic radiation at different wavelengths. This radiation is detected and turned into

electronic signals that are converted into concentration of the different elements in the samples (Fig. 7B) (Boss and Fredeen, 2004).

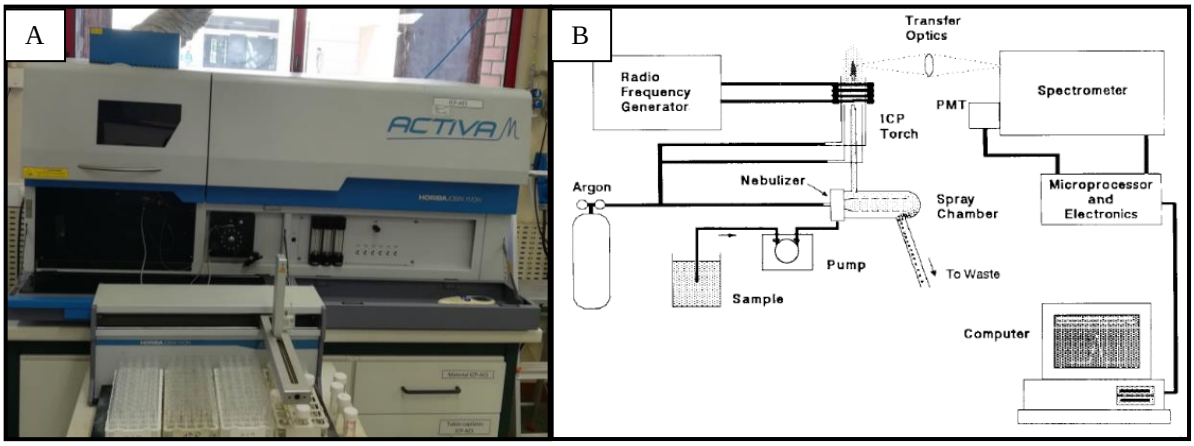

Fig. 7 A: ICP-OES used for the quantification of Ti in water and mussel's samples; B: Representation of the layout of a typical ICP-OES instrument (in: Boss and Fredeen, 2004).

2.5. Histopathological measurements

Histopathological changes were identified in gills and digestive glands of mussels, from each condition. The assessment of histopathological alterations is an important method to evaluate the impacts of pollutants in bivalves (Calabrese *et al*., 1984; Bignell *et al*., 2011; Cuevas *et al*., 2015). Gills are one of the major target organs for contaminants because they are in direct contact with the surrounding environment, playing an important role in respiration (Evans, 1987; Au, 2004; Rajalakshmi and Mohandas, 2005). The digestive gland of bivalves is the main organ for xenobiotic biotransformation, a mechanism of immune defense and homeostatic regulation (Moore and Allen, 2002; Livingstone *et al*., 2006), being also extensively used for toxicity assessment (Bignell *et al*., 2008; Marigómez *et al*., 2013).

After the exposure period, one mussel per aquarium was fixed in Bouin's solution (5% of acetic acid, 9% of formaldehyde, 0.9% of picric acid) for 24 h at 4 °C. Subsequently, samples were kept in 70-75% ethanol for one month, replacing the ethanol daily until the total removal of the fixative (Fig. 8A). After this, a transverse histological sample of approximately 1 cm thickness of the anterior part of each organism was excised and samples were dehydrated in ethanol (75% for 15 min, 85% for 15 min, 95% for 15 min twice and 100% for 15 min twice) and placed in xylene for 30 min twice. Afterwards, samples were immersed in paraffin (58 °C) in a vacuum stove overnight (Fig. 8B). After this step, paraffin

was removed and samples were once again embedded in new paraffin for 45 min. This procedure was repeated twice. At last, samples were placed in paper molds filled with paraffin over night to solidify (Fig. 8C) (D'Aniello *et al*., 2016, Polese *et al*., 2016; Zupo *et al*., 2019).

Fig. 8 A: Mussels in ethanol 70%; B: Vacuum stove with the samples embedded in paraffin; C: Paper molds with samples and paraffin.

Histological sections of 7 µm were cut with a microtome (Fig. 9A) and placed on slides covered with glycerin/albumin. For histological staining, the samples were placed in xylene for 30 min twice, rehydrated through a descending series of alcohol (100% twice, 95% twice, 85%, 75% each one during 5 min) and distilled water for 5 min to remove the paraffin. Then, half of the sections were stained with hematoxylin for 5 min (to assess tissue health), followed by washing in tap water (5 min) and distilled water (rapid passage). After this, samples were dehydrated by ascending series of alcohol and xylene and subsequently held with permount for their preservation (Fig. 9B) (Polese *et al*., 2016; Zupo *et al*., 2019). The other half of sections were stained with toluidine blue (0.2% of toluidine blue in sodium acetate buffer) for 30 min (to assess the abundance of hemocytes), followed by a rapid passage in sodium acetate buffer (pH 4.2), 5 min in molybdate (5%), various passages in water and a rapid passage in 100% ethanol, 10 min in xylene twice and held with permount (Gabe, 1968).

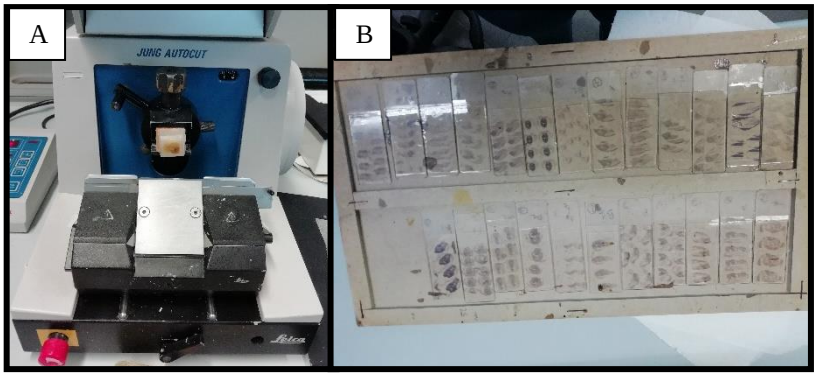

Fig. 9 A: Microtome with one sample; B: Slides of samples stained with hematoxylin and held with permount.

The individual histopathological condition index (I_h) was estimated for gills ($I_{h\,G}$) and digestive glands ($I_{h\,DG}$), based on Bernet *et al*. (1999) and modifications performed by Costa *et al*. (2013). The I_h was calculated following the concepts of the differential biological significance of each surveyed alteration (weight) and its degree of dissemination (score) and was calculated following the formula:

$$I_h = \frac{\sum_1^j w_j a_{jh}}{\sum_1^j M_j}$$

where I_h is the histophatological index for the individual h; w_j the weight of the j_{th} histopathological alteration; a_{jh} the score attributed to the h_{th} individual for the j_{th} alteration and M_j is the maximum attributable value for the j_{th} alteration. The condition weights proposed were based on Costa *et al*. (2013) and ranges between 1 (minimum severity) and 3 (maximum severity) while the score ranges between 0 (none) and 6 (diffuse). Weight for the histopathological alteration considered in this study are reported in Table 1.

Table 1 Weight for the histopathological alteration (Costa et al., 2013).

Tissue	Histopathological alteration	Weight (w)
Gills	Lipofuscin aggregates	1
	Loss of cilia	2
	Enlarged central vessel	1
	Heamocyte infiltration	1
Digestive tubules	Lipofuscin aggregates	1
	Heamocyte infiltration	1
	Atrophy	2
	Necrosis	3

2.6. Biochemical parameters

With the purpose to evaluate the biochemical alterations induced in mussels after exposure to rutile and anatase NPs and the combinations of rutile NPs and warming, biomarkers related to metabolic capacity (electron transport system (ETS) activity), energy reserves (content of glycogen (GLY) and total protein (PROT)), oxidative stress (activity of antioxidant and biotransformation enzymes (superoxide dismutase (SOD); catalase (CAT); glutathione peroxidase (GPx); glutathione reductase (GRed); glutathione S-transferases (GSTs)); levels of lipid peroxidation (LPO) and protein carbonylation (PC)); and neurotoxicity (acetylcholinesterase (AChE) activity) were assessed.

The ETS activity has been used to obtain an indication of organisms' metabolic status (De Coen and Janssen, 1997). When organisms are exposed to stressful conditions, they may increase metabolism, in this case ETS, in mitochondria, for the maintenance of homeostasis, survival and reproduction (Gagné *et al*., 2006), or may decrease or maintain the ETS activity by activating behavioral adaptations as valves closure (Gosling, 2003). Usually along with the decrease of ETS activity organisms are able to preserve their energy reserves (GLY and PROT) as a defense mechanism. Organisms may also decrease the content in GLY and PROT resulting from the expenditure of their energy reserves to fuel up defense mechanisms.

Under stressful conditions organisms, including mussels, normally increase the production of reactive oxygen species (ROS) and in order to avoid cellular damages they activate their antioxidant defenses, including the activity of the antioxidant enzymes (SOD, CAT, GPx and GRed) (Regoli and Giuliani, 2014). Along with the activation of antioxidant

defenses, organisms exposed to stress conditions also activate biotransformation enzymes, namely glutathione S-transferases (GSTs) (Townsend and Tew, 2003; Sturve *et al*., 2008).

Lipid peroxidation (LPO) has been generally used as a biomarker for cell damage (Moreira *et al*., 2016) because when the defense mechanisms are insufficient to protect the cells, the lipids of cell membranes are attacked by ROS, promoting an autocatalytic oxidation process (Almeida *et al*., 2007). Also, if defense mechanisms fail, the excess of ROS may promote a protein oxidation known as protein carbonylation (PC) (Suzuki *et al*., 2010).

The activity of AChE is used as a biomarker of exposure to neurotoxic compounds in aquatic organisms. This enzyme is important to the functioning of the neuro–muscular system and it is responsible for the degradation of the neural transmitter acetylcholine to choline in cholinergic synapses and neuromuscular junctions (Matozzo *et al*., 2005).

To guarantee the validity of the results, the determination of the biochemical parameters was done in duplicate. For each biomarker, the extraction was performed with specific buffers using a proportion of 1:2 (w/v) with the homogenized tissue. For GLY, PROT, SOD, CAT, GPx, GRed, GSTs, PC and AChE the supernatants were extracted in potassium phosphate buffer (50 mmol/L potassium dihydrogen phosphate; 50 mmol/L potassium phosphate dibasic; 1 mmol/L ethylenediamine tetraacetic acid disodium salt dihydrate (EDTA); 1% (v/v) Triton X-100; 1% (w/v) polyvinylpyrrolidone (PVP); 1 mmol/L dithiothreitol (DTT); pH 7.0). For ETS supernatants were extracted in 0.1 mol/L Tris- HCl buffer (pH 8.5, 15% (w/v) PVP, 153 μmol/L magnesium sulfate (MgSO) and 0.2% (v/v) Triton X-100). For LPO quantification supernatants were extracted in 20% (w/v) trichloroacetic acid (TCA). All samples were sonicated using a TissueLyser II (Qiagen) for 90 s, after which they were centrifuged for 20 min at 10,000 g (3,000 g for ETS) and 4 °C. Supernatants were stored at -80 °C or immediately used. All measurements were done using a microplate reader (Biotek).

2.6.1. Metabolic capacity and energy reserves

The activity of ETS was measured using the method of King and Packard (1975) and the modifications implemented by De Coen and Janssen (1997). Absorbance was measured at 490 nm during 10 min with intervals of 25 s. The amount of formazan formed was calculated using the extinction coefficient (Ɛ) 15,900 $(mmol/L)^{-1}$ cm^{-1}. The results were expressed in nmol per min per g FW.

The GLY content was determined following the sulfuric acid method (Dubois *et al*. 1956). Glucose standards (0-10 mg/mL) were used to obtain a calibration curve. Absorbance was measured at 492 nm, after incubation during 30 min at room temperature, and the results were expressed in mg per g FW.

The PROT content was quantified according to the spectrophotometric Biuret method descibed by Robinson and Hogden (1940). Bovine serum albumin (BSA) was used as standards in the range 0–40 mg/mL to obtain a calibration curve. Absorbance was measured at 540 nm and results were expressed in mg per g FW.

2.6.2. Antioxidant and biotransformation defenses

The activity of SOD was determined based on the method described by Beauchamp and Fridovich (1971) with modifications implemented by Carregosa *et al*. (2014). SOD standards (0.25 - 60 U/mL) were used in order to obtain a calibration curve. Absorbance was read at 560 nm after 20 min of incubation at room temperature. Results were expressed in U per g FW, where one unit (U) represents the amount of the enzyme that catalyzes the conversion of 1 μmol of substrate per min.

The activity of CAT was quantified according to the Johansson and Borg (1988) method. Formaldehyde standards (0 - 150 μmol/L) were used in order to obtain a calibration curve. Absorbance was measured at 540 nm and the activity was expressed in U per g FW, where U represents the amount of enzyme that caused the formation of 1.0 nmol formaldehyde per min.

The activity of GPx was determined using the method of Paglia and Valentine (1967). Absorbance was measured at 340 nm during 5 min in 10 s intervals. The enzymatic activity was determined using the extinction coefficient (Ɛ) 6.22 $(mmol/L)^{-1}cm^{-1}$. The results were expressed as U per g FW, where U represents the quantity of enzymes that caused the formation of 1.0 μmol NADPH oxidized per min.

The activity of GRed was quantified following the method described by Carlberg and Mannervik (1985). Absorbance was measured at 340 nm and the activity was determined using the extinction coefficient (Ɛ) 6.22 $(mmol/L)^{-1}$ cm^{-1}. The activity was expressed in U per g FW, where U represent the enzymes amount that caused the formation of 1.0 μmol NADPH oxidized per min.

The activity of GSTs was measured following Habig *et al*. (1974) with adaptations performed by Carregosa *et al*. (2014). Absorbance was measured spectrophotometrically at 340 nm during 5 min in 10 s intervals. The amount of thioether formed was calculated using the extinction coefficient (Ɛ) 9.6 $(mmol/L)^{-1}$ cm^{-1}. The enzymatic activity was expressed in U per g FW, where U is defined as the quantity of enzyme that causes the formation of 1 μmol of dinitrophenyl thioether per min.

2.6.3. Cellular damage

Levels of LPO were assessed trough the measurement of malondialdehyde (MDA) content, following the method described by Ohkawa *et al*. (1979). Absorbance was measured at 535 nm and the amount of MDA formed was calculated using the extinction coefficient (Ɛ) 156 $(mmol/L)^{-1}$ cm^{-1}. The results were expressed in nmol per g FW.

Levels of PC were determined based on the reaction between 2,4-dinitrophenylhydrazine (DNPH) with carbonyl groups, known as DNPH alkaline method described by Mesquita *et al*. (2014). Absorbance was measured at 450 nm and PC levels were determined using the extinction coefficient (Ɛ) 0.022 $(mmol/L)^{-1}$ cm^{-1}. The results were expressed in nmol of protein carbonyls groups formed per g FW.

2.6.4. Neurotoxicity

The activity of AChE was measured using acetylthiocholine iodide (ATChI, 5 mmol/L) substrates, following the method of Ellman *et al*. (1961) with alterations performed by Mennillo *et al*. (2017). Enzyme activity was recorded at 412 nm during 5 min and expressed in nmol per min per g FW using the extinction coefficient (Ɛ) $13.6x10^3$ $(mol/L)^{-1}cm^{-1}$.

2.7. Statistical analyses

The results were divided in two experimental datasets. In the first dataset rutile and anatase exposure conditions at control temperature were examined, and in the second one rutile at 18 °C and 22 °C were considered.

For the first experiment, results on Ti concentrations, histopathological indexes ($I_{h\ G}$ and $I_{h\ DG}$) and biochemical markers (ETS, PROT, GLY, SOD, CAT, GPx, GRed, GSTs,

LPO, PC and AChE) obtained for mussels exposed to rutile and anatase NPs were submitted to a statistical hypothesis testing, using permutational analysis of variance, employing the PERMANOVA+add-on in PRIMER v6 (Anderson *et al*., 2008). The pseudo-F *p*-values in the PERMANOVA main tests were evaluated in terms of significance. When significant differences were observed in the main test, pairwise comparisons were performed. Values lower than 0.05 ($p < 0.05$) were considered as significantly different. The null hypotheses tested were: i) for each TiO_2 NPs (rutile or anatase), biological response (histopathological and biochemical markers) and Ti concentration in mussels tissues, no significant differences existed among exposure concentrations (0, 5, 50 and 100 µg/L), with significant differences represented in figures with different lowercase letters for rutile NPs and uppercase letter for anatase NPs; ii) for each biological response (histopathological and biochemical marker) and Ti concentration in mussels tissues, no significant differences existed between TiO_2 NPs (rutile and anatase), with significant differences represented in figures with an asterisk.

For the second experiment, results on Ti concentrations, histopathological indexes ($I_{h\,G}$ and $I_{h\,DG}$), and biochemical markers (ETS, PROT, GLY, SOD, CAT, GPx, GSTs, LPO and AChE) obtained for mussels exposed to rutile at 18 °C and at 22 °C were submitted to a statistical hypothesis testing using permutational analysis of variance, employing the PERMANOVA+add-on in PRIMER v6 (Anderson *et al*., 2008). The pseudo-F *p*-values in the PERMANOVA main tests were evaluated in terms of significance. When significant differences were observed in the main test, pairwise comparisons were performed. Values lower than 0.05 ($p < 0.05$) were considered as significantly different. The null hypotheses tested were: i) for each temperature (18 and 22 °C), biological response (histopathological and biochemical markers) and Ti concentration in mussels tissues, no significant differences existed among exposure concentrations (0, 5, 50 and 100 µg/L), with significant differences represented in figures with different lowercase letters for 18 °C and uppercase letters for 22 °C; ii) for each biological response (histopathological and biochemical marker) and Ti concentration in mussels tissues, no significant differences existed between temperatures (18 and 22 °C), with significant differences represented in figures with an asterisk.

For both experimental datasets, the matrix gathering the biological responses (histopathological and biochemical markers) and Ti concentrations in mussels tissues was used to calculate the Euclidean distance similarity matrix. This similarity matrix was simplified through the calculation of the distance among centroids matrix based on the

exposure condition, which was then submitted to ordination analysis, performed by Principal Coordinates (PCO). Pearson correlation vectors of biological responses and Ti concentration in mussels tissues (correlation >0.75) were provided as supplementary variables being superimposed on the top of the PCO graph.

Chapter 3

Results

3. RESULTS

3.1. Rutile and Anatase nanoparticles

3.1.1. Rutile and Anatase characterization

The physical and textural properties of both anatase and rutile samples were studied by X-ray diffraction (XRD), scanning electron microscopy (SEM) and -196 °C N_2 adsorption-desorption isotherms. The characterization obtained by SEM showed that both TiO_2 NPs presented 8 and 3 m^2/g for anatase and rutile, respectively of specific surface area (S_{BET}). From the XRD analyses it was verified that both samples were monophasic, presenting pure anatase ($I4_1/amd$) and rutile ($P4_2/mnm$) tetragonal phases. The anatase lattice parameters were $a=b$=3.7924 and c=9.5304 Å. The rutile lattice constants were $a=b$=4.5922 and c=2.9578 Å. The densities of the anatase and rutile particles were calculated from the lattice parameters as 3.38 and 4.27 g/cm^3, respectively. The SEM micrographs (not shown) demonstrated that the rutile particles were more agglomerated than the anatase ones. The diameters of particles measured on SEM micrographs (calculated based in diameter of 45 particles) were for rutile 694 nm and for anatase 94 nm (Table 2).

Table 2 Summary of structural and morphological features of commercial TiO_2 particles.

Sample	Crystal system (cell parameters)	ρoxide [a] ($g.cm^{-3}$)	$d$parBET [b] (nm)	$d$parXRD [c] (nm)	$d$parSEM [d] (nm)	SBET ($m^2.g^{-1}$)	Source
np-*a*TO	Tetragonal (anatase) (*a*=*b*=3.7924 *c*=9.5304)	3.38	186	50	94	8	Merck
mp-*r*TO	Tetragonal (rutile) (*a*=*b*=4.5922 *c*=2.9578)	4.27	428	-	694[e]	3	Alfa Aesar

[a] Calculated using the lattice parameters; [b] calculated through the equation: $d_{par} = \frac{6}{S_{BET}\rho}$ considering the spherical shape of the particles where S_{BET} corresponds to specific surface area and ρ is the density; [c] crystallite size obtained through the Scherrer equation: $d_{parXRD} = \frac{k_{sf}\lambda_{Cu}}{FWHM\cos(\theta)}$ where k_{sf} corresponds at dimension less shape factor, λ_{Cu} is the wavelength of the X-ray (Cu Kα radiation, λ = 1.5406 Å), FWHM is full width of peak at half maximum in radians and θ is the Bragg angle; [d] calculated based in diameter of 45 particles; [e] aggregates.

Concerning the particles characterization for both forms of TiO_2 NPs in the exposure synthetic seawater, it was not possible to detect the particles on the collected water samples.

3.1.2. Titanium concentration in water and mussel's tissues

In all the collected water samples Ti concentration was below the detection limit (2 µg/L).

Ti concentration in *M. galloprovincialis* exposed to rutile NPs increased along the exposure gradient, with significant differences only at the highest exposure concentration in comparison to the remaining conditions (Table 3). Similarly, Ti concentration in mussels exposed to anatase NPs significantly increased along the exposure gradient, with significantly higher values in organisms exposed to 100 µg/L in comparison to the remaining conditions. Comparing Ti concentration in mussels exposed to rutile and anatase NPs, no significant differences was observed at each exposure concentration.

Table 3 Concentrations of Ti (µg/g) in mussel's soft tissues after 28 days of exposure to each condition of rutile and anatase NPs (CTL, 5, 50 and 100 µg/L of Ti). Results are mean ± standard deviation. Significant differences ($p < 0.05$) among conditions are represented with different letters (lowercase letters for rutile NPs; uppercase letters for anatase NPs). Significant differences ($p < 0.05$) between the two forms of TiO_2 NPs at each exposure concentration are represented with an asterisk.

	Exposure conditions	**[Ti] (µg/g)**
	CTL	2.1±0.3 $^{a, A}$
Rutile	5 µg/L	2.4±1.0 ^{a}
	50 µg/L	2.5±0.4 ^{a}
	100 µg/L	4.5±0.3 ^{b}
Anatase	5 µg/L	2.3±0.8 ^{A,B}
	50 µg/L	2.8±0.2 ^{B}
	100 µg/L	5.3±0.7 ^{C}

3.1.3. Histopathological parameters

The exposure to both forms of TiO_2 NPs at different concentrations lead to an increase of damage severity in gills in a dose dependent manner. In particular, along the increasing exposure gradient, gills of *M. galloprovincialis* exposed to rutile NPs showed a progressive increase of lipofuscin aggregates, enlargement of the central vessel and hemocytes infiltration (Fig. 10). Similarly, gills of mussels exposed to anatase NPs showed

a progressive increase of lipofuscin aggregates, enlargement of the central vessel, loss of cilia and hemocytes infiltration with the increasing exposure concentration (Fig. 10).

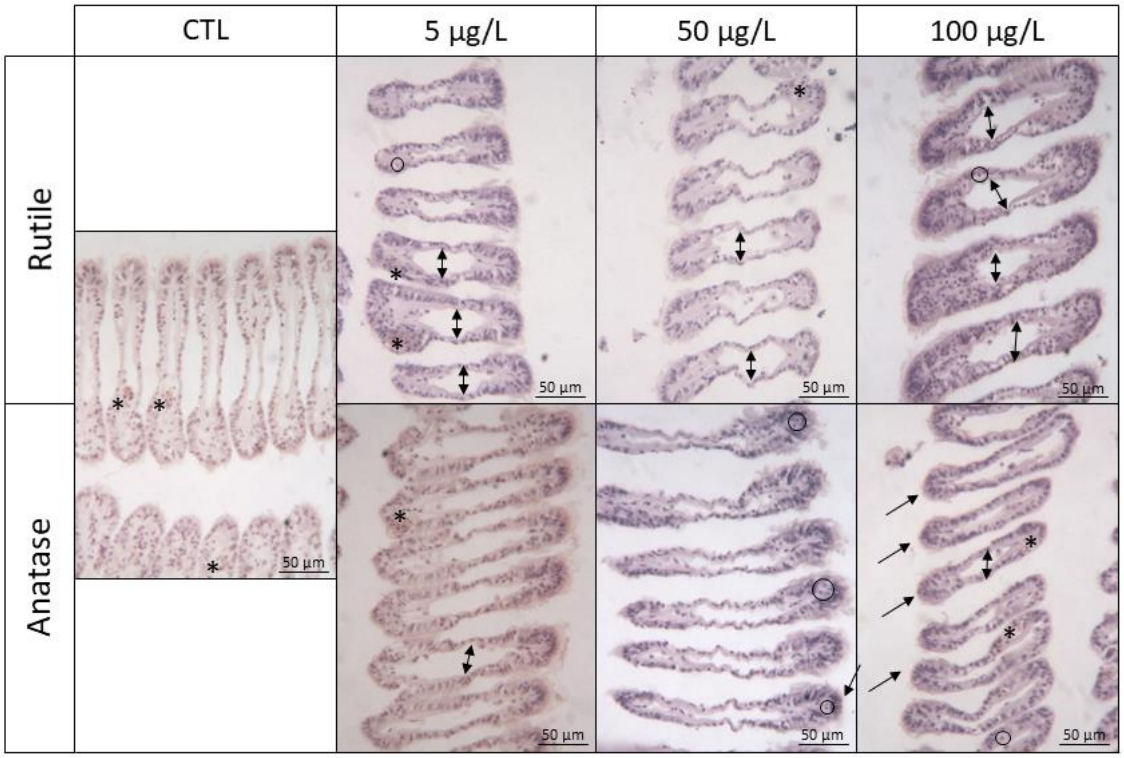

Fig. 10 Micrographs of histopathological alterations observed in the gills of Mytilus galloprovincialis exposed to different Ti concentrations of rutile and anatase NPs stained with hematoxylin: lipofuscin aggregates (*); enlargement of the central vessel; hemocytes infiltration (circles) and loss of cilia (arrows). Scale bar 50 µm.

Mussel's digestive glands (Fig. 11) showed that exposure to rutile NPs lead to an increase of accumulation of lipofuscin, atrophy and hemocytes infiltration. In mussels exposed to anatase NPs (Fig. 11) an increase of atrophy and hemocytes infiltration was observed and lipofuscin aggregates were higher at 5 and 50 µg/L of Ti. No necrosis was observed at any concentration for both forms of TiO_2 NPs.

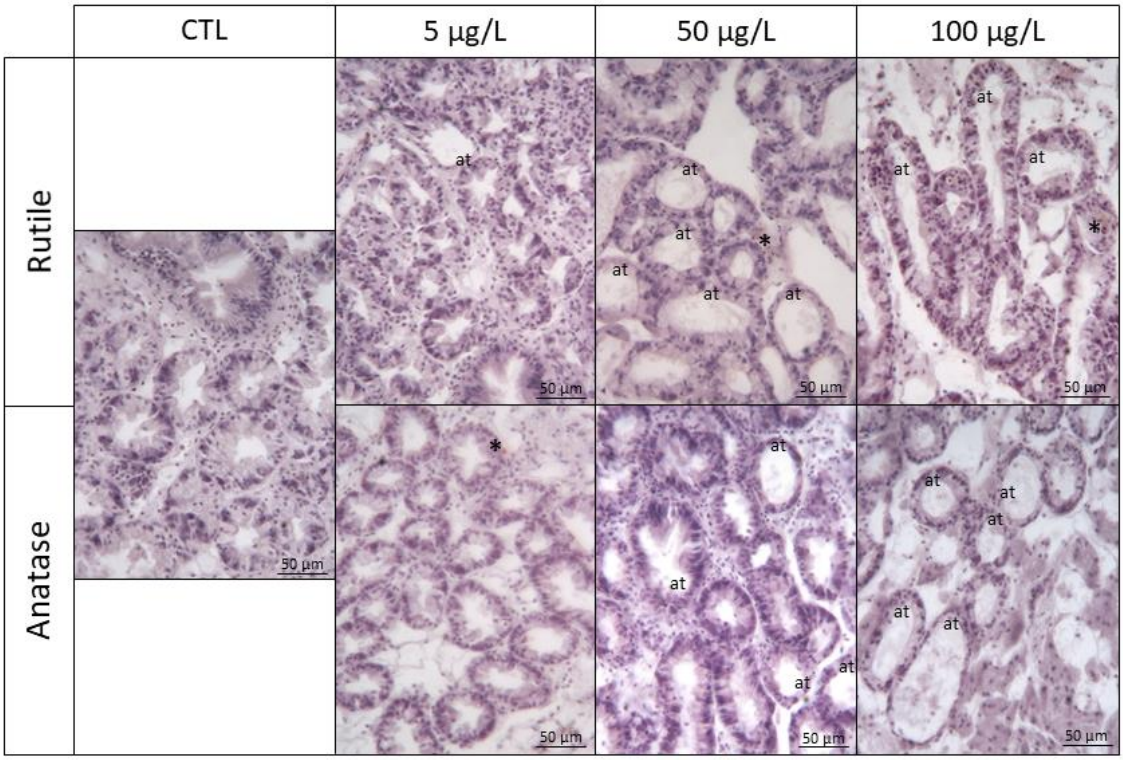

Fig. 11 Micrographs of histopathological alterations observed in the digestive tubules of Mytilus galloprovincialis exposed to different Ti concentrations of rutile and anatase NPs stained with hematoxylin: atrophied digestive tubule (at) and lipofuscin accumulation (*). Scale bar 50 µm.

Regarding the I_h of mussel's gills (Fig. 12A) the values significantly increased along the exposure gradient under both forms of TiO_2 NPs, with the highest values at the highest tested concentrations. No significant differences were observed between rutile and anatase NPs for each of the tested concentrations. The I_h regarding digestive gland of mussels exposed to rutile NPs (Fig. 12B) significantly increased along the exposure gradient, with the highest values at the highest exposure concentration. The I_h regarding the digestive gland of mussels exposed to anatase NPs (Fig. 12B) was significantly higher in contaminated mussels in comparison to non-contaminated ones. No significant differences were observed between rutile and anatase NPS for each of the tested concentrations.

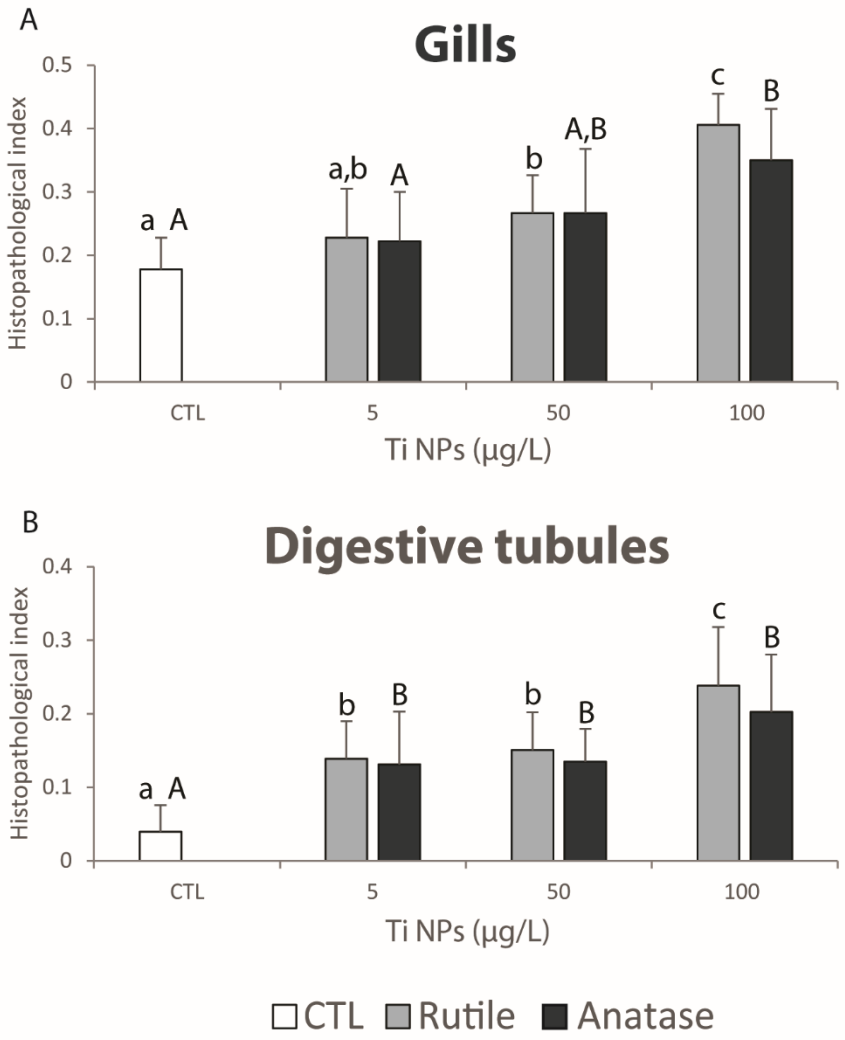

Fig. 12 A: Histopathological index in gills ($I_{h\ G}$); B: Histopathological index in digestive tubules ($I_{h\ DG}$), in Mytilus galloprovincialis exposed to different Ti concentrations of rutile and anatase NPs. Results are mean + standard deviation. Significant differences ($p < 0.05$) among conditions are represented with different letters (lowercase letters for rutile NPs; uppercase letters for anatase NPs). Significant differences ($p < 0.05$) between the two forms of TiO_2 NPs at each exposure concentration are represented with an asterisk.

3.1.4. Biochemical parameters

3.1.4.1. Metabolic capacity and energy reserves

In terms of ETS values, *M. galloprovincialis* exposed to rutile NPs showed no significant differences in comparison to non-contaminated mussels. In organisms exposed to anatase NPs significantly higher ETS values were observed at 50 µg/L of Ti in comparison

to mussels under control. No significant differences were observed between rutile and anatase NPs for each of the tested concentrations (Fig. 13A).

In mussels exposed to both tested forms of TiO_2 NPs the GLY content was significantly higher in contaminated mussels in comparison to non-contaminated ones. No significant differences were observed between rutile and anatase NPs for each of the tested concentrations (Fig. 13B).

The PROT content in mussels exposed to rutile NPs was lower in contaminated mussels in comparison to non-contaminated ones, with significant differences only between organisms under control and exposed to 5 µg/L of Ti. In mussels exposed to anatase NPs significantly lower PROT content was showed in organisms exposed to 5 and 100 µg/L of Ti in comparison to organisms at control and exposed to 50 µg/L of Ti. No significant differences were observed between rutile and anatase NPs for each of the tested concentrations (Fig. 13C).

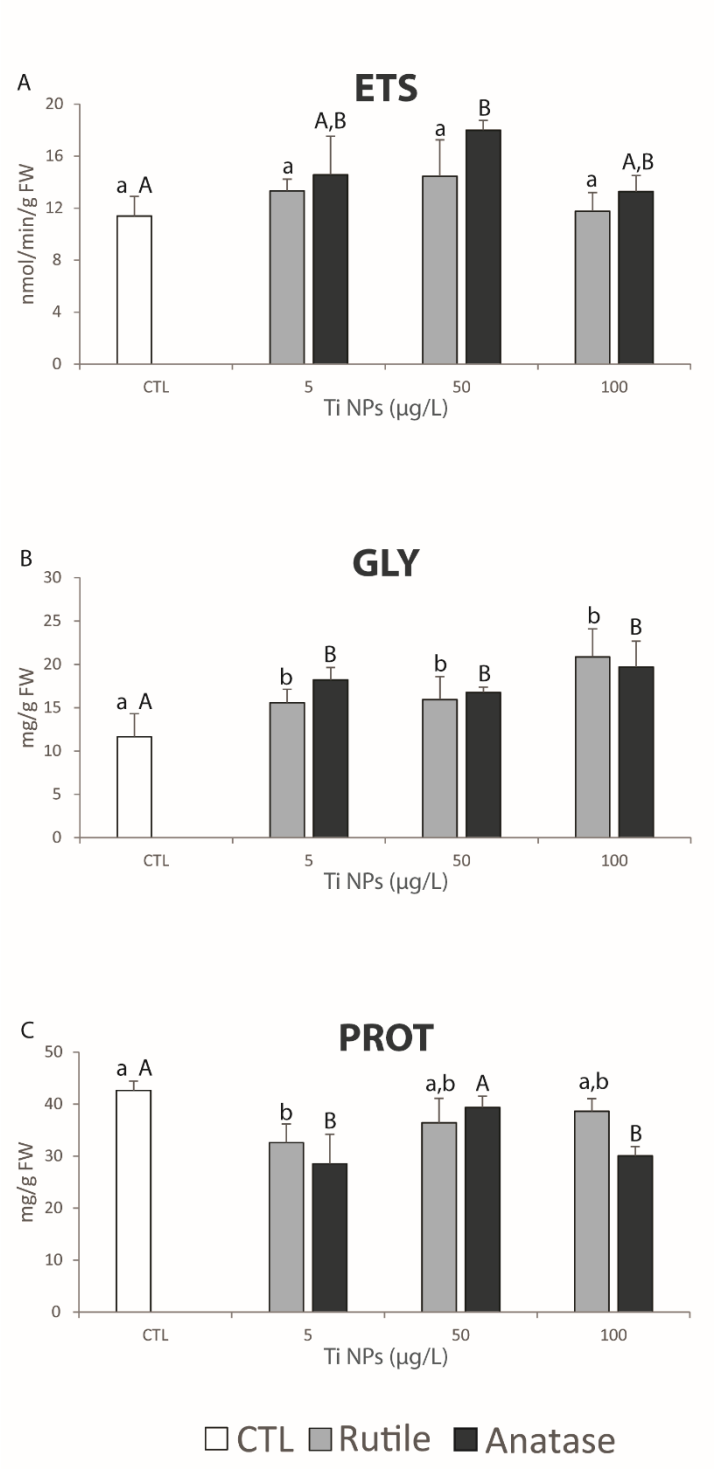

Fig. 13 A: Electron transport system activity (ETS), B: Glycogen content (GLY) and C: Protein content (PROT), in Mytilus galloprovincialis exposed to different Ti concentrations of rutile and anatase NPs. Results are mean + standard deviation. Significant differences ($p < 0.05$) among conditions are represented with different letters (lowercase letters for rutile NPs; uppercase letters for anatase NPs). Significant differences ($p < 0.05$) between the two forms of TiO_2 NPs at each exposure concentration are represented with an asterisk.

3.1.4.2. Antioxidant and biotransformation defenses

In mussels exposed to rutile NPs SOD activity increased at the lowest exposure concentration (5 µg/L of Ti) while significantly decreased at 50 and 100 µg/L of Ti. The activity of SOD in mussels exposed to anatase NPs significantly increased in mussels exposed to 50 µg/L of Ti. Comparing both forms of TiO_2 NPs, SOD activity was significantly higher in organisms exposed to rutile NPs at 5 µg/L of Ti while an opposite pattern was observed at 50 µg/L of Ti (Fig. 14A).

The activity of CAT showed no significant differences among mussels exposed to rutile NPs and non-contaminated mussels. In mussels exposed to anatase NPs significantly higher CAT activity was observed at 50 µg/L of Ti. Differences between rutile and anatase NPs were only observed in organisms exposed to 50 µg/L of Ti, with the highest activity in mussels exposed to anatase (Fig. 14B).

Mussels exposed to rutile NPs showed significantly higher GPx activity in comparison to non-contaminated mussels. Significantly higher GPx activity was observed in mussels exposed to anatase NPs at higher exposure concentrations (50 and 100 µg/L of Ti). Comparing both forms of TiO_2 NPs, significant differences were observed in organisms exposed to 5 µg/L of Ti, with the highest activity in mussels exposed to rutile (Fig. 14C).

The activity of GRed in mussels exposed to rutile NPs was significantly higher at the lowest exposure concentration (5 µg/L of Ti) in comparison to mussels at control and organisms exposed to 50 µg/L of Ti. The activity of GRed in mussels exposed to anatase NPs was significantly higher at 5 µg/L of Ti in comparison to the remaining conditions. When comparing rutile and anatase NPs, significant differences were observed in organisms exposed to 50 µg/L of Ti, with the highest activity in mussels exposed to anatase (Fig. 14D).

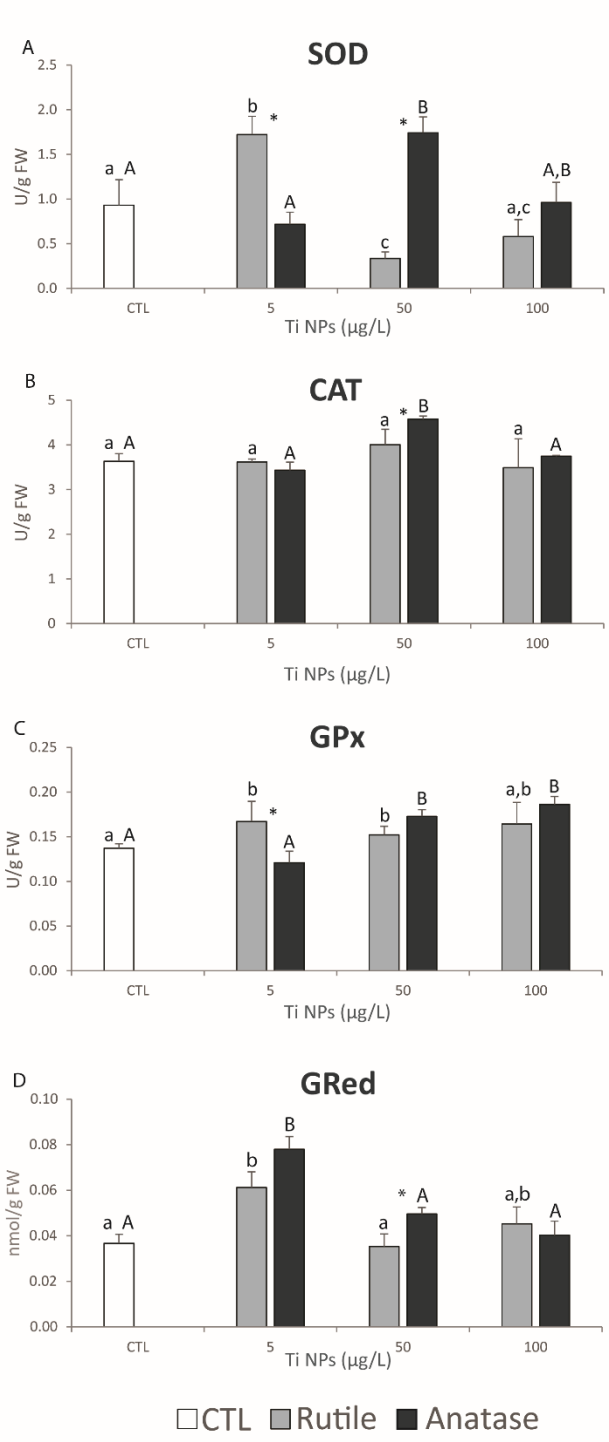

Fig. 14 A: Superoxide dismutase activity (SOD); B: Catalase activity (CAT); C: Glutathione peroxidase activity (GPx); and D: Glutathione reductase activity (GRed), in Mytilus galloprovincialis exposed to different Ti concentrations of rutile and anatase NPs. Results are mean + standard deviation. Significant differences ($p < 0.05$) among conditions are represented with different letters (lowercase letters for rutile NPs; uppercase letters for anatase NPs). Significant differences ($p < 0.05$) between the two forms of TiO_2 NPs at each exposure concentration are represented with an asterisk.

The activity of GSTs in mussels exposed to rutile NPs was significantly higher at the highest exposure concentration (100 µg/L of Ti) while in mussels exposed to anatase NPs GSTs activity significantly decreased at higher exposure concentrations (50 and 100 µg/L of Ti) in comparison to mussels exposed to control and 5 µg/L of Ti. Comparing both tested forms of TiO_2 NPs, significant differences were observed in organisms exposed to 50 and 100 µg/L of Ti, with the highest activity in mussels exposed rutile (Fig. 15).

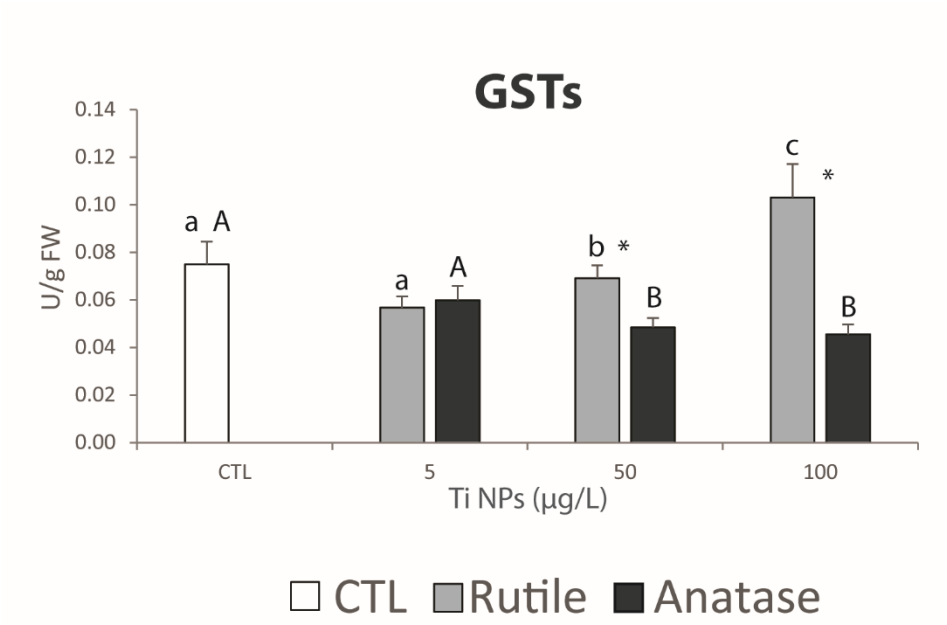

Fig. 15 Glutathione S-transferases activity (GSTs), in Mytilus galloprovincialis exposed to different Ti concentrations of rutile and anatase NPs. Results are mean + standard deviation. Significant differences ($p < 0.05$) among conditions are represented with different letters (lowercase letters for rutile NPs; uppercase letters for anatase NPs). Significant differences ($p < 0.05$) between the two forms of TiO_2 NPs at each exposure concentration are represented with an asterisk.

3.1.4.3. Cellular damage indicators

Mussels exposed to rutile NPs significantly decrease their LPO levels at the lowest exposure concentration in comparison to mussels under control and exposed to 50 µg/L of Ti. LPO levels were significantly higher in mussels exposed to anatase NPs in comparison to non-contaminated mussels. Significant differences between rutile and anatase NPs were observed in contaminated mussels, with the highest values in mussels exposed to anatase (Fig. 16A).

PC levels in mussels exposed to rutile NPs were significantly lower at the lowest exposure concentration and significantly higher at the intermediate exposure concentration in comparison to control and the highest concentration. PC levels in organisms exposed to anatase NPs were significantly lower only at the highest exposure concentration in comparison to the remaining conditions. Comparing both forms of TiO_2 NPs, the levels of PC were significantly higher in organisms exposed to anatase at 5 µg/L of Ti while an opposite pattern was observed at 50 and 100 µg/L of Ti (Fig. 16B).

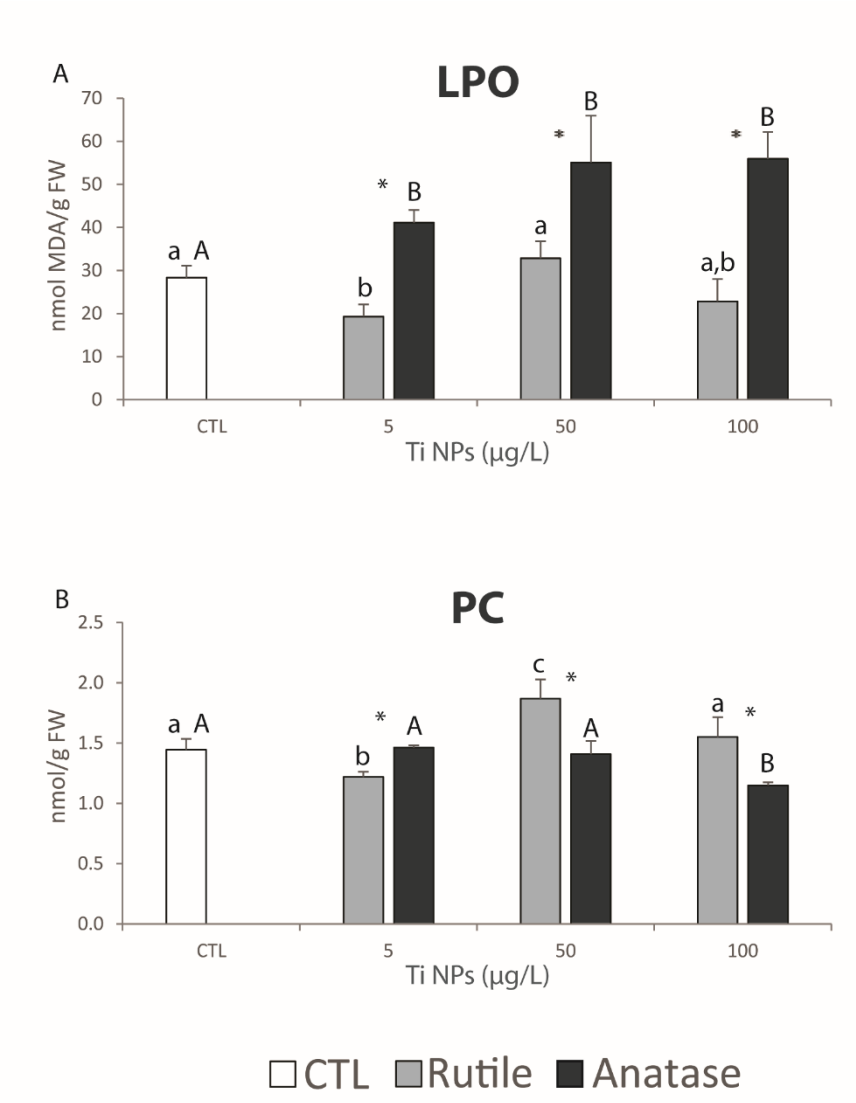

Fig. 16 A: Lipid peroxidation levels (LPO); B: Protein carbonylation levels (PC), in Mytilus galloprovincialis exposed to different Ti concentrations of rutile and anatase NPs. Results are mean + standard deviation. Significant differences ($p < 0.05$) among conditions are represented with different letters (lowercase letters for rutile NPs; uppercase letters for anatase NPs). Significant differences ($p < 0.05$) between the two forms of TiO_2 NPs at each exposure concentration are represented with an asterisk.

3.1.4.4. Neurotoxicity

In mussels exposed to rutile NPs the activity of AChE significantly increased at 50 and 100 µg/L of Ti. Mussels exposed to anatase NPs showed significantly higher AChE activity in comparison to non-contaminated mussels. Comparing both forms of TiO_2 NPs, AChE values were significantly higher in mussels exposed to anatase at 5 µg/L of Ti (Fig. 17).

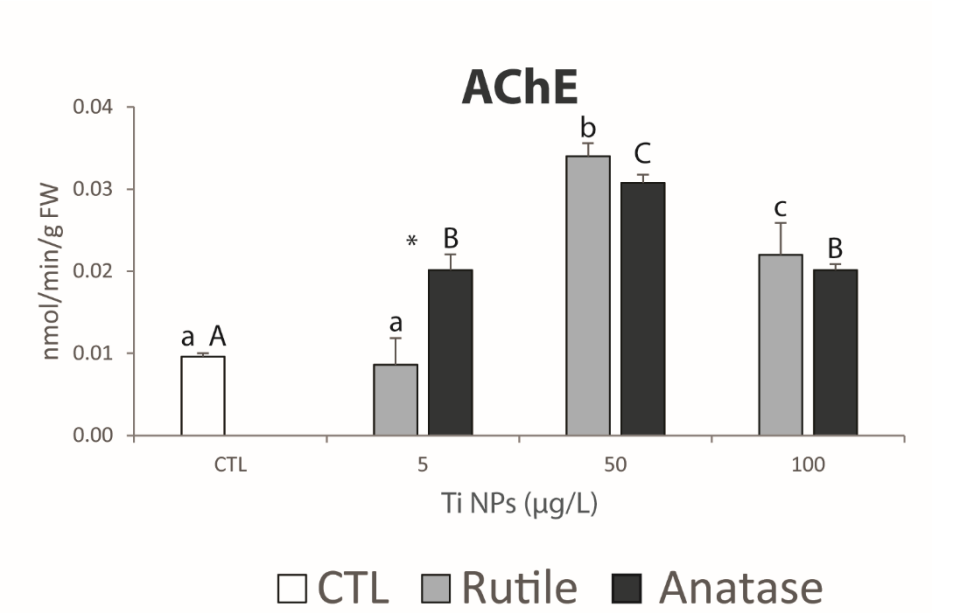

Fig. 17 Acetylcholinesterase activity (AChE), in Mytilus galloprovincialis exposed to different Ti concentrations of rutile and anatase NPs. Results are mean + standard deviation. Significant differences ($p < 0.05$) among conditions are represented with different letters (lowercase letters for rutile NPs; uppercase letters for anatase NPs). Significant differences ($p < 0.05$) between the two forms of TiO_2 NPs at each exposure concentration are represented with an asterisk.

3.1.5. Multivariate analysis

Results from the PCO analysis are presented in Fig. 18. The first principal component axis (PCO1), which represents 32.3% of the variability, clearly separated organisms exposed to control and the lowest Ti concentration for both rutile and anatase (positive side) from organisms exposed to higher concentrations of both forms (negative side). PCO2 axis explained 24.7% of the variability, separating organisms exposed higher rutile concentrations (negative side) from organisms exposed to remaining conditions (positive

side). Ti concentration, histopatological indices, GLY and GPx were the variables best correlated with PCO1 negative side (r > 0.75), being associated with 100 µg/L of Ti both for rutile and anatase NPs. The variables LPO, ETS and SOD were highly correlated with PCO2 positive side (r > 0.75), being close related to 50 µg/L of Ti for anatase NPs.

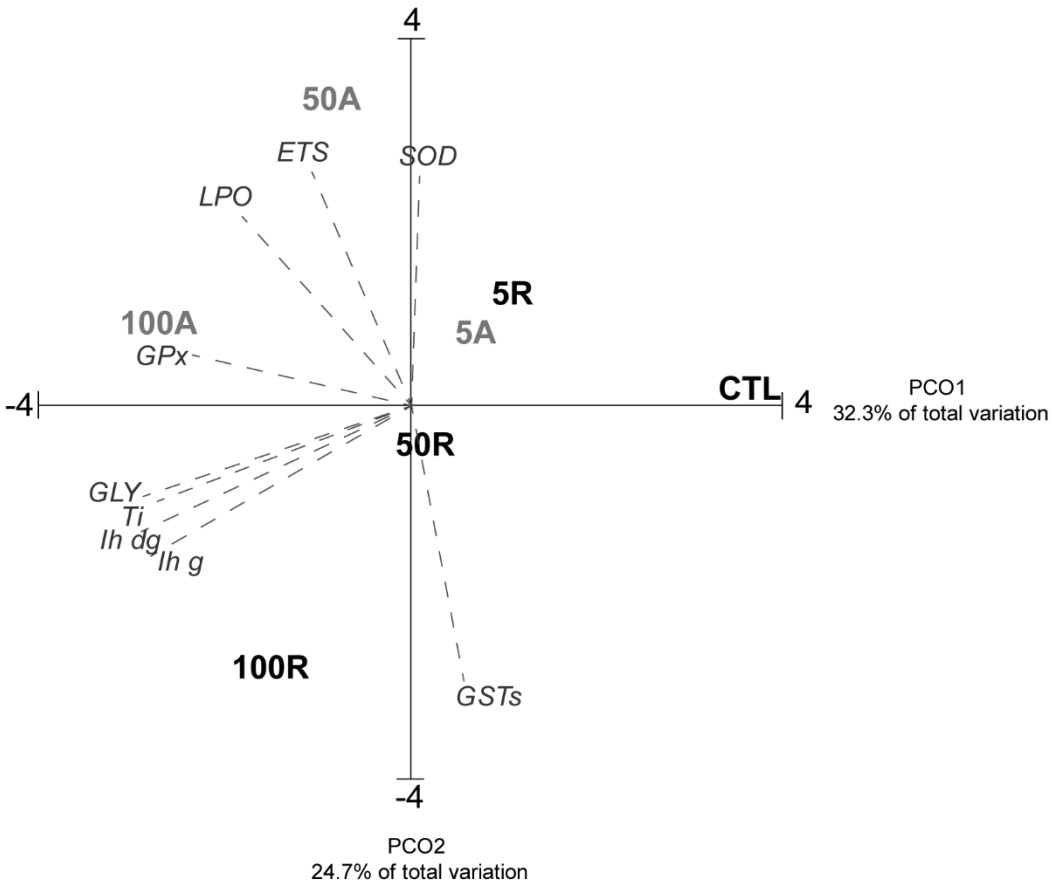

Fig. 18 Centroids ordination diagram (PCO) based on biochemical descriptors, histopathological indices and Ti concentration, measured in Mytilus galloprovincialis exposed to different Ti concentrations of rutile (5, 50 and 100 R) and anatase (5, 50 and 100 A) NPs. Pearson correlation vectors are superimposed as supplementary variables (r > 0.75): Ti, $I_{h\,G}$; $I_{h\,DG}$; ETS; GLY; PROT; SOD; CAT; GPx; GRed; GSTs; LPO; PC; AChE.

3.2. Rutile nanoparticles and warming conditions

3.2.1. Rutile characterization

The structural and microstructural characterization of rutile NPs was verified by XRD, -196 °C N_2-sorption isotherms and SEM techniques. It was confirmed that the particles used presented rutile tetragonal phase with lattice parameters of a=b=4.5922 Å and c=2.9578 Å. The density of the NPs was determined from XRD pattern using the lattice

parameters and had a value of 4.27 g/cm^3. The diameter of particles was measured on 45 particles of the SEM micrographs (not shown) and had an average value of 694 nm. The diameter of the particles calculated using the specific surface area (S_{BET}, determined as being equal to 3 m^2/g) was 428 nm. The difference between the particle diameter calculated from the SEM and S_{BET} measurements indicate the agglomeration of the particles (aggregates) (Table 2).

Regarding the particles characterization in the exposure medium, it was not possible to detect the particles on the collected water samples.

3.2.2. Ti concentrations in water and mussel's samples

In all the collected water samples Ti concentration was below the detection limit (2 µg/L).

Under both temperatures, Ti concentration in *M. galloprovincialis* was significantly higher in mussels exposed to the highest concentration (100 µg/L of Ti) (Table 4). When comparing temperatures, significant differences were only obtained at the highest tested concentration, with higher values at 18 °C.

Table 4 Concentrations of Ti (µg/g) in mussel's soft tissues after 28 days of exposure to each condition (CTL, 5, 50 and 100 µg/L of Ti) and both temperatures (18 and 22 °C). Results are mean ± standard deviation. Significant differences ($p < 0.05$) among conditions are represented with different letters (lowercase letters for 18 °C; uppercase letters for 22 °C). Significant differences ($p < 0.05$) between the two temperatures at each exposure concentration are represented with an asterisk.

	Exposure conditions	[Ti] (µg/g)
18 °C	CTL	2.1±0.3 ^{a}
	5 µg/L	2.4±1.0 ^{a}
	50 µg/L	2.5±0.4 ^{a}
	100 µg/L	4.5±0.3 ^{b*}
22 °C	CTL	1.8±0.7 ^{A}
	5 µg/L	2.3±0.6 ^{A}
	50 µg/L	2.2±0.6 ^{A}
	100 µg/L	3.3±0.4 ^{B*}

3.2.3. Histopathological parameters

Mussel's gills and digestive glands showed several histopathological alterations that were detectable and measurable.

The present results showed that exposure to rutile NPs at different concentrations leads to an increase of damage severity in a dose dependent manner in mussel's gills under both temperatures. At 18 °C, exposed mussel' gills showed a progressive increase of hemocytes infiltration, lipofuscin aggregates and enlargement of the central vessel (Fig. 19). At 22 °C there was a progressive increase of hemocytes infiltration and lipofuscin aggregates. Also, at increased temperature both the loss of cilia and the enlargement of the central vessel were higher at the highest concentration (Fig. 19).

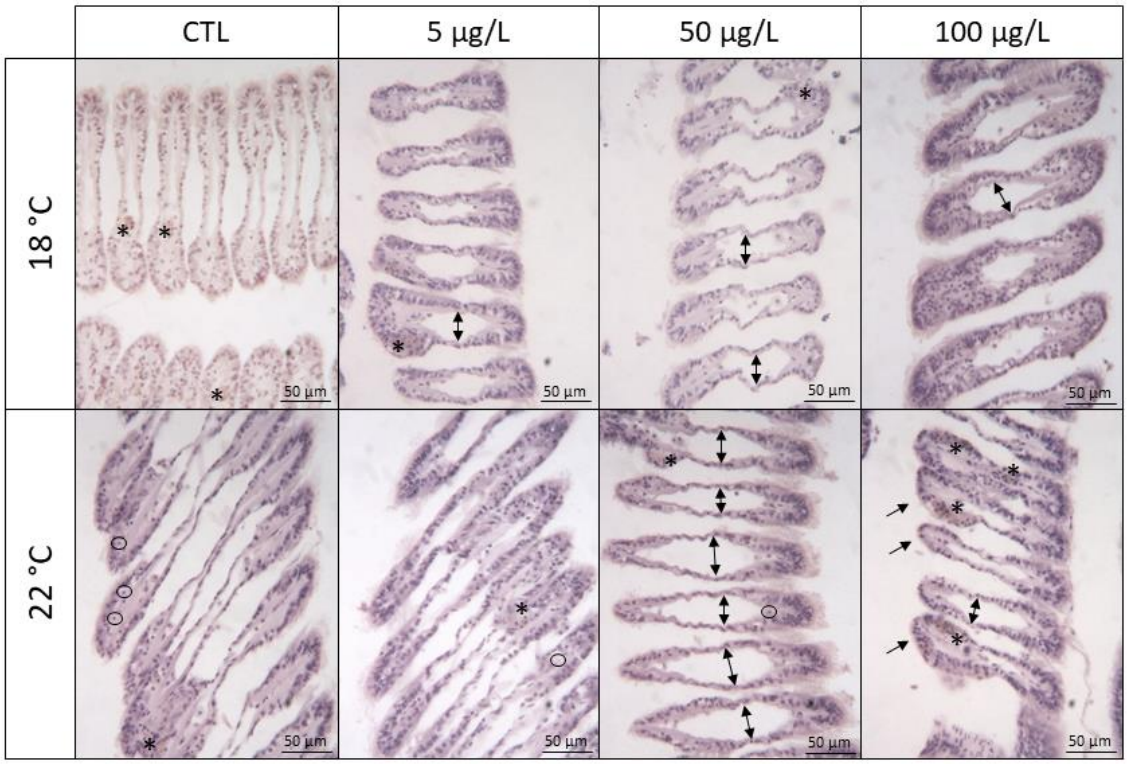

Fig. 19 Micrographs of histopathological alterations observed in the gills of Mytilus galloprovincialis exposed to different Ti concentrations stained with hematoxylin: lipofuscin aggregates (*); enlargement of the central vessel; hemocytes infiltration (circles) and loss of cilia (arrows). Scale bar 50 µm.

The analysis of the digestive gland (Fig. 20) showed that at 18 °C, exposed mussel's digestive glands presented a progressive increase of hemocytes infiltration, atrophy and

accumulation of lipofuscin. No necrosis was found at any concentration. At 22 °C there was a progressive increase of hemocytes infiltration and atrophy. The necrosis alterations appeared at concentrations of 50 and 100 µg/L of Ti (Fig. 20).

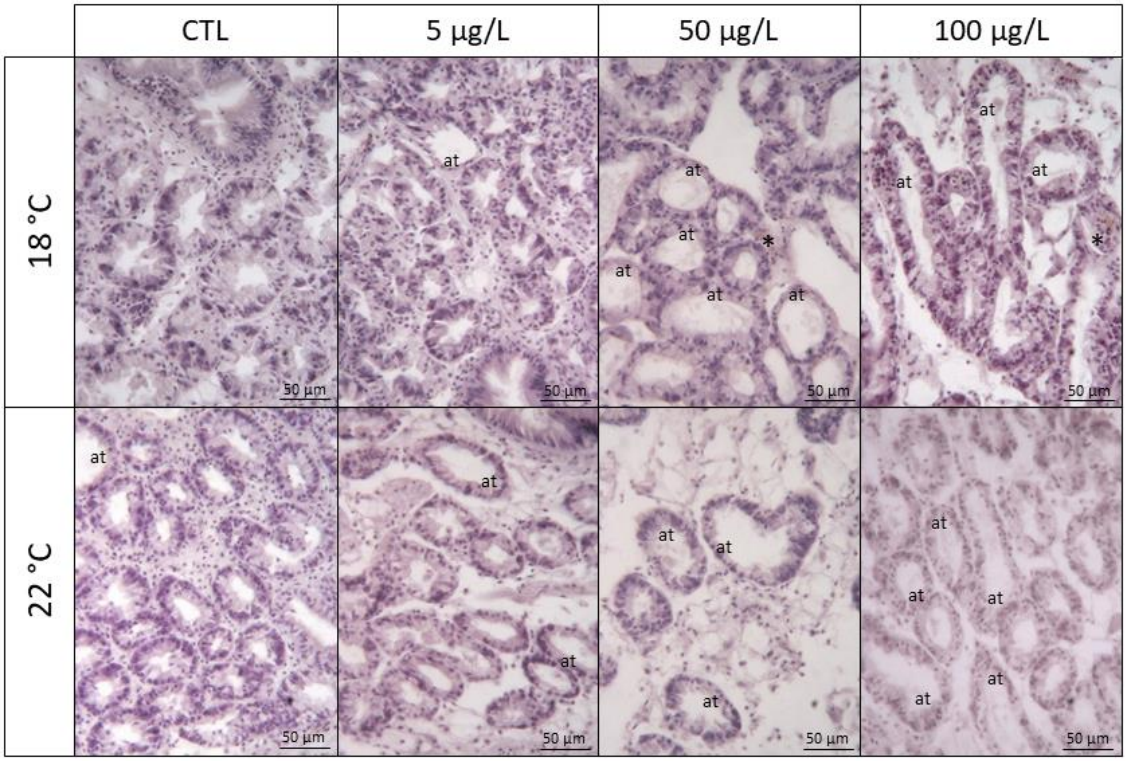

Fig. 20 Micrographs of histopathological alterations observed in the digestive tubules of Mytilus galloprovincialis exposed to different Ti concentrations stained with hematoxylin: atrophied digestive tubule (at) and lipofuscin accumulation (*). Scale bar 50 µm.

Under both temperatures, the histopathological index (I_h) obtained for mussel's gills (Fig. 21A) significantly increased along the exposure gradient, with the highest values in mussels exposed to the highest concentration. Comparing temperatures, I_h was significantly higher at 22 °C in organisms exposed to 50 µg/L of Ti. Under both temperatures the I_h obtained for mussel's digestive gland (Fig. 21B) was significantly higher in rutile NPs exposed mussels, with the highest values in mussels exposed to the highest concentration. Comparing temperatures, I_h was significantly higher at 22 °C in organisms under control condition.

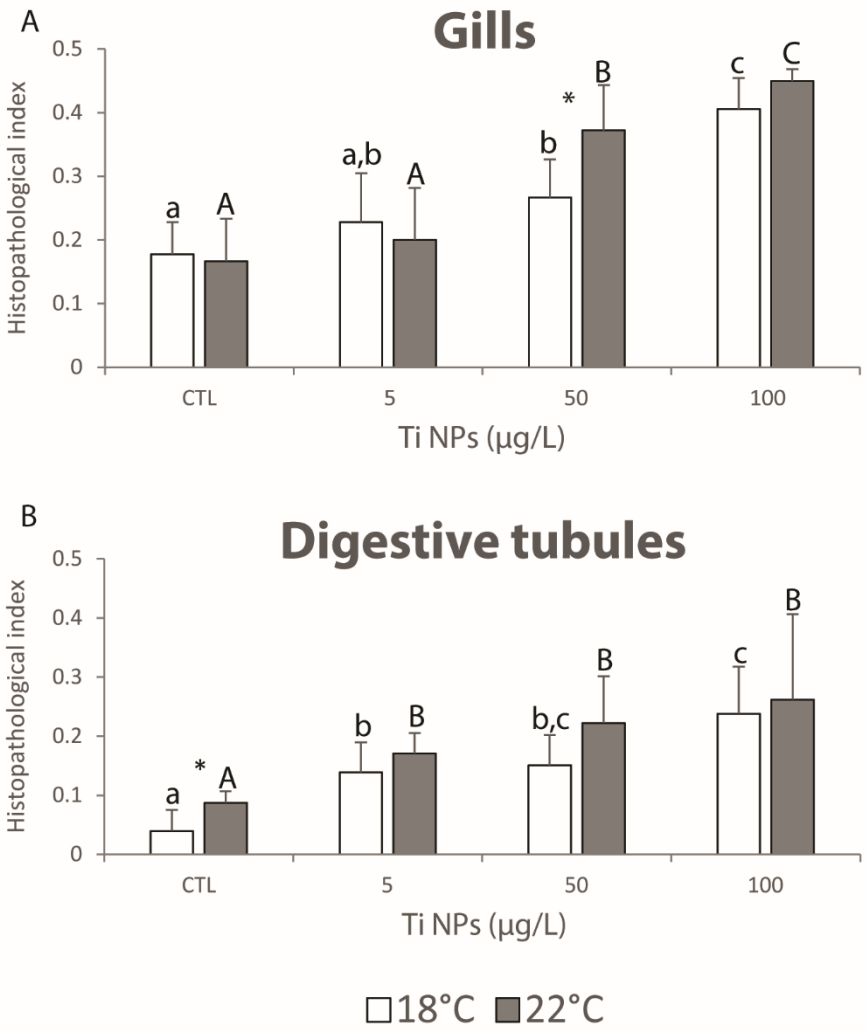

Fig. 21 A: Histopathological index in gills ($I_{h\ G}$); B: Histopathological index in digestive tubules ($I_{h\ DG}$), in Mytilus galloprovincialis exposed to different Ti concentrations of rutile NPs under different temperatures (18 °C and 22 °C). Results are mean + standard deviation. Significant differences ($p < 0.05$) among conditions are represented with different letters (lowercase letters for 18 °C; uppercase letters for 22 °C). Significant differences ($p < 0.05$) between the two temperatures at each exposure concentration are represented with an asterisk.

3.2.4. Biochemical parameters

3.2.4.1. Metabolic capacity and energy reserves

Under control temperature (18 °C) no significant differences were observed in terms of ETS values between contaminated and non-contaminated mussels. At 22 °C significantly

higher ETS values were observed in mussels exposed to 5 and 50 µg/L of Ti in comparison to mussels and control and the highest exposure concentration (100 µg/L of Ti). Significant differences between temperatures were only observed in mussels exposed to the lowest Ti concentration (5 µg/L), with the highest values in mussels under increased temperature (Fig. 22A).

The GLY content in mussels exposed to 18 °C was significantly higher in contaminated mussels in comparison to non-contaminated ones. At warming conditions significantly higher values were observed at the highest exposure concentration. No significant differences were observed between both temperatures for each of the tested concentrations, while in non-contaminated mussels significantly higher GLY content was observed in organisms under temperature rise (Fig. 22B).

In terms of PROT content, under control temperature contaminated mussels tended to present lower values than control organisms, but significant differences were only observed between control and 5 µg/L exposed organisms. At 22 °C mussels exposed to rutile NPs presented significantly lower PROT content in comparison to control organisms. No significant differences were observed between temperatures for each of the tested concentrations (Fig. 22C).

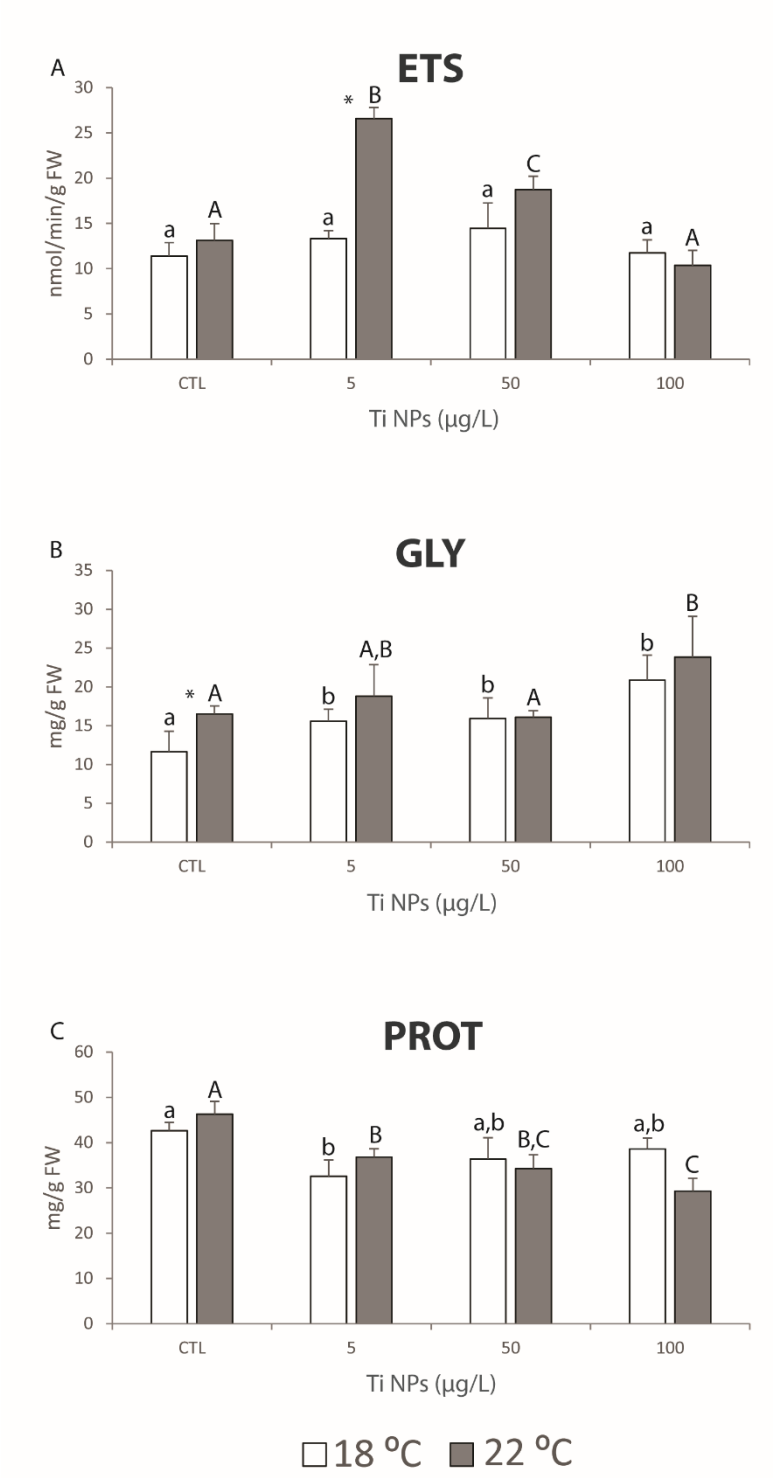

Fig. 22 A: Electron transport system activity (ETS), B: Glycogen content (GLY) and C: Protein content (PROT), in Mytilus galloprovincialis exposed to different Ti concentrations of rutile NPs under different temperatures (18 °C and 22 °C). Results are mean + standard deviation. Significant differences ($p < 0.05$) among conditions are represented with different letters (lowercase letters for 18 °C; uppercase letters for 22 °C). Significant differences ($p < 0.05$) between the two temperatures at each exposure concentration are represented with an asterisk.

3.2.4.2. Antioxidant and biotransformation defenses

In comparison to control values, at 18 °C the activity of SOD increased at the lowest exposure concentration (5 µg/L of Ti) while significantly decreased at higher exposure concentrations (50 and 100 µg/L of Ti). At warming conditions SOD activity significantly increased along the exposure gradient, with the highest values in mussels exposed to the highest concentration. Comparing temperatures, SOD activity was significantly higher at 18 °C in organisms exposed to the control and the lowest tested concentration while an opposite pattern was observed at higher concentrations (Fig. 23A).

The activity of CAT showed no significant differences among tested conditions under control temperature. At 22 °C contaminated mussels tended to decreased their CAT activity with the lowest value in organisms exposed to 50 µg/L of Ti. When comparing temperatures significantly higher CAT values were observed in organisms exposed to 5 and 100 µg/L of Ti at 22 °C (Fig. 23B).

Under control temperature contaminated mussels showed significantly higher GPx activity that non-contaminated mussels. Under increased temperature no significant differences were observed among conditions. Differences between temperatures were only observed in organisms exposed to 50 µg/L of Ti, with the highest activity at the highest temperature (Fig. 23C).

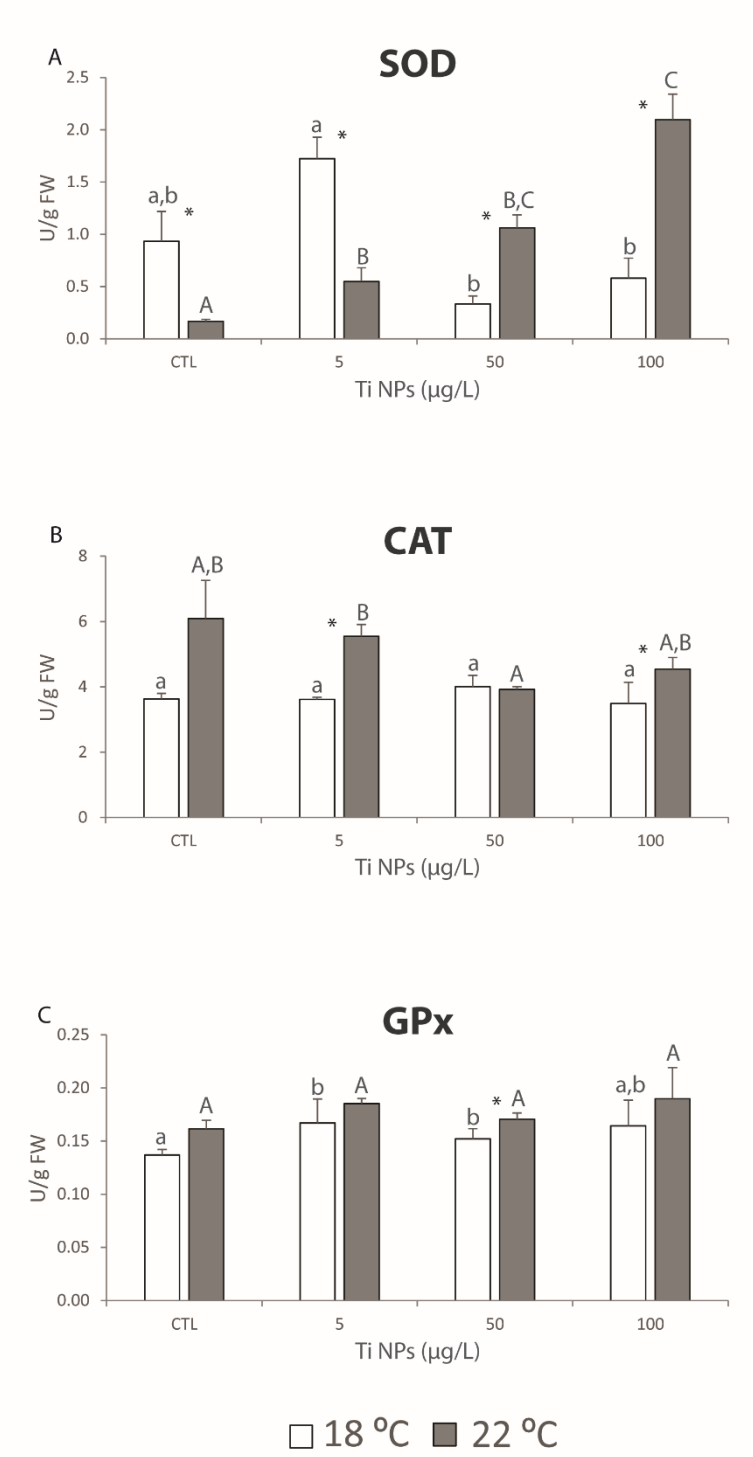

Fig. 23 A: Superoxide dismutase activity (SOD); B: Catalase activity (CAT); and C: Glutathione peroxidase activity (GPx), in Mytilus galloprovincialis exposed to different Ti concentrations of rutile NPs under different temperatures (18 °C and 22 °C). Results are mean + standard deviation. Significant differences ($p < 0.05$) among conditions are represented with different letters (lowercase letters for 18 °C; uppercase letters for 22 °C). Significant differences ($p < 0.05$) between the two temperatures at each exposure concentration were represented with an asterisk.

Mussels maintained at control temperature showed significantly higher GSTs activity at the highest exposure concentration. At increased temperature mussels tended to maintain similar GSTS levels, but a significant decrease was observed in organisms exposed to 50 µg/L of Ti in comparison to the ones exposed to 5 µg/L. Mussels maintained at 18 °C showed significantly higher GSTs values, except at 5 µg/L (Fig. 24).

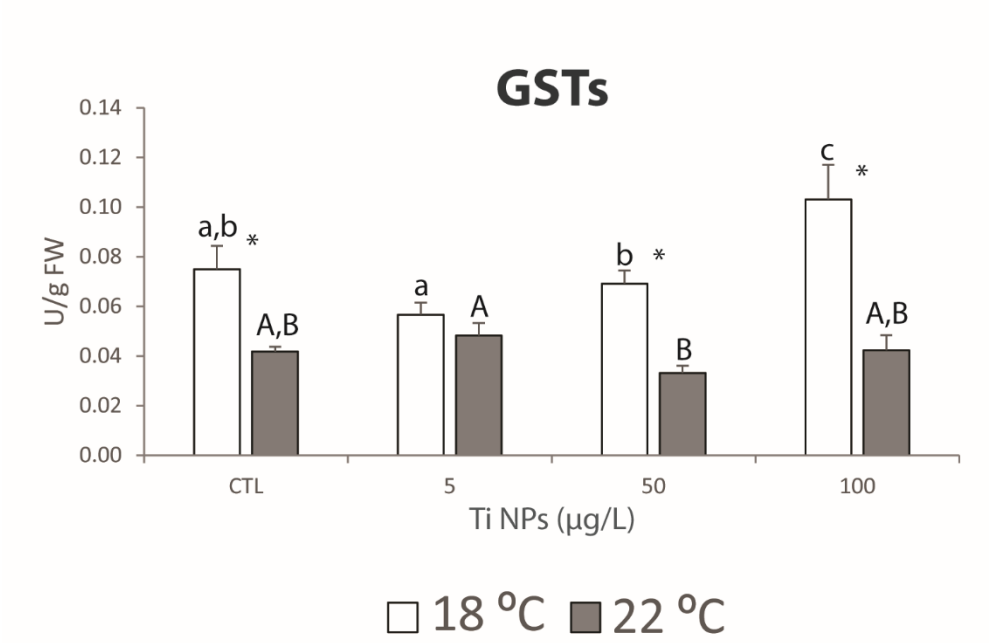

Fig. 24 Glutathione S-transferases activity (GSTs), in Mytilus galloprovincialis exposed to different Ti concentrations of rutile NPs under different temperatures (18 °C and 22 °C). Results are mean + standard deviation. Significant differences ($p < 0.05$) among conditions are represented with different letters (lowercase letters for 18 °C; uppercase letters for 22 °C). Significant differences ($p < 0.05$) between the two temperatures at each exposure concentration were represented with an asterisk.

3.2.4.3. Cellular damage

Organisms under control temperature tended to maintain their LPO levels, with significantly lower values only at the lowest exposure concentration in comparison to the remaining conditions. At increased temperature contaminated mussels showed lower LPO levels than non-contaminated ones, but significant differences to the control were only observed at 5 µg/L of Ti. Significantly higher LPO levels were observed in mussels exposed to warming conditions in comparison to the ones maintained at 18 °C (Fig. 25).

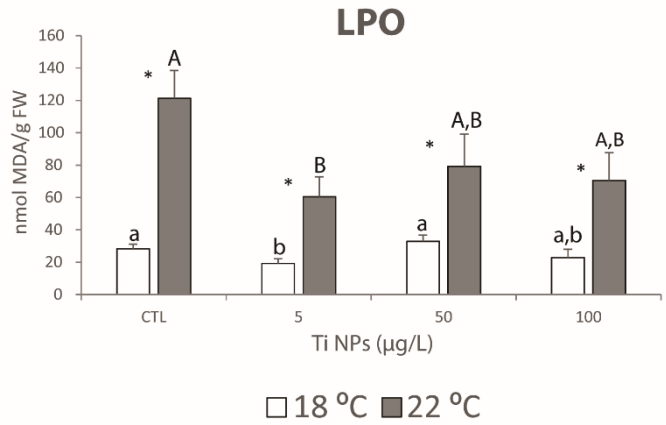

Fig. 25 Lipid peroxidation levels (LPO) in Mytilus galloprovincialis exposed to different Ti concentrations of rutile NPs under different temperatures (18 °C and 22 °C). Results are mean + standard deviation. Significant differences ($p < 0.05$) among conditions are represented with different letters (lowercase letters for 18 °C; uppercase letters for 22 °C). Significant differences ($p < 0.05$) between the two temperatures at each exposure concentration were represented with an asterisk.

3.2.4.4. Neurotoxicity

Under control temperature the activity of AChE was significantly increased at 50 and 100 µg/L of Ti, while at 22 °C no significant differences were observed among conditions. Comparing both temperatures, AChE values were significantly higher at 22 °C under control and the lowest exposure concentration, and significantly higher at 18 °C under the intermediate concentration (Fig. 26).

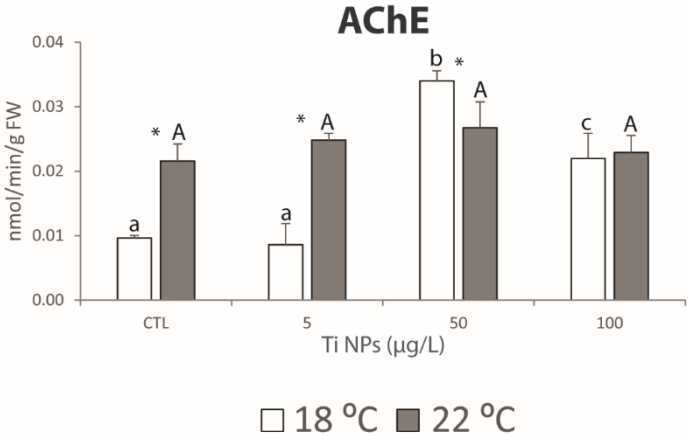

Fig. 26 Acetylcholinesterase activity (AChE), in Mytilus galloprovincialis exposed to different Ti concentrations of rutile NPs under different temperatures (18 °C and 22 °C). Results are mean + standard deviation. Significant differences ($p < 0.05$) among conditions are represented with different letters (lowercase letters for 18 °C; uppercase letters for 22 °C). Significant differences ($p < 0.05$) between the two temperatures at each exposure concentration were represented with an asterisk.

3.2.5. Multivariate analysis

Results from the PCO analysis are presented in Fig. 27. The first principal component axis (PCO1), which represents 33.8% of the variability, separated non-contaminated organisms (control conditions at both temperatures) and mussels exposed to 5 and 50 µg/L under 22 °C in the positive side from the remaining conditions in the negative side. PCO2 axis explained 29.4% of the variability, clearly separating organisms exposed to the control temperature (18 °C) (positive side) from organisms exposed to warming conditions (negative side). PROT was positively associated to PCO1 positive axis, while Ti concentration was highly correlated with PCO1 negative axis (r > 0.75). CAT and LPO levels were close associated with organisms exposed to higher temperature and lower Ti concentrations (5 and 50 µg/L) while histopathological indices ($I_{h\,G}$ and $I_{h\,DG}$), GPx, and GLY were close related with organisms exposed to the highest Ti concentration at 22 °C (r > 0.75). GSTs were close related to organisms exposed to rutile NPs at 18 °C (r > 0.75).

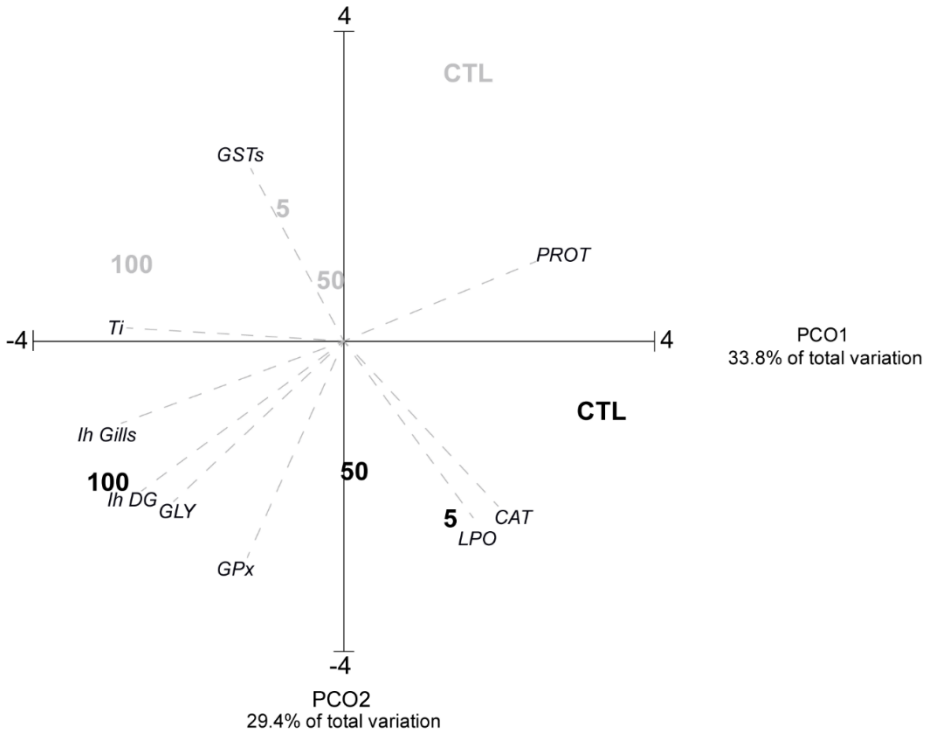

Fig. 27 Centroids ordination diagram (PCO) based on biochemical descriptors, histopathological indices and Ti concentration, measured in Mytilus galloprovincialis exposed to different Ti concentrations of rutile NPs under different temperatures (18 °C and 22 C). Pearson correlation vectors are superimposed as supplementary variables (r > 0.75): Ti, $I_{h\,G}$; $I_{h\,DG}$; ETS; GLY; PROT; SOD; CAT; GPx; GRed; GSTs; LPO; PC; AChE.

Chapter 4

Discussion

4. DISCUSSION

The present study evaluated the impacts induced by rutile and anatase NPs, as well as temperature rise in the species *M. galloprovincialis* assessing mussel's Ti bioaccumulation, histopathological alterations and biochemical effects, including impacts on organisms metabolism, energy reserves, oxidative and neurotoxic status.

4.1. Rutile and Anatase characterization and quantification in water samples

In the present study, it was no possible to characterize and quantify the particles on water samples collected from exposure assays, which may be related to the fact that TiO_2 NPs rapidly agglomerates in seawater and tend to precipitate to the bottom of the aquaria. Also Canesi *et al*. (2010) and Zhu *et al*. (2011) showed that TiO_2 NPs form agglomerates in artificial seawater and tend to sink rapidly, they correlated this with the high ionic strength of the seawater. This happens because with increasing ionic strength the barrier to avoid agglomeration decreased (Jiang *et al*., 2009). Therefore, it was not possible to associate the detected differences in terms of biological effects to differences in rutile and anatase behaviour in seawater.

4.2. Rutile and Anatase nanoparticles

The histopathological and biochemical impacts observed in mussels were clearly associated with the Ti concentration observed in their soft tissues, which increased along the exposure gradient, with the highest impacts and Ti concentrations in mussels at the highest tested concentration regardless the TiO_2 form (rutile or anatase). Ciacci *et al*. (2012) showed that aggregation increases with increasing concentration and Ward and Kach (2009) demonstrated that bivalves more efficiently capture and ingest NPs that are incorporated into agglomerates compared to those freely dispersed. So, the present results may indicate that higher concentration may result into larger or more aggregates and higher accumulation, leading to higher toxicity.

In detail, histopathological observations confirmed that both forms of TiO_2 NPs induced alterations in mussel's gills and digestive tubules. Since gills interact with the surrounding environment, they are one of the main target organs for contaminants (Evans,

1987; Au, 2004; Rajalakshmi and Mohandas, 2005). In the present study, the exposure to rutile and anatase NPs resulted in abundance of lipofuscin aggregates, hemocyte infiltration and enlargement of the central vessel. The presence of lipofuscin aggregates was previously associated with oxidative stress in bivalves (Livingstone *et al*., 2006), which is in accordance with the present results obtained in mussels exposed to anatase NPs. However, in mussels exposed to rutile NPs the appearance of these aggregates was not accompanied by cellular damage which may indicate the low toxicity of rutile in terms of biochemical changes and, on the other hand, higher responsiveness of mussels in terms of histopathological changes towards this TiO_2 form. In what regards to hemocytes infiltration these alterations are clearly a consequence of mussels exposure to rutile and anatase NPs. Similar alterations were already observed by Bignell *et al*. (2011) and Amachree *et al*. (2014) in mussels exposed to other stressful conditions, namely the presence of pathogens and mercury, respectively. The loss of cilia was only observed in mussels exposed to anatase NPs, which again can indicate higher toxicity of these NPs in comparison to rutile. According to Pagano *et al*. (2016), the loss of cilia may lead to difficulties in filtering food and breathing problems, highlighting possible physiological impairments in mussels exposed to these NPs which can compromise mussels growth and reproduction success. Previous studies conducted by D'Agata *et al*. (2014) also showed that mussels suffered histopathological alterations in gills due to exposure to 'bulk' TiO_2 and TiO_2 NPs, while Sunila (1988) demonstrate similar impacts due to cadmium, copper, lead, cobalt, iron and silver.

Bivalves' digestive gland has also been widely used for toxicity evaluation (Bignell *et al*., 2008; Marigómez *et al*., 2013) because it is the major organ involved in organism's homeostatic regulation, immune defense mechanisms and metabolism (Moore and Allen, 2002; Livingstone *et al*., 2006). The results obtained in the present study showed that rutile and anatase NPs caused atrophy of this organ that according to Cuevas *et al*. (2015) corresponds to a reduction in the thickness of epithelia followed by the expansion of the digestive tubule lumen. Rutile and anatase NPs also caused hemocytes infiltration and accumulation of lipofuscin in digestive tubules. Previous studies also demonstrated that diamond NPs (Cid *et al*., 2015), cadmium-based quantum dots (Jimeno-Romero *et al*., 2019) and copper (Calabrese *et al*., 1984) induced similar histological alterations in bivalves' digestive gland.

Regarding mussels biochemical changes, and in particular mussels metabolism, the results obtained showed that organisms metabolic capacity was not altered when exposed to rutile NPs, which may indicate that the Ti concentrations tested under this form were not enough to impact mussel's metabolism. Other authors also demonstrated that low concentrations of mercury and carbon NPs had no effects on mussel's metabolism (Coppola *et al*., 2017; Andrade *et al*., 2019). However, when mussels were exposed to anatase NPs an increase on their metabolic capacity was observed, especially at intermediate Ti concentration, showing that mussels exposed to this TiO_2 form were probably trying to prevent the effects of Ti, namely activating antioxidant and biotransformation defense mechanisms which requires higher metabolic capacity. Similarly, Monteiro *et al*. (2019b) demonstrated that *M. galloprovincialis* exposed to high concentration of Ti (100 µg/L) increased their metabolic capacity. In this way, the present findings may indicate that although Ti concentrations were similar in mussels exposed to both TiO_2 forms, it seems that anatase can induce greater metabolic alterations than rutile. Thus, in accordance to published studies and the present findings, it seems that mussel's metabolic capacity may depend on the contaminant type and the concentration tested, with higher concentrations exerting higher impacts.

Regarding mussels energy reserves, the present study demonstrated that organisms were able to avoid the expenditure of GLY, regardless the TiO_2 form. These results followed the ability of mussels to maintain their ETS activity when exposed to rutile NPs, indicating that in stressful conditions mussels try to prevent the impacts by limiting their metabolic activity and saving GLY expenditure. The ability to maintain the ETS activity followed by the increased of GLY content was observed by Coppola *et al*. (2018) in *M. galloprovincialis* after exposure to arsenic. The results obtained further revealed that the increased of metabolic capacity in mussels exposed to anatase NPs was not high enough to lead to the expenditure of GLY. Once again, such results may highlight that the Ti concentrations tested were not high enough to lead to mussel's energy reserves expenditure or other energy reserves (such as lipids) were used to fuel up defense mechanisms. This pattern was also observed by Monteiro *et al*. (2019b) in *M. galloprovincialis* after exposure to Ti. Nevertheless, in what regards to PROT content, this reserve decreased in mussels exposed to rutile and anatase NPs, indicating that organisms were using proteins and were not able

to increase their production under the exposure conditions, probably because the stress induced was not sufficient to activate the production of enzymes.

In what regards to oxidative stress, my findings suggest that the activity of antioxidant defenses in mussels exposed to rutile NPs were, for most of the enzymes, not increased with the increasing exposure concentration, corroborating the hypothesis that the conditions tested were not sufficient to induce biochemical changes in mussels, namely increase on their antioxidant defenses. Another possibility is that biotransformation defenses, namely GSTs enzymes, were involved in cells detoxification from Ti, which was noticed at the highest exposure concentration and, for this reason, there was no need for antioxidant enzymes activation. The GSTs are an important group of enzymes whose function is catalyze the conjugation of a xenobiotic with glutathione (GSH) (Townsend and Tew, 2003) as well as inactivate lipid peroxidation products through the use of GSH as a reducing agent (Sturve *et al*., 2008). Previous studies demonstrated the non-activation of antioxidant enzymes while GSTs were activated, namely in *M. galloprovincialis* exposed to arsenic (Coppola *et al*., 2018) and in the same species exposed to silver NPs (Ale *et al*., 2019). Nevertheless, in mussels exposed to anatase NPs an opposite behaviour was detected, with mussels increasing their antioxidant defenses while decreasing the biotransformation defenses (GSTs). These findings may result from the higher ROS production resulting from higher toxicity of anatase but also from the activation of mussel's metabolic capacity, assessed by the activity of ETS, since the mitochondrial transport system is one of the main ROS generators, leading to the activation of antioxidant enzymes.

As a consequence of low rutile toxicity, the results obtained revealed low cellular damages in mussels exposed to this TiO_2 form. Since antioxidant defenses were not significantly activated, the present results highlight the low toxicity of rutile NPs as well as the efficiency of the biotransformation defense system to detoxify rutile NPs. Nonetheless, mussels exposed to anatase NPs suffered cellular damages despite the increase in antioxidant defenses. In this case, cellular damages may result from the excessive production of ROS and the inefficient ability of mussels to activate GSTs. Similarly, Andrade *et al*. (2019) also demonstrated that *M. galloprovincialis* exposed to carbon nanotubes lead to cellular damages and decreased in GSTs activity.

Overall, the present study showed that, although at each exposure concentration similar Ti concentrations were observed in mussels exposed to both forms, higher metabolic

and oxidative stress impacts were caused by anatase. These results are in agreement with several studies that already proved that anatase NPs are more toxic than rutile NPs (Braydich-Stolle *et al*., 2009; Zhang *et al*., 2013), which authors associated with the structure and the lower particle size of anatase. In particular, Zhang *et al*. (2013) demonstrated that the 25 nm anatase particles induced the strongest cytotoxicity and oxidative stress, followed by 5 and 100 nm anatase particles; in contrast, 100 nm rutile particles induced the lowest toxicity. The results showed that the diameters of particles measured on SEM micrographs (calculated based in diameter of 45 particles) were 694 nm for rutile and 94 nm for anatase, which may explain higher toxicity of anatase. Also Iswarya *et al*. (2016) demonstrated that anatase NPs were highly toxic than rutile NPs under visible irradiation in *Ceriodaphnia dubia*, and also correlated with crystalline form and the aggregation of NPs.

The present study further revealed that rutile and anatase NPs induced neurotoxicity in mussels. The increased in AChE activity is probably due to organisms' attempts to reduce neurotransmitter excess in the synaptic clefts (Pan *et al*., 2012; Rajkumar, 2013). It has been reported the increase on AChE activities reflected neurotoxicity of TiO_2 NPs in the scallop *Chlamys farreri* (Xia *et al*., 2017), with higher values in contaminated organisms.

4.3. Rutile nanoparticles and warming conditions

The present study revealed that differences in Ti concentrations found in mussel's tissues were only observed at the highest exposure concentration, with higher values at lower temperature (18 ºC, control). These findings may be explained by Ti behavior at higher temperature. Studies conducted by Mikulášek *et al*. (1997) revealed that the interactive forces of TiO_2 are affected by temperature, showing that the increase of the temperature leads to a reduction of dispersion shear stress of these NPs. The authors explained this effect as a result of a decrease in the interactive forces between particles with temperature. For this reason, it was expected that at higher temperature higher aggregation occurred which, previous studies identified as a factor that contributes to higher accumulation and toxicity. In particular, Ward and Kach (2009) demonstrated that bivalves more efficiently capture and ingest NPs that are incorporated into agglomerates compared to those freely dispersed. However, in the present study higher accumulation was observed at lower temperature (smaller particles). Therefore, at higher temperature the lowest accumulation may be explained by higher precipitation of larger aggregates limiting the availability and

accumulation of the NPs. Canesi et al. (2010) and Zhu et al. (2011) showed that TiO_2 NPs form aggregates in artificial seawater and thus tend to precipitate rapidly. Therefore, higher aggregates at higher temperature may precipitate faster.

In terms of histopathological impacts, the present study clearly revealed that both gills and digestive glands were responsive to rutile NPs, in a dose-dependent response, with higher alterations observed at increased temperature (22 °C). In particular, the results obtained demonstrated that rutile NPs and temperature induced histopathological alterations in gills and digestive tubules of contaminated mussels. Regarding gills, the presence of rutile NPs caused mainly hemocyte infiltration which, according to different authors (Bignell et al., 2011; Costa et al., 2013; Cuevas et al., 2015; Rocha et al., 2016), are associated with inflammatory responses. Also, rutile NPs caused enlargement of the central vessel and abundance of lipofuscin aggregates. According to Höhn and Grune (2013), the presence of lipofuscin aggregates may indicate oxidative stress in the affected cells, which corroborates LPO levels observed in mussels exposed to 22 ºC. On the other hand, at 18 ºC there were no evidences of LPO which may show the low toxicity of rutile NPs at control temperature in terms of biochemical changes despite the effects in terms of histopathological changes. At increased temperature contaminated organisms also evidenced loss of cilia that can lead to difficulties in filtering food and breathing problems (Pagano *et al*., 2016). Therefore, the present findings are in line with other studies that already demonstrated histological alterations in bivalve's gills when exposed to pollutants, namely lanthanum (La) (Pinto *et al*., 2019), mercury (Amachree *et al*., 2014), and 'bulk' TiO_2 and TiO_2 NPs (D'Agata *et al*., 2014).

Regarding digestive tubules, for both temperatures the exposure to rutile NPs caused mainly hemocytes infiltration, accumulation of lipofuscin and atrophy that consists in a reduction in the thickness of epithelia accompanied by the enlargement of the digestive tubule lumen (Cuevas *et al*., 2015). At 22 °C, mussels exposed to 50 and 100 µg/L of rutile NPs showed signs of necrosis that is characterized by cellular rupture (do Amaral *et al*., 2019). Similarly, studies assessing impacts of contaminants, such as La (Pinto *et al*., 2019), cadmium-based quantum dots (Rocha *et al*., 2016) and various metals (cadmium, chromium, copper, mercury, nickel, lead, zinc) (Cuevas *et al*., 2015) demonstrated histological alterations in digestive tubules in mussels.

The results obtained further evidenced that temperature greatly influenced mussel's biochemical performance, however, the present study also demonstrated that rutile NPs were responsible for biochemical alterations in mussels. This response may be related to higher Ti bioaccumulation in mussels exposed to the highest exposure concentration. Furthermore, temperature influenced the accumulation of Ti in mussel's tissues, with higher accumulation levels at 18 °C. Therefore, differences in mussel's biochemical responses observed at both temperatures may be related to increased sensitivity of organisms to rutile due to temperature rise. Previous studies already demonstrated that bivalves increased the accumulation of pollutants along an increasing exposure gradient (Velez *et al*., 2015, 2016) while studies with TiO_2 demonstrated significantly higher accumulation in mussel's tissues only at the highest exposure concentration (5, 50, 100 µg/L, Monteiro *et al*., 2019b). Studies assessing the impacts of pollutants under warming conditions evidenced contrasting results, with higher accumulation levels of arsenic in mussels under increased temperatures (Coppola *et al*., 2018), while triclosan concentrations were higher in mussels exposed to control temperature and no temperature effects were noticed on chromium bioaccumulation (Pirone *et al*., 2019). Thus, the present findings and results from studies already published may indicate that under temperature rise bioaccumulation of pollutants may differ with the pollutant.

The present results also demonstrated that the effects caused by the presence of rutile NPs and temperature seemed to be additive for some of the responses measured, with higher impacts in contaminated organisms exposed to warming conditions (22 °C) compared to contaminated mussels at control temperature (18 °C). In particular, the metabolic capacity of mussels was not altered in organisms exposed to rutile NPs at 18 °C, revealing that the concentrations tested were not enough to impact mussel's metabolism. However, when exposed to increased temperature the impacts of the NPs on mussel's metabolism were noticed, especially at 5 and 50 µg/L, evidencing that the toxicity of rutile NPs may be enhanced under warming conditions or, on the other hand, the sensitivity of mussels to these NPs may increase under higher temperature. Because non-contaminated mussels exposed to 22 °C did not show any significant alteration on ETS activity compared to non-contaminated mussels exposed to 18 °C I may hypothesize that alterations on mussel's metabolism resulted from the increased toxicity of rutile NPs under 22 °C, with mussels increasing their metabolic capacity to activate defense mechanisms. These results can indicate that mussels

exposed to higher temperature and lower rutile concentrations were able to activate their metabolism probably to fight against high stress levels, but with increasing exposure concentrations mussels were no longer able to maintain this behaviour. Metabolic depression was already described in mussels as a response to pollutants exposure, normally associated with bivalve's capacity to maintain their valves closed and reduce the filtration rate and avoid accumulation of xenobiotics. Thus, the present findings are in agreement with previous studies also conducted with *M. galloprovincialis* which demonstrated a metabolic depression as a response to the exposure to pollutants, namely Ti (Monteiro *et al*., 2019a), La (Pinto *et al*., 2019) and gadolinium (Henriques *et al.*, 2019).

In terms of energy reserves the present study showed that mussels were able to preserve the expenditure of GLY, especially noticed at the most stressful conditions (100 µg/L at both temperatures). These results follow the decreased of ETS activity at 22 °C, indicating that higher stressful conditions mussels try to prevent the impacts by limiting their metabolic activity and saving GLY. Previous studies already evidenced the capacity of bivalves to preserve their energy reserves when under stressful conditions, a behaviour normally associated with a decreasing metabolic activity. In particular, Monteiro *et al*. (2019a,b) showed an increase in GLY content in *M. galloprovincialis* with increasing Ti concentration. Also, Duquesne *et al*. (2004) demonstrated the same pattern in *Macoma balthica* exposed to cadmium.

However, in what concerns to PROT content the results obtained showed a different response, with a tendency to decrease the PROT content with the increase of rutile NPs exposure concentration, especially noticed at higher temperature. These findings may indicate that mussels were not able to increase the production of proteins under the stress conditions, which can point out that the stress induced was not enough to increase the production of proteins (namely enzymes) and therefore this energy resource tended to decrease, especially at the highest exposure concentration. De Marchi *et al*. (2018) showed a decrease in PROT content in *Ruditapes philippinarum* exposed to carbon nanotubes.

In terms of oxidative stress the present results suggest that at 18 °C the activity of antioxidant defenses was not activated with the increasing exposure concentration, corroborating the hypothesis that the concentrations tested were not enough to activate antioxidant defenses, or other mechanisms of defense, such as detoxification mechanisms, were enough to prevent impacts especially at higher concentrations. In fact, the limited

increase in mussel's antioxidant defenses could be related to increased activity of their detoxification capacity, here evidenced by increased glutathione-S-transferases (GSTs) activity, especially at higher rutile concentrations. When exposed to pollutants organisms develop mechanisms of defense that are responsible for lowering the stress induced. Such mechanisms involve the detoxification of xenobiotic substances as the case of GSTs that main function is to catalyse the conjugation of a diverse array of electrophilic compounds with glutathione (Regoli and Giulianni, 2014). Coppola *et al*. (2018) demonstrated that at control temperature and in the presence of arsenic the activity of antioxidant defenses (SOD and CAT) in *M. galloprovincialis* were not significantly increased which was associated with the capacity of bivalves to activate detoxification mechanisms (GSTs). Also Ale *et al*. (2019) showed that the activity of CAT was not activated in *M. galloprovincialis* exposed to silver NPs while the activity of GSTs was activated. A study conducted by Mezni *et al*. (2018) showed that the activity of SOD was not significantly increased in digestive glands of *M. galloprovincialis* at control temperature exposed to a gradients of TiO_2 NPs. Monteiro *et al*. (2019a) demonstrated an increase of GSTs activity with increasing exposure concentrations of Ti in *M. galloprovincialis*. Nevertheless, at higher temperature an opposite behaviour was observed, with mussels increasing the activity of SOD with the increase of rutile NPs concentration while CAT was inhibited in contaminated organisms. Such findings may result from the inefficient capacity of GSTs to detoxify rutile at warming conditions which, in turn, resulted into higher stress levels and activation of antioxidant defenses (SOD) and inhibition of CAT that could result from extreme stress conditions. It was already demonstrated that GSTs may be inhibited in bivalves exposed to warming conditions which may result into higher stress levels and inhibition of antioxidant enzymes at extreme conditions. Coppola *et al*. (2018) showed that *M. galloprovincialis* increased the activity of antioxidant defenses when exposed to 1 mg/L of arsenic and under warming conditions. Pirone *et al*. (2019) also demonstrated that the activity of antioxidant defenses was not activated in *M. galloprovincialis* at control temperature exposed to 50 μg/L of lead but at 22 °C mussels increased the activity of SOD. The inhibition of GSTs was demonstrated by Andrade *et al*. (2019) when exposed *M. galloprovincialis* to carbon nanotubes under warming conditions.

In what regards to cellular damage, the results here presented showed that no lipid peroxidation (LPO) occurred in contaminated mussels at 18 °C evidencing that no cellular

damage was observed in mussels exposed to rutile NPs under control temperature, probably due to low toxicity of rutile. These results also highlight the efficiency of the biotransformation defense system to detoxify rutile NPs. Such response may result from the increased capacity of mussels to activate their detoxification mechanisms, preventing organisms from cellular damage and oxidative stress. On the other hand, at increased temperature cellular damages were observed although antioxidant mechanisms were enhanced in contaminated organisms resulting into a general oxidative status in mussels exposed to higher temperature and rutile NPs. This situation may also result from the inefficient capacity of mussels to activate GSTs and eliminate rutile NPs. Previous studies conducted by Coppola *et al*. (2017, 2018) have already showed that no LPO occurred in contaminated mussels (*M. galloprovincialis*) exposed mercury and arsenic respectively during 14 days at control temperature, while under higher temperature (22 °C) LPO levels increased. Also Freitas *et al*. (2017) showed higher LPO levels in *M. galloprovincialis* exposed to mercury under warming conditions compared to control temperature.

The present study further demonstrated the neurotoxic capacity of rutile NPs at control temperature while no changes were observed at warming conditions. Such results may indicate that at 18 °C the activity of AChE is enhanced probably because the organisms attempt to reduce neurotransmitter excess in the synaptic clefts, which was already showed in the bivalve *Perna indica* exposed to arsenic (Rajkumar, 2013) and in *Scrobicularia plana* exposed to gold nanoparticles (Pan *et al*., 2012). At higher temperature it seems that the effect of temperature overlaps the effect of rutile NPs. It has been reported that TiO_2 NPs may induced alterations in the nervous system (Skocaj *et al*., 2011).

Chapter 5

Conclusions

5. CONCLUSIONS

This study provides information concerning the potential risk of anatase and rutile TiO_2 NPs and warming conditions for the aquatic environment and inhabiting organisms, by assessing biochemical and histopathological effects in *Mytilus galloprovincialis,* a species with high ecological and economical relevance.

The most common form of TiO_2 is rutile and this study demonstrate that rutile NPs induced less biochemical alterations in *M. galloprovincialis* in comparison to anatase NPs, especially in term of oxidative stress. In particular, the increase in cellular damage and antioxidant defenses. However, both forms of TiO_2 NPs were responsible for Ti bioaccumulation as well as histopathological alterations in mussels, in a concentration-dependent way, with higher injuries identified in mussels exposed to higher Ti concentrations, regardless the TiO_2 form. From the results obtained it is possible to identify that the most sensitive biomarkers for the different NPs were the ETS, representing the metabolic capacity, antioxidant defenses (SOD and CAT), biotransformation defenses (GSTs) and cellular damage (LPO), because they demonstrated that anatase NPs induce higher toxic effect in this species than rutile.

When organisms are exposed to rutile NPs at two different temperatures, higher toxic impacts are revealed under warming conditions in comparison to mussels exposed to rutile NPs at control temperature, suggesting that temperature rise may significantly increase the sensitivity of bivalves towards pollutants. Such increased under warming conditions can result from the inefficient capacity of biotransformation enzymes (GSTs) that under increase temperature were inhibited. The most sensitive biomarkers for temperature were the ETS, SOD, GSTs, LPO and AChE, since they showed that warming increased the toxicity of rutile NPs.

In future works it is important to investigate the effects of anatase NPs in combination with warming and the combination of both forms of TiO_2 NPs, as well as the NPs under other climate stressors, such as pH and salinity variations.

It is possible to conclude that both TiO_2 forms may generate ecological and socio-economic consequences, such as mussels reproductive and feeding capacity, growth and, consequently, mussels heath and survival, which may eventually result in biodiversity loss and socio-economic impacts in cultures of this species.

Chapter 6

References

6. REFERENCES

Abdel-Maksoud, Y.K., Imam, E., Ramadan, A.R. (2018). TiO_2 water-bell photoreactor for wastewater treatment. Solar Energy, 170: 323–335.

Ale, A., Liberatori, G., Vannuccini, M.L., Bergami, E., Ancora, S., Mariotti, G., Bianchi., N., Galdopórpora, J.M., Desimone, M.F., Cazenave, J., Corsi, I. (2019). Exposure to a nanosilver-enabled consumer product results in similar accumulation and toxicity of silver nanoparticles in the marine mussel *Mytilus galloprovincialis*. Aquatic Toxicology, 211: 46–56.

Allen, N.S., Edge, M., Verran, J., Caballero, L., Abrusci, C., Stratton, J., Maltby, J., Bygott, C. (2010). Photocatalytic surfaces: environmental benefits of nanotitania. The Open Materials Science Journal, 3: 6–27.

Almeida, E., Bainy, A.C.D., Loureiro, A.P.M., Martinez, G.R., Miyamoto, S., Onuki, J., Barbosa, L.F., Garcia, C.C.M., Prado, F.M., Ronsein, G.E., Sigolo, C.A., Brochini, C.B., Martins, A.M.G., Medeiros, M.H.G.M., Di Mascio, P. (2007). Oxidative stress in *Perna perna* and other bivalves as indicators of environmental stress in the Brazilian marine environment: Antioxidants, lipid peroxidation and DNA damage. Comparative Biochemistry and Physiology Part A: Molecular & Integrative Physiology, 146: 588–600.

Amachree, D., Moody, A.J., Handy, R.D. (2014). Comparison of intermittent and continuous exposures to inorganic mercury in the mussel, *Mytilus edulis*: Accumulation and sub-lethal physiological effects. Ecotoxicology and Environmental Safety, 109: 133–142.

Amorim, S.M., Suave, J., Andrade, L., Mendes, A.M., José, H.J., Moreira, R.F.P.M. (2018). Towards an efficient and durable self-cleaning acrylic paint containing mesoporous TiO_2 microspheres. Progress in Organic Coatings, 118: 48–56.

Amtout, A., Leonelli, R. (1995). Optical properties of rutile near its fundamental band gap. Physical Review B, 51(11): 6842–6851.

Anderson, M.J., Gorley, R.N., Clarke, K.R. (2008). PERMANOVA+ for PRIMER: Guide to Software and Statistical Methods. PRIMER-E, Plymouth.

Andrade, M., De Marchi, L., Soares, A.M.V.M., Rocha, R.J.M., Figueira, E., Freitas, R. (2019). Are the effects induced by increased temperature enhanced in *Mytilus galloprovincialis* submitted to air exposure? Science of the Total Environment, 647: 431–440.

Angel, M.V. (1991). Variations in time and space: is biogeography relevant to studies of long-time scale change? Journal of the Marine Biological Association of the United Kingdom, 71(1): 191–206.

Artifon, V., Zanardi-Lamardo, E., Fillmann, G. (2019). Aquatic organic matter: Classification and interaction with organic microcontaminants. Science of The Total Environment, 649: 1620–1635.

Au, D.W.T. (2004). The application of histo-cytopathological biomarkers in marine pollution monitoring: a review. Marine Pollution Bulletin, 48(9–10): 817–834.

Azizi, G., Layachi, M., Akodad, M., Yáñez-Ruiz, D. R., Martín-García, A. I., Baghour, M., Mesfioui, A., Skalli, A., Moumen, A. (2018). Seasonal variations of heavy metals content in mussels (*Mytilus galloprovincialis*) from Cala Iris offshore (Northern Morocco). Marine Pollution Bulletin, 137: 688–694.

Baalousha, M., Stolpe, B., Lead, J. R. (2011). Flow field-flow fractionation for the analysis and characterization of natural colloids and manufactured nanoparticles in environmental systems: A critical review. Journal of Chromatography A, 1218(27): 4078–4103.

Banerjee, S., Dubey, S., Gautam, R.K., Chattopadhyaya, M.C., Sharma, Y.C. (2017). Adsorption characteristics of alumina nanoparticles for the removal of hazardous dye, Orange G from aqueous solutions. Arabian Journal of Chemistry, In Press.

Banni, M., Hajer, A., Sforzini, S., Oliveri, C., Boussetta, H., Viarengo, A. (2014). Transcriptional expression levels and biochemical markers of oxidative stress in *Mytilus galloprovincialis* exposed to nickel and heat stress. Comparative Biochemistry and Physiology Part C: Toxicology & Pharmacology, 160: 23–29.

Barbosa, J.S., Neto, D.M.A., Freire, R.M., Rocha, J.S., Fechine, L.M.U.D., Denardin, J.C., Valentini, A., de Araújo, T.G., Mazzetto, S.E., Fechine, P.B.A. (2018). Ultrafast

sonochemistry-based approach to coat TiO_2 commercial particles for sunscreen formulation. Ultrasonics Sonochemistry, 48: 340–348.

Barmo, C., Ciacci, C., Canonico, B., Fabbri, R., Cortese, K., Balbi, T., Marcomini, A., Pojana, G., Gallo, G., Canesi, L. (2013). In vivo effects of n-TiO_2 on digestive gland and immune function of the marine bivalve *Mytilus galloprovincialis*. Aquatic Toxicology, 132–133: 9–18.

Barreto, A., Luis, L.G., Pinto, E., Almeida, A., Paíga, P., Santos, L.H.M.L.M., Delerue-Matos, C., Trindade, T., Soares, A.M.V.M., Hylland, K., Loureiro, S., Oliveira, M. (2019). Effects and bioaccumulation of gold nanoparticles in the gilthead seabream (*Sparus aurata*) – Single and combined exposures with gemfibrozil. Chemosphere, 215: 248–260.

Batley, G.E., Kirby, J.K., McLaughlin, M.J. (2013). Fate and Risks of Nanomaterials in Aquatic and Terrestrial Environments. Accounts of Chemical Research, 46(3): 854–862.

Beauchamp, C., Fridovich, I. (1971). Superoxide dismutase: improved assays and an assay applicable to acrylamide gels. Analytical Biochemistry, 44 (1): 276–287.

Benali, I., Boutiba, Z., Grandjean, D., de Alencastro, L.F., Rouane-Hacene, O., Chèvre, N. (2017). Spatial distribution and biological effects of trace metals (Cu, Zn, Pb, Cd) and organic micropollutants (PCBs, PAHs) in mussels *Mytilus galloprovincialis* along the Algerian west coast. Marine Pollution Bulletin, 115(1–2): 539–550.

Bernet, D., Schmidt, H., Meier, W., Burkhardt-Holm, P., Wahli, T. (1999). Histopathology in fish: proposal for a protocol to assess aquatic pollution. Journal of Fish Diseases, 22: 25–34.

Bignell, J.P., Dodge, M.J., Feist, S.W., Lyons, B., Martin, P.D., Taylor, N.G.H., Stone, D., Travalent, L., Stentiford, G.D. (2008). Mussel histopathology: Effects of season, disease and species. Aquatic Biology, 2(1): 1–15.

Bignell, J.P., Stentiford, G.D., Taylor, N.G.H., Lyons, B.P. (2011). Histopathology of mussels (*Mytilus sp*.) from the Tamar estuary, UK. Marine Environmental Research, 72(1–2): 25–32.

Boss, C.B., Fredeen, K.J. (2004). ICP-OES instrumentation. In: Concepts, instrumentation and techniques in inductively coupled plasma optical emission spectrometry. Third Edition. PerkinElmer, 2–35.

Boukadida, K., Banni, M., Gourves, P.Y., Cachot, J. (2016). High sensitivity of embryo-larval stage of the Mediterranean mussel, *Mytilus galloprovincialis* to metal pollution in combination with temperature increase. Marine Environmental Research, 122: 59–66.

Branch, G.M., Steffani, C.N. (2004). Can we predict the effects of alien species? A case-history of the invasion of South Africa by *Mytilus galloprovincialis* (Lamarck). Journal of Experimental Marine Biology and Ecology, 300: 189–215.

Brar, S.K., Verma, M., Tyagi, R.D., Surampalli, R.Y. (2010). Engineered nanoparticles in wastewater and wastewater sludge – Evidence and impacts. Waste Management, 30(3): 504–520.

Braydich-Stolle, L.K., Schaeublin, N.M., Murdock, R.C., Jiang, J., Biswas, P., Schlager, J.J., Hussain, S.M. (2009). Crystal structure mediates mode of cell death in TiO_2 nanotoxicity. Journal of Nanoparticle Research, 11(6): 1361–1374.

Cai, Y., Li, C., Wu, D., Wang, W., Tan, F., Wang, X., Wong, P.K., Qiao, X. (2017). Highly active MgO nanoparticles for simultaneous bacterial inactivation and heavy metal removal from aqueous solution. Chemical Engineering Journal, 312: 158–166.

Calabrese, A., MacInnes, J.R., Nelson, D.A., Greig, R.A., Yevich, P.P. (1984). Effects of long-term exposure to silver or copper on growth, bioaccumulation and histopathology in the blue mussel *Mytilus edulis*. Marine Environmental Research, 11(4): 253–274.

Caldeira, K., Wickett, M.E. (2003). Anthropogenic carbon and ocean pH. Nature, 425: 365.

Canesi, L., Ciacci, C., Fabbri, R., Marcomini, A., Pojana, G., Gallo, G. (2012). Bivalve molluscs as a unique target group for nanoparticle toxicity. Marine Environmental Research, 76: 16–21.

Canesi, L., Fabbri, R., Gallo, G., Vallotto, D., Marcomini, A., Pojana, G. (2010). Biomarkers in *Mytilus galloprovincialis* exposed to suspensions of selected nanoparticles (Nano carbon black, C60 fullerene, Nano-TiO_2, Nano-SiO_2). Aquatic Toxicology, 100(2): 168–177.

Carlberg, I., Mannervik, B. (1985). Glutahione reductase. Methods Enzymol, 113: 484–490.

Carregosa, V., Figueira, E., Gil, A.M., Pereira, S., Pinto, J., Soares, A.M.V.M., Freitas, R. (2014). Tolerance of *Venerupis philippinarum* to salinity: Osmotic and metabolic aspects. Comparative Biochemistry and Physiology Part A: Molecular & Integrative Physiology, 171: 36–43.

Casse, M., Montero-Serrano, J.C., St-Onge, G., Poirier, A. (2019). REE distribution and Nd isotope composition of estuarine waters and bulk sediment leachates tracing lithogenic inputs in eastern Canada. Marine Chemistry, 211: 117–130.

Catsiki, V.-A., Florou, H. (2006). Study on the behavior of the heavy metals Cu, Cr, Ni, Zn, Fe, Mn and ^{137}Cs in an estuarine ecosystem using *Mytilus galloprovincialis* as a bioindicator species: the case of Thermaikos gulf, Greece. Journal of Environmental Radioactivity, 86(1): 31–44.

Cho, W.S., Kang, B.C., Lee, J.K., Jeong, J., Che, J.H., Seok, S.H. (2013). Comparative absorption, distribution, and excretion of titanium dioxide and zinc oxide nanoparticles after repeated oral administration. Particle and Fibre Toxicology, 10: 9.

Ciacci, C., Canonico, B., Bilaniĉovă, D., Fabbri, R., Cortese, K., Gallo, G., Marcomini, A., Pojana, G., Canesi, L. (2012). Immunomodulation by different types of N-Oxides in the hemocytes of the marine bivalve *Mytilus galloprovincialis*. PLoS ONE, 7(5): e36937.

Cid, A., Picado, A., Correia, J.B., Chaves, R., Silva, H., Caldeira, J., de Matos, A.P.A., Diniz, M.S. (2015). Oxidative stress and histological changes following exposure to diamond nanoparticles in the freshwater Asian clam *Corbicula fluminea* (Müller, 1774). Journal of Hazardous Materials, 284: 27–34.

Clarke, A. (2003). Costs and consequences of evolutionary temperature adaptation. Trends in Ecology & Evolution, 18(11): 573–581.

Collins, M., Knutti, R., Arblaster, J., Dufresne, J.-L., Fichefet, T., Friedlingstein, P., Gao, X., Gutowski, W.J., Johns, T., Krinner, G., Shongwe, M., Tebaldi, C., Weaver, A.J., Wehner, M. (2013). Long-term Climate Change: Projections, Commitments and Irreversibility. In: Climate Change 2013: The Physical Science Basis. Contribution of Working Group I to the Fifth Assessment Report of the Intergovernmental Panel on

Climate Change [Stocker, T.F., Qin, D., Plattner, G.-K., Tignor, M., Allen, S.K., Boschung, J., Nauels, A., Xia, Y., Bex, V. Midgley, P.M. (eds.)]. Cambridge University Press, Cambridge, United Kingdom and New York, NY, USA.

Colvin, V.L. (2003). The potential environmental impact of engineered nanomaterials. Nature Biotechnology, 21: 1166–1170.

Coppola, F., Almeida, Â., Henriques, B., Soares, A.M.V.M., Figueira, E., Pereira, E., Freitas, R. (2017). Biochemical impacts of Hg in *Mytilus galloprovincialis* under present and predicted warming scenarios. Science of the Total Environment, 601–602: 1129–1138.

Coppola, F., Almeida, Â., Henriques, B., Soares, A.M.V.M., Figueira, E., Pereira, E., Freitas, R. (2018). Biochemical responses and accumulation patterns of *Mytilus galloprovincialis* exposed to thermal stress and Arsenic contamination. Ecotoxicology and Environmental Safety, 147: 954–962.

Coppola, F., Tavares, D.S., Henriques, B., Monteiro, R., Trindade, T., Soares, A.M.V.M., Figueira, E., Polese, G., Pereira, E., Freitas, R. (2019). Remediation of arsenic from contaminated seawater using manganese spinel ferrite nanoparticles: Ecotoxicological evaluation in *Mytilus galloprovincialis*. Environmental Research, 175: 200–212.

Costa, P.M., Carreira, S., Costa, M.H., Caeiro, S. (2013). Development of histopathological indices in a commercial marine bivalve (*Ruditapes decussatus*) to determine environmental quality. Aquatic Toxicology, 126: 442–454.

Cuevas, N., Zorita, I., Costa, P.M., Franco, J., Larreta, J. (2015). Development of histopathological indices in the digestive gland and gonad of mussels: Integration with contamination levels and effects of confounding factors. Aquatic Toxicology, 162: 152–164.

Cui, S., Yang, L., Wang, J., Wang, X. (2016). Fabrication of a sensitive gas sensor based on PPy/TiO_2 nanocomposites films by layer-by-layer self-assembly and its application in food storage. Sensors and Actuators B: Chemical, 233: 337–346.

D'Agata, A., Fasulo, S., Dallas, L.J., Fisher, A.S., Maisano, M., Readman, J.W., Jha, A.N. (2014). Enhanced toxicity of 'bulk'' titanium dioxide compared to "fresh'' and "aged''

nano-TiO_2 in marine mussels (*Mytilus galloprovincialis*). Nanotoxicology, 8(5): 549–558.

Dame, R.F. (2008). Estuaries. In Encyclopedia of Ecology (Second Edition), 2: 484–490. Chichester, UK: Elsevier.

D'Aniello, B., Polese, G., Luongo, L., Scandurra, A., Magliozzi, L., Aria, M., Pinelli, C. (2016). Neuroanatomical relationships between FMRFamide-immunoreactive components of the nervus terminalis and the topology of olfactory bulbs in teleost fish. Cell and Tissue Research, 364(1): 43–57.

Dauvin, J.-C., Ruellet, T. (2009). The estuarine quality paradox: Is it possible to define an ecological quality status for specific modified and naturally stressed estuarine ecosystems? Marine Pollution Bulletin, 59(1–3): 38–47.

Dayton, P., Curran, S., Kitchingman, A., Wilson, M., Catenazzi, A., Birkeland, C., Blaber, S., Saifullah, S., Branch, G., Boersma, D., Nixon, S., Dugan, P., Davidson, N.,n Vörösmarty, C. (2005). Coastal systems. In: Ecosystems and Human Well-being: Current State and Trends, 513–549.

De Coen, W., Janssen, C.R. (1997). The use of biomarkers in Daphnia magna toxicity testing. IV.Cellular Energy Allocation: a new methodology to assess the energy budget of toxicant-stressed Daphnia populations. Journal of Aquatic Ecosystem Stress and Recovery, 6(1): 43–55.

de la Calle, I., Menta, M., Klein, M., Séby, F. (2017). Screening of TiO_2 and Au nanoparticles in cosmetics and determination of elemental impurities by multiple techniques (DLS, SP-ICP-MS, ICP-MS and ICP-OES). Talanta, 171: 291–306.

De Marchi, L., Neto, V., Pretti, C., Chiellini, F., Morelli, A., Soares, A. M. V. M., Figueira, E., Freitas, R. (2019a). The influence of Climate Change on the fate and behavior of different carbon nanotubes materials and implication to estuarine invertebrates. Comparative Biochemistry and Physiology Part C: Toxicology & Pharmacology, 219: 103–115.

De Marchi, L., Neto, V., Pretti, C., Figueira, E., Chiellini, F., Morelli, A., Soares, A.M.V.M., Freitas, R. (2018). Toxic effects of multi-walled carbon nanotubes on bivalves:

Comparison between functionalized and nonfunctionalized nanoparticles. Science of the Total Environment, 622–623: 1532–1542.

De Marchi, L., Pretti, C., Chiellini, F., Morelli, A., Neto, V., Soares, A.M.V.M., Figueira, E., Freitas, R. (2019b). The influence of simulated global ocean acidification o--+'n the toxic effects of carbon nanoparticles on polychaetes. Science of The Total Environment, 666: 1178–1187.

Desbiolles, F., Malleret, L., Tiliacos, C., Wong-Wah-Chung, P., Laffont-Schwob, I. (2018). Occurrence and ecotoxicological assessment of pharmaceuticals: Is there a risk for the Mediterranean aquatic environment? Science of The Total Environment, 639:1334–1348.

Dey, C., Baishya, K., Ghosh, A., Goswami, M.M., Ghosh, A., Mandal, K. (2017). Improvement of drug delivery by hyperthermia treatment using magnetic cubic cobalt ferrite nanoparticles. Journal of Magnetism and Magnetic Materials, 427: 168–174.

Dias, J.M., Lopes, J., Dekeyser, I. (1999). Hydrological characterisation of Ria de Aveiro, Portugal, in early summer. Oceanologica Acta, 22(5): 473–485.

Dias, J.M., Lopes, J.F., Dekeyser, I. (2000). Tidal propagation in Ria de Aveiro lagoon, Portugal. Physics and Chemistry of the Earth, Part B: Hydrology, Oceans and Atmosphere, 25(4): 369–374.

do Amaral, Q.D.F., Da Rosa, E., Wronski, J.G., Zuravski, L., Querol, M.V.M., dos Anjos, B., de Andrade, C.F.F., Machado, M.M., de Oliveira, L.F.S. (2019). Golden mussel (*Limnoperna fortunei*) as a bioindicator in aquatic environments contaminated with mercury: Cytotoxic and genotoxic aspects. Science of The Total Environment, 675: 343–353.

Dorier, M., Béal, D., Tisseyre, C., Marie-Desvergne, C., Dubosson, M., Barreau, F., Houdeau, E., Herlin-Boime, N., Rabilloud, T., Carriere, M. (2019). The food additive E171 and titanium dioxide nanoparticles indirectly alter the homeostasis of human intestinal epithelial cells *in vitro*. Environmental Science: Nano, 6(5): 1549–1561.

Dubois, M., Gilles, K.A., Hamilton, J.K.J., Rebers, P.A., Smith, F. (1956). Colorimetric method for determination of sugars and related substances. Analytical Chemistry, 28 (3): 350–356.

Duquesne, S., Liess, M., Bird, D.J. (2004). Sub-lethal effects of metal exposure: Physiological and behavioural responses of the estuarine bivalve *Macoma balthica*. Marine Environmental Research, 58(2–5): 245–250.

Elderfield, H., Upstill-Goddard, R., Sholkovitz, E. R. (1990). The rare earth elements in rivers, estuaries, and coastal seas and their significance to the composition of ocean waters. Geochimica et Cosmochimica Acta, 54(4): 971–991.

Ellman, G.L., Courtney, K.D., Andres, V., Featherstone, R.M. (1961). A new and rapid colorimetric determination of acetylcholinesterase activity. Biochemical Pharmacology, 7(2): 88–95.

Evans, D.H. (1987). The fish gill: site of action and model for toxic effects of environmental pollutants. Environmental Health Perspectives, 71: 47–58.

Fadeel, B., Garcia-Bennett, A.E. (2010). Better safe than sorry: Understanding the toxicological properties of inorganic nanoparticles manufactured for biomedical applications. Advanced Drug Delivery Reviews, 62(3): 362–374.

FAO, Food and Agriculture Organization of the United Nations. (1998). Integrated coastal area management and agriculture, forestry and fisheries. FAO guidelines. Rome.

FAO, Food and Agriculture Organization of the United Nations (2019). Species Facts Sheets: *Mytilus galloprovincialis* (Lamarck, 1819). In: FAO Fisheries and Aquaculture Department [online]. Rome.

Fernández-Rubio, J., Rodríguez-Gil, J.L., Postigo, C., Mastroianni, N., López de Alda, M., Barceló, D., Valcárcel, Y. (2019). Psychoactive pharmaceuticals and illicit drugs in coastal waters of North-Western Spain: Environmental exposure and risk assessment. Chemosphere, 224: 379–389.

Freitas, R., Coppola, F., Costa, S., Pretti, C., Intorre, L., Meucci, V., Soares, A.M.V.M., Solé, M. (2019). The influence of temperature on the effects induced by Triclosan and Diclofenac in mussels. Science of The Total Environment, 663: 992–999.

Freitas, R., Coppola, F., Henriques, B., Wrona, F., Figueira, E., Pereira, E., Soares, A.M.V.M. (2017). Does pre-exposure to warming conditions increase *Mytilus galloprovincialis* tolerance to Hg contamination? Comparative Biochemistry and Physiology Part C: Toxicology & Pharmacology, 203: 1–11.

Gabe, M. (1968). Metachromacity of products of secretion rich in cystine after oxidation by certain peracids. Comptes Rendus des Séances de l'Académie des Sciences. Série D: Seances Naturelles, 267(6): 666-668.

Gagné, F., Blaise, C., Fournier, M., Hansen, P.D. (2006). Effects of selected pharmaceutical products on phagocytic activity in *Elliptio complanata* mussels. Comparative Biochemistry and Physiology Part C: Toxicology & Pharmacology, 143(2): 179-86.

Gambardella, C., Morgana, S., Bari, G. Di, Ramoino, P., Bramini, M., Diaspro, A., Falugi, C., Faimali, M. (2015). Multidisciplinary screening of toxicity induced by silica nanoparticles during sea urchin development. Chemosphere, 139: 486–495.

Gao, W., Wang, W., Yao, S., Wu, S., Zhang, H., Zhang, J., Jing, F., Mao, H., Jin, Q., Cong, H., Jia, C., Zhang, G., Zhao, J. (2017). Highly sensitive detection of multiple tumor markers for lung cancer using gold nanoparticle probes and microarrays. Analytica Chimica Acta, 958: 77–84.

Gao, Y., Zhou, C., Gaulier, C., Bratkic, A., Galceran, J., Puy, J., Zhang, H., Leermakers, M., Baeyens, W. (2019). Labile trace metal concentration measurements in marine environments: From coastal to open ocean areas. TrAC Trends in Analytical Chemistry, 116, 92–101.

Gondikas, A.P., Kammer, F. von der, Reed, R.B., Wagner, S., Ranville, J.F., Hofmann, T. (2014). Release of TiO_2 Nanoparticles from Sunscreens into Surface Waters: A One-Year Survey at the Old Danube Recreational Lake. Environmental Science & Technology 48(10): 5415–5422.

Gong, X.-Q., Selloni, A. (2007). First-principles study of the structures and energetics of stoichiometric brookite TiO_2 surfaces. Physical Review B, 76: 235307.

Google Maps. (2019). Accessed July 2019. Available at: https://www.google.com/maps

Gosling, E. (2003). Circulation, respiration, excretion and osmoregulation. In: Bivalve Molluscs: Biology, Ecology and Culture. Blackwell Publishing, 201-225.

Gottschalk, F., Nowack, B. (2011). The release of engineered nanomaterials to the environment. Journal of Environmental Monitoring, 13(5): 1145–1155.

Grant, W.S., Cherry, M.I. (1985). *Mytilus galloprovincialis* Lmk. in Southern Africa. Journal of Experimental Marine Biology and Ecology, 90: 179–191.

Grätzel, M. (2001). Photoelectrochemical cells. Nature, 414: 338–344.

Guzman, K.A.D., Finnegan, M.P., Banfield, J.F. (2006). Influence of surface potential on aggregation and transport of titania nanoparticles. Environmental Science & Technology, 40(24): 7688–7693.

Habig, W.H., Pabst, M.J., Jakoby, W.B. (1974). Glutathione S-Transferases. The fist enzymatic step in mercapturic acid formation. The Journal of Biological Chemistry, 249(22): 7130–7139.

Harley, C.D.G., Hughes, A.H., Hultgren, K.M., Miner, B.G., Sorte, C.J.B., Thornber, C.S., Rodriguez, L.F., Tomanek, L., Williams, S.L. (2006). The impacts of climate change in coastal marine systems. Ecology Letters, 9(2), 228–241.

Henriques, B., Coppola, F., Monteiro, R., Pinto, J., Viana, T., Pretti, C., Soares, A., Freitas, R., Pereira, E. (2019). Toxicological assessment of anthropogenic Gadolinium in seawater: Biochemical effects in mussels *Mytilus galloprovincialis*. Science of the Total Environment, 664: 626–634.

Hoffmann, M.R., Martin, S.T., Choi, W., Bahnemann, D.W. (1995). Environmental Applications of Semiconductor Photocatalysis. Chemical Reviews, 95(1): 69–96.

Hoffmann, A.A., Sørensen, J.G., Loeschcke, V. (2003). Adaptation of *Drosophila* to temperature extremes: Bringing together quantitative and molecular approaches. Journal of Thermal Biology, 28(3): 175–216.

Hofmann, G.E., Todgham, A.E. (2010). Living in the Now: Physiological Mechanisms to Tolerate a Rapidly Changing Environment. Annual Review of Physiology, 72: 127–145.

Höhn, A., Grune, T. (2013). Lipofuscin: Formation, effects and role of macroautophagy. Redox Biology, 1(1): 140–144.

Hood, E. (2004). Nanotechnology: Looking As We Leap. Environmental Health Perspectives, 112(13).

Hosseinzadeh, F., Shirazian, F., Shahsavari, R., Khoei, A.R. (2016). Local density variation of gold nanoparticles in aquatic environments. Physica E: Low-Dimensional Systems and Nanostructures, 84: 489–497.

Huang, J., Nkrumah, P.N., Anim, D.O., Mensah, E. (2014). E-waste disposal effects on the aquatic environment: Accra, Ghana. In: Reviews of Environmental Contamination and Toxicology. Springer, 229: 19-34.

Im, H.J., Koo, B., Kim, M.-S., Lee, J.E. (2019). Solvothermal synthesis of Sb_2Te_3 nanoplates under various synthetic conditions and their thermoelectric properties. Applied Surface Science, 475: 510–514.

IPCC. (2007). Climate change 2007: the physical science basis. In: Contribution of Work Group I to the Fourth Assessment Report of the Intergovernmental Panel on Climate. Cambridge University Press, Cambridge, UK.

IPCC. (2014). Climate Change 2014: Synthesis Report. Contribution of Working Groups I, II and III to the Fifth Assessment Report of the Intergovernmental Panel on Climate Change [Core Writing Team, R.K. Pachauri and L.A. Meyer (eds.)]. IPCC, Geneva, Switzerland, 151 pp.

Islam, M.S., Tanaka, M. (2004). Impacts of pollution on coastal and marine ecosystems including coastal and marine fisheries and approach for management: a review and synthesis. Marine Pollution Bulletin, 48(7–8): 624–649.

ISO, International Standards Organisation. (2015). Nanotechnologies – Vocabulary – Part 2: Nano-Objects. ISO 80004-2, Geneva, Switzerland.

Iswarya, V., Bhuvaneshwari, M., Alex, S.A., Iyer, S., Chaudhuri, G., Chandrasekaran, P.T., Bhalerao, G.M., Chakravarty, S., Raichur, A.M., Chandrasekaran, N., Mukherjee, A. (2015). Combined toxicity of two crystalline phases (anatase and rutile) of Titania nanoparticles towards freshwater microalgae: *Chlorella sp*. Aquatic Toxicology, 161: 154–169.

Iswarya, V., Bhuvaneshwari, M., Chandrasekaran, N., Mukherjee, A. (2016). Individual and binary toxicity of anatase and rutile nanoparticles towards *Ceriodaphnia dubia*. Aquatic Toxicology, 178: 209–221.

Iswarya, V., Bhuvaneshwari, M., Chandrasekaran, N., Mukherjee, A. (2018). Trophic transfer potential of two different crystalline phases of TiO_2 NPs from *Chlorella sp*. to *Ceriodaphnia dubia*. Aquatic Toxicology, 197: 89–97.

Iswarya, V., Palanivel, A., Chandrasekaran, N., Mukherjee, A. (2019). Toxic effect of different types of titanium dioxide nanoparticles on *Ceriodaphnia dubia* in a freshwater system. Environmental Science and Pollution Research, 26(12): 11998–12013.

Izagirre, U., Errasti, A., Bilbao, E., Múgica, M., Marigómez, I. (2014). Combined effects of thermal stress and Cd on lysosomal biomarkers and transcription of genes encoding lysosomal enzymes and HSP70 in mussels, *Mytilus galloprovincialis*. Aquatic Toxicology, 149: 145–156.

Jansen, J.M., Hummel, H., Bonga, S.W., (2009). The respiratory capacity of marine mussels (*Mytilus galloprovincialis*) in relation to the high temperature threshold. Comparative Biochemistry and Physiology Part A: Molecular & Integrative Physiology, 153(4): 399–402.

Jiang, J., Oberdörster, G., Biswas, P. (2009). Characterization of size, surface charge, and agglomeration state of nanoparticle dispersions for toxicological studies. Journal of Nanoparticle Research, 11(1): 77–89.

Jimeno-Romero, A., Bilbao, E., Valsami-Jones, E., Cajaraville, M.P., Soto, M., Marigómez, I. (2019). Bioaccumulation, tissue and cell distribution, biomarkers and toxicopathic effects of CdS quantum dots in mussels, *Mytilus galloprovincialis*. Ecotoxicology and Environmental Safety, 167: 288–300.

Johansson, L.H., Borg, L.A.H. (1988). A spectrophotometric method for determination of catalase activity in small tissue samples. Analytical Biochemistry, 174(1): 331–336.

Johnson, A.C., Bowes, M.J., Crossley, A., Jarvie, H.P., Jurkschat, K., Jürgens, M.D., Lawlor, A.J., Park, B., Rowland, P., Spurgeon, D., Svendsen, C., Thompson, I.P., Barnes, R.J., Williams, R.J ., Xu, N. (2011). An assessment of the fate, behaviour and environmental

risk associated with sunscreen TiO_2 nanoparticles in UK field scenarios. Science of the Total Environment, 409(13): 2503–2510.

Kaegi, R., Ulrich, A., Sinnet, B., Vonbank, R., Wichser, A., Zuleeg, S., Simmler, H., Brunner, S., Vonmont, H., Burkhardt, M., Boller, M. (2008). Synthetic TiO_2 nanoparticle emission from exterior facades into the aquatic environment. Environmental Pollution, 156(2): 233–239.

Kennedy, V.C., Zellweger, G.W., Jones, B.F. (1974). Filter pore-size effects on the analysis of Al, Fe, Mn, and Ti in water. Water Resources Research, 10(4): 785–790.

Kimbrough, K.L., Johnson, W.E., Lauenstein, G.G., Christensen, J.D., Apeti, D.A. (2008). An assessment of two decades of contaminant monitoring in the nation's coastal zone. NOAA Technical Memorandum NOS NCCOS 74. Silver Spring, MD. 105 pp.

King, F.D., Packard, T.T. (1975). Respiration and the activity of the respiratory electron transport system in marine zooplankton. Limnology and Oceanography, 20: 849–854.

Kiser, M.A., Westerhoff, P., Benn, T., Wang, Y., Pérez-Rivera, J., Hristovski, K. (2009). Titanium nanomaterial removal and release from wastewater treatment plants. Environmental Science & Technology, 43(17): 6757–6763.

Lecoanet, H.F., Wiesner, M.R. (2004). Velocity effects on fullerene and oxide nanoparticle deposition in porous media. Environmental Science & Technology, 38(16): 4377–4382.

Leong, H.J., Oh, S.-G. (2018). Preparation of antibacterial TiO_2 particles by hybridization with azelaic acid for applications in cosmetics. Journal of Industrial and Engineering Chemistry, 66: 242–247.

Livingstone, D.R., Dixon, D.R., Donkin, P., Lowe, D.M., Moore, M.N., Widdows, J. (1989). Molecular, cellular and physiological responses of the common mussel *Mytilus edulis* to pollution: uses in environmental monitoring and management. Ecotoxicology, The Institute of Biology, London, pp. 26–30.

Livingstone, D.R., Martinez, P.G., Michel, X., Narbonne, J.F., O'Hara, S., Ribera, D., Winston, G.W. (2006). Oxyradical Production as a Pollution-Mediated Mechanism of Toxicity in the Common Mussel, *Mytilus edulis* L., and Other Molluscs. Functional Ecology, 4(3): 415-424.

Liu, W.-T. (2006). Nanoparticles and their biological and environmental applications. Journal of Bioscience and Bioengineering, 102(1): 1–7.

Lopes, C.L., Azevedo, A., Dias, J.M. (2013). Flooding assessment under sea level rise scenarios: Ria de Aveiro case study. Journal of Coastal Research, 65: 766–771.

Lower, W.R., Kendall, R. (1990). Sentinel Species and Sentinel Bioassay. In: Biomarkers of Environmental Contamination. Lewis Publishers, 309–331 pp.

Lu, P.J., Huang, S.C., Chen, Y.P., Chiueh, L.C., Shih, D.Y.C. (2015). Analysis of titanium dioxide and zinc oxide nanoparticles in cosmetics. Journal of Food and Drug Analysis, 23(3): 587–594.

Manciocco, A., Calamandrei, G., Alleva, E. (2014). Global warming and environmental contaminants in aquatic organisms: The need of the etho-toxicology approach. Chemosphere, 100: 1–7.

Marigómez, I., Garmendia, L., Soto, M., Orbea, A., Izagirre, U., Cajaraville, M.P. (2013). Marine ecosystem health status assessment through integrative biomarker indices: A comparative study after the Prestige oil spill "Mussel Watch". Ecotoxicology, 22(3): 486–505.

Markert, B.A., Breure, A.M., Zechmeister, H.G. (2003). Definitions, strategies and principles for bioindication/biomonitoring of the environment. Trace Metals and other Contaminants in the Environment, 6: 3–39).

Martín-Pozo, L., de Alarcón-Gómez, B., Rodríguez-Gómez, R., García-Córcoles, M.T., Çipa, M., Zafra-Gómez, A. (2019). Analytical methods for the determination of emerging contaminants in sewage sludge samples. A review. Talanta, 192: 508–533.

Măruţescu, L., Chifiriuc, M.C., Postolache, C., Pircalabioru, G.G., Bolocan, A. (2019). Nanoparticles' toxicity for humans and environment. In: Nanomaterials for Drug Delivery and Therapy. Elsevier, 515–535 pp.

Maskos, M., Stauber, R.H. (2016). 3.21 Characterization of Nanoparticles in Biological Environments. Comprehensive Biomaterials II, 3: 467–481.

Masunga, N., Mmelesi, O.K., Kefeni, K.K., Mamba, B.B. (2019). Recent advances in copper ferrite nanoparticles and nanocomposites synthesis, magnetic properties and application in water treatment: Review. Journal of Environmental Chemical Engineering, 7(3): 103179.

Matozzo, V., Tomei, A., Marin, M.G. (2005). Acetylcholinesterase as a biomarker of exposure to neurotoxic compounds in the clam *Tapes philippinarum* from the Lagoon of Venice. Marine Pollution Bulletin, 50(12): 1686–1693.

Menard, A., Drobne, D., Jemec, A. (2011). Ecotoxicity of nanosized TiO_2. Review of in vivo data. Environmental Pollution, 159(3): 677–684.

Mennillo, E., Casu, V., Tardelli, F., De Marchi, L., Freitas, R., Pretti, C. (2017). Suitability of cholinesterase of polychaete *Diopatra neapolitana* as biomarker of exposure to pesticides: In vitro characterization. Comparative Biochemistry and Physiology Part C: Toxicology & Pharmacology, 191: 152–159.

Mesquita, C.S., Oliveira, R., Bento, F., Geraldo, D., Rodrigues, J.V., Marcos, J.C. (2014). Simplified 2,4-dinitrophenylhydrazine spectrophotometric assay for quantification of carbonyls in oxidized proteins. Analytical Biochemistry, 458: 69–71.

Mezni, A., Alghool, S., Sellami, B., Saber, N.B., Altalhi, T. (2018). Titanium dioxide nanoparticles: synthesis, characterisations and aquatic ecotoxicity effects. Chemistry and Ecology, 34(3): 288–299.

Middlemas, S., Fang, Z.Z., Fan, P. (2013). A new method for production of titanium dioxide pigment. Hydrometallurgy, 131–132: 107–113.

Mikulášek, P., Wakeman, R.J., Marchant, J Q. (1997). The influence of pH and temperature on the rheology and stability of aqueous titanium dioxide dispersions. Chemical Engineering Journal, 67(2): 97–102.

Mnasri, N., Charnay, C., de Ménorval, L.-C., Elaloui, E., Zajac, J. (2016). Rod-shaped silica particles derivatized with elongated silver nanoparticles immobilized within mesopores. Journal of Solid State Chemistry, 243: 207–214.

Moellmann, J., Ehrlich, S., Tonner, R., Grimme, S. (2012). A DFT-D study of structural and energetic properties of TiO_2 modifications. Journal of Physics: Condensed Matter, 24(42): 424206.

Mogilevsky, G., Chen, Q., Kleinhammes, A., Wu, Y. (2008). The structure of multilayered titania nanotubes based on delaminated anatase. Chemical Physics Letters, 460(4–6): 517–520.

Monteiro, R., Costa, S., Coppola, F., Freitas, R., Vale, C., Pereira, E. (2019a). Evidences of metabolic alterations and cellular damage in mussels after short pulses of Ti contamination. Science of the Total Environment, 650: 987–995.

Monteiro, R., Costa, S., Coppola, F., Freitas, R., Vale, C., Pereira, E. (2019b). Toxicity beyond accumulation of Titanium after exposure of *Mytilus galloprovincialis* to spiked seawater. Environmental Pollution, 244: 845–854.

Moore, M.N., Allen, J.I. (2002). A computational model of the digestive gland epithelial cell of marine mussels and its simulated responses to oil-derived aromatic hydrocarbons. Marine Environmental Research, 54(3–5): 579–584.

Moreira, A., Figueira, E., Soares, A.M.V.M., Freitas, R. (2016). The effects of arsenic and seawater acidification on antioxidant and biomineralization responses in two closely related *Crassostrea species*. Science of Total Environment, 545-546: 569-581.

Mubiana, V.K., Blust, R. (2007). Effects of temperature on scope for growth and accumulation of Cd, Co, Cu and Pb by the marine bivalve *Mytilus edulis*. Marine Environmental Research, 63(3): 219–235.

Murawski, S.A. (1993). Climate Change and Marine Fish Distributions: Forecasting from Historical Analogy. Transactions of the American Fisheries Society, 122(5): 647–658.

Nardi, A., Mincarelli, L.F., Benedetti, M., Fattorini, D., D'Errico, G., Regoli, F. (2017). Indirect effects of climate changes on cadmium bioavailability and biological effects in the Mediterranean mussel *Mytilus galloprovincialis*. Chemosphere, 169: 493–502.

Nowack, B., Bucheli, T.D. (2007). Occurrence, behavior and effects of nanoparticles in the environment. Environmental Pollution, 150(1): 5–22.

Nowack, B., Ranville, J.F., Diamond, S., Gallego-Urrea, J.A., Metcalfe, C., Rose, J., Horne, N., Koelmans, A.A., Klaine, S.J. (2012). Potential scenarios for nanomaterial release and subsequent alteration in the environment. Environmental Toxicology and Chemistry, 31(1): 50–59.

Ohkawa, H., Ohishi, N., Yagi, K. (1979). Assay for lipid peroxides in animal tissues by thiobarbituric acid reaction. Analytical Biochemistry, 95(2): 351–358.

Orr, J.C., Fabry, V.J., Aumont, O., Bopp, L., Doney, S.C., Feely, R.A., Gnanadesikan, A., Gruber, N., Ishida, A., Joos, F., Key, R.M., Lindsay, K., Maier-Reimer, E., Matear, R., Monfray, P., Mouchet, A., Najjar, R.G., Plattner, G.-K., Rodgers, K.B., Sabine, C.L., Sarmiento, J.L., Schlitzer, R., Slater, R.D., Totterdell, I.J., Weirig, M.-F., Yamanaka, Y., Yool, A. (2005). Anthropogenic ocean acidification over the twenty-first century and its impact on calcifying organisms. Nature, 437: 681–686.

Pagano, M., Capillo, G., Sanfilippo, M., Palato, S., Trischitta, F., Manganaro, A., Faggio, C. (2016). Evaluation of functionality and biological responses of *Mytilus galloprovincialis* after exposure to quaternium-15 (Methenamine 3-Chloroallylochloride). Molecules, 21(2): 1–12.

Paglia, D.E., Valentine, W.N. (1967). Studies on the quantitative and qualitative characterization of erythrocyte glutathione peroxidase. The Journal of Laboratory and Clinical Medicine, 70(1): 158–169.

Pan, J.F., Buffet, P.E., Poirier, L., Amiard-Triquet, C., Gilliland, D., Joubert, Y., Pilet, P., Guibbolini, M., de Faverney, C.R., Roméo, M., Valsami-Jones, E., Mouneyrac, C. (2012). Size dependent bioaccumulation and ecotoxicity of gold nanoparticles in an endobenthic invertebrate: The Tellinid clam *Scrobicularia plana*. Environmental Pollution, 168: 37–43.

Paz, Y. (2010). Application of TiO_2 photocatalysis for air treatment: Patents' overview. Applied Catalysis B: Environmental, 99(3–4): 448–460.

Pinto, J., Costa, M., Leite, C., Borges, C., Coppola, F., Henriques, B., Monteiro, R., Russo, T., Di Cosmo, A., Soares, A.M.V.M., Polese, G., Pereira, E., Freitas, R. (2019). Ecotoxicological effects of lanthanum in *Mytilus galloprovincialis*: Biochemical and histopathological impacts. Aquatic Toxicology, 211: 181–192.

Pirone, G., Coppola, F., Pretti, C., Soares, A.M.V.M., Solé, M., Freitas, R. (2019). The effect of temperature on Triclosan and Lead exposed mussels. Comparative Biochemistry and Physiology Part B: Biochemistry and Molecular Biology, 232: 42–50.

Polese, G., Bertapelle, C., Di Cosmo, A. (2016). Olfactory organ of *Octopus vulgaris*: morphology, plasticity, turnover and sensory characterization. Biology Open, 5: 611–619.

Pörtner, H.-O. (2010). Oxygen- and capacity-limitation of thermal tolerance: a matrix for integrating climate-related stressor effects in marine ecosystems. Journal of Experimental Biology, 213: 881–893.

Pörtner, H.-O., Karl, M.D., Boyd, P.W., Cheung, W.W.L., Lluch-Cota, S.E., Nojiri, Y., Schmidt D.N., Zavialov P.O. (2014). Impacts, adaptation, and vulnerability. Part A: Global and Sectoral Aspects. Contribution of Working Group II to the Fifth Assessment Report of the Intergovernmental Panel on Climate Change, Cambridge University Press.

Pörtner, H.-O., Knust, R. (2007). Climate change affects marine fishes through the oxygen limitation of thermal tolerance. Science, 315(5808): 95–97.

Pörtner, H.-O., Langenbuch, M., Michaelidis, B. (2005). Synergistic effects of temperature extremes, hypoxia, and increases in CO_2 on marine animals: From earth history to global change. Journal of Geophysical Research, 110: 2156–2202.

Pörtner, H.O., Peck, L., Somero, G. (2007). Thermal limits and adaptation in marine Antarctic ectotherms: An integrative view. Philosophical Transactions of the Royal Society B: Biological Sciences, 362(1488): 2233–2258.

Priyadarshini, E., Pradhan, N. (2017). Gold nanoparticles as efficient sensors in colorimetric detection of toxic metal ions: A review. Sensors and Actuators B: Chemical, 238: 888–902.

Quintino, V., Azevedo, A., Magalhães, L., Sampaio, L., Freitas, R., Rodrigues, A.M., Elliott, M. (2012). Indices, multispecies and synthesis descriptors in benthic assessments: Intertidal organic enrichment from oyster farming. Estuarine, Coastal and Shelf Science, 110: 190–201.

Rajalakshmi, S., Mohandas, A. (2005). Copper-induced changes in tissue enzyme activity in a freshwater mussel. Ecotoxicology and Environmental Safety, 62(1): 140–143.

Rajkumar, J.S.I. (2013). Reduced glutathione and acetylcholinesterase expressions in *Perna indica* exposed to trivalent arsenic. International Journal of Biological Research, 1(1): 1–4.

Regoli, F., Giuliani, M.E. (2014). Oxidative pathways of chemical toxicity and oxidative stress biomarkers in marine organisms. Marine Environmental Research, 93: 106–117.

Robinson, H., Hodgen, C. (1940). The biuret reaction in the determination of serum proteins: a study of the conditions necessary for the production of a stable color which bears a quantitative relationship to the protein concentration. Journal of Biological Chemistry, 135: 707–725.

Rodriguez-Narvaez, O.M., Peralta-Hernandez, J.M., Goonetilleke, A., Bandala, E.R. (2017). Treatment technologies for emerging contaminants in water: A review. Chemical Engineering Journal, 323: 361–380.

Rocha, T.L., Sabóia-Morais, S.M.T., Bebianno, M.J. (2016). Histopathological assessment and inflammatory response in the digestive gland of marine mussel *Mytilus galloprovincialis* exposed to cadmium-based quantum dots. Aquatic Toxicology, 177: 306–315.

Santos, S., Cardoso, J.F.M.F., Carvalho, C., Luttikhuizen, P.C., van der Veer, H.W. (2011). Seasonal variability in somatic and reproductive investment of the bivalve *Scrobicularia plana* (da Costa, 1778) along a latitudinal gradient. Estuarine, Coastal and Shelf Science, 92(1): 19–26.

Shi, X., Li, Z., Chen, W., Qiang, L., Xia, J., Chen, M., Zhu, L., Alvarez, P.J.J. (2016). Fate of TiO_2 nanoparticles entering sewage treatment plants and bioaccumulation in fish in the receiving streams. NanoImpact, 3–4: 96–103.

Skocaj, M., Filipic, M., Petkovic, J., Novak, S. (2011). Titanium dioxide in our everyday life; Is it safe? Radiology and Oncology, 45(4): 227–247.

Skrabal, S.A. (2006). Dissolved titanium distributions in the Mid-Atlantic Bight. Marine Chemistry, 102(3–4): 218–229.

Sokolova, I.M. (2004). Cadmium effects on mitochondrial function are enhanced by elevated temperatures in a marine poikilotherm, *Crassostrea virginica* Gmelin (Bivalvia: Ostreidae). Journal of Experimental Biology, 207: 2639–2648.

Sousa, A.I., Santos, D.B., da Silva, E.F., Sousa, L.P., Cleary, D.F.R., Soares, A.M.V.M., Lillebø, A.I. (2017). 'Blue Carbon' and Nutrient Stocks of Salt Marshes at a Temperate Coastal Lagoon (Ria de Aveiro, Portugal). Scientific Reports, 7: 41225.

Starling, M.C.V.M., Amorim, C.C., Leão, M.M.D. (2019). Occurrence, control and fate of contaminants of emerging concern in environmental compartments in Brazil. Journal of Hazardous Materials, 372: 17–36.

Sturve, J., Almroth, B.C., Förlin, L. (2008). Oxidative stress in rainbow trout (*Oncorhynchus mykiss*) exposed to sewage treatment plant effluent. Ecotoxicology and Environmental Safety, 70(3): 446–452.

Su, C., Tseng, C.-M., Chen, L.-F., You, B.-H., Hsu, B.-C., Chen, S.-S. (2006). Sol–hydrothermal preparation and photocatalysis of titanium dioxide. Thin Solid Films, 498(1–2): 259–265.

Sunila, I. (1988). Acute histological responses of the gill of the mussel, *Mytilus edulis*, to exposure by environmental pollutants. Journal of Invertebrate Pathology, 52(1): 137–141.

Sureda, A., Capó, X., Busquets-Cortés, C., Tejada, S. (2018). Acute exposure to sunscreen containing titanium induces an adaptive response and oxidative stress in *Mytillus galloprovincialis*. Ecotoxicology and Environmental Safety, 149: 58–63.

Suzuki, Y.J., Carini, M., Butterfield, D.A. (2010). Protein Carbonylation. Antioxidants & Redox Signaling, 12(3): 323-325.

The European Commission. (2011). Commission recommendation of 18 October 2011 on the definition of nanomaterial. Official Journal of the European Union, 696: 38–40.

Townsend, D.M., Tew, K.D. (2003). The role of glutathione-S-transferase in anti-cancer drug resistance. Oncogene, 22: 7369–7375.

Velez, C., Figueira, E., Soares, A.M.V.M., Freitas, R. (2016). Accumulation and sub-cellular partitioning of metals and As in the clam *Venerupis corrugata*: Different strategies towards different elements. Chemosphere, 156: 128–134.

Velez, C., Figueira, E., Soares, A.M.V.M., Freitas, R. (2017). Effects of seawater temperature increase on economically relevant native and introduced clam species. Marine Environmental Research, 123: 62–70.

Velez, C., Galvão, P., Longo, R., Malm, O., Soares, A.M.V.M., Figueira, E., Freitas, R. (2015). *Ruditapes philippinarum* and *Ruditapes decussatus* under Hg environmental contamination. Environmental Science and Pollution Research, 22(15): 11890–11904.

Verlecar, X.N., Jena, K.B., Chainy, G.B.N. (2007). Biochemical markers of oxidative stress in *Perna viridis* exposed to mercury and temperature. Chemico-Biological Interactions, 167(3): 219–226.

Viarengo, A., Dondero, F., Pampanin, D.M., Fabbri, R., Poggi, E., Malizia, M., Bolognesi, C., Perrone, E., Gollo, E., Cossa, G.P. (2007). A biomonitoring study assessing the residual biological effects of pollution caused by the HAVEN wreck on marine organisms in the Ligurian sea (Italy). Archives of Environmental Contamination and Toxicology, 53(4): 607–616.

Wahie, S., Lloyd, J.J., Farr, P.M. (2007). Sunscreen ingredients and labelling: A survey of products available in the UK. Clinical and Experimental Dermatology, 32(4): 359–364.

Wang, Y., Huang, Y., Ho, W., Zhang, L., Zou, Z., Lee, S. (2009). Biomolecule-controlled hydrothermal synthesis of C–N–S-tridoped TiO_2 nanocrystalline photocatalysts for NO removal under simulated solar light irradiation. Journal of Hazardous Materials, 169(1–3): 77–87.

Wang, Z., Li, Y., Chen, H., Fan, J., Wang, X., Ma, X. (2019). Correlation between the radius of acceptor ion and the dielectric properties of co-doped TiO_2 ceramics. Ceramics International, 45(12): 14625-14633.

Wang, W.-X, Fisher, N.S., Luoma, S.N. (1996). Kinetic determinations of trace element bioaccumulation in the mussel *Mytilus edulis*. Marine Ecology Progress Series, 140: 91–113.

Wang, J., Zhou, G., Chen, C., Yu, H., Wang, T., Ma, Y., Jia, G., Gao, Y., Li, B., Sun, J., Li, Y., Jiao, F., Zhao, Y., Chai, Z. (2007). Acute toxicity and biodistribution of different sized titanium dioxide particles in mice after oral administration. Toxicology Letters, 168(2): 176–85.

Ward, J.E., Kach, D.J. (2009). Marine aggregates facilitate ingestion of nanoparticles by suspension-feeding bivalves. Marine Environmental Research, 68(3): 137–142.

Weir, A., Westerhoff, P., Fabricius, L., Hristovski, K., von Goetz, N. (2012). Titanium dioxide nanoparticles in food and personal care products. Environmental Science & Technology, 46(4): 2242–2250.

Winkler, J. (2003). Production of Titanium Dioxide Pigments. European Coatings Literature, Vincentz, pp. 37–40.

Xia, B., Zhu, L., Han, Q., Sun, X., Chen, B., Qu, K. (2017). Effects of TiO_2 nanoparticles at predicted environmental relevant concentration on the marine scallop *Chlamys farreri*: An integrated biomarker approach. Environmental Toxicology and Pharmacology, 50: 128–135.

Yan, L., Stallard, R.F., Key, R.M., Crerar, D.A. (1991). Trace metals and dissolved organic carbon in estuaries and offshore waters of New Jersey, USA. Geochimica et Cosmochimica Acta, 55(12): 3647–3656.

Yang, W.-E., Hsu, M.-L., Lin, M.-C., Chen, Z.-H., Chen, L.-K., Huang, H.-H. (2009). Nano/submicron-scale TiO_2 network on titanium surface for dental implant application. Journal of Alloys and Compounds, 479(1–2): 642–647.

Yang, K., Xing, B. (2009). Sorption of Phenanthrene by Humic Acid-Coated Nanosized TiO_2 and ZnO. Environmental Science & Technology, 43(6): 1845–1851.

Yazdi, M.H., Sepehrizadeh, Z., Mahdavi, M., Shahverdi, A.R., Faramarzi, M.A. (2016). Metal, metalloid, and oxide nanoparticles for therapeutic and diagnostic oncology. Nano Biomedicine and Engineering, 8(4): 246–267.

Yokoi, K., van den Berg, C.M.G. (1991). Determination of titanium in sea water using catalytic cathodic stripping voltammetry. Analytica Chimica Acta, 245: 167–176.

Yuzer, B., Guida, M., Ciner, F., Aktan, B., Aydin, M.I., Meric, S., Selcuk, H. (2016). A multifaceted aggregation and toxicity assessment study of sol–gel-based TiO_2 nanoparticles during textile wastewater treatment. Desalination and Water Treatment, 57(11): 4966–4973.

Zanjani, J.S.M., Oğuz, O., Okan, B.S., Yildiz, M., Menceloğlu, Y.Z. (2018). Polymer Composites Containing Functionalized Nanoparticles and the Environment. In: Polymer Composites with Functionalized Nanoparticles, 437–466.

Zhang, J., Song, W., Guo, J., Zhang, J., Sun, Z., Li, L., Ding, F., Gao, M. (2013). Cytotoxicity of different sized TiO_2 nanoparticles in mouse macrophages. Toxicology and Industrial Health, 29(6): 523–533.

Zhang, X., Zheng, J. (2019). Hollow carbon sphere supported Ag nanoparticles for promoting electrocatalytic performance of dopamine sensing. Sensors and Actuators B: Chemical, 290: 648–655.

Zhou, X., Xu, C., Jin, Y., Li, B. (2019). Visual chiral recognition of D/L-leucine using cube-shaped gold nanoparticles as colorimetric probes. Spectrochimica Acta Part A: Molecular and Biomolecular Spectroscopy, 223: 117263.

Zhu, Z., Cai, H., Sun, D.W. (2018). Titanium dioxide (TiO_2) photocatalysis technology for nonthermal inactivation of microorganisms in foods. Trends in Food Science & Technology, 75: 23–35.

Zhu, X., Zhou, J., Cai, Z. (2011). TiO_2 Nanoparticles in the Marine Environment: Impact on the Toxicity of Tributyltin to Abalone (*Haliotis diversicolor supertexta*) Embryos. Environmental Science & Technology, 45(8): 3753–3758.

Zupo, V., Glaviano, F., Paolucci, M., Ruocco, N., Polese, G., Di Cosmo, A., Costantini, M., Mutalipassi, M. (2019). Roe enhancement of *Paracentrotus lividus*: Nutritional effects of fresh and formulated diets. Aquaculture Nutrition, 25(1): 26–38.